NASA CR-134729
R74AEG410

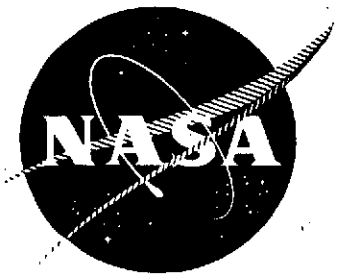

STATOR HUB TREATMENT STUDY

by

D.C. Wisler
D.E. Hilvers

GENERAL ELECTRIC COMPANY

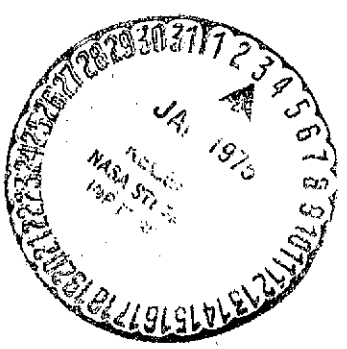

Prepared For

National Aeronautics and Space Administration

NASA Lewis Research Center
Contract NAS3-17359

1. Report No.	2. Government Accession No.	3. Recipient's Catalog No.
NASA CR-134729		

4. Title and Subtitle	5. Report Date
Stator Hub Treatment Study	December 1974
	6. Performing Organization Code

7. Author(s)	8. Performing Organization Report No.
D.C. Wisler, D.E. Hilvers	R74AEG410
	10. Work Unit No.

9. Performing Organization Name and Address	11. Contract or Grant No.
General Electric Company Aircraft Engine Group Cincinnati, Ohio 45215	NAS3-17359
	13. Type of Report and Period Covered
12. Sponsoring Agency Name and Address	Final June 1973-Dec. 1974
National Aeronautics and Space Administration Washington, D.C. 20546	14. Sponsoring Agency Code

15. Supplementary Notes

Project Manager, Everett E. Bailey
NASA-Lewis Research Center
Cleveland, Ohio 44135

16. Abstract

The results of an experimental research program to investigate the potential of improving compressor stall margin by the application of hub treatment are presented. The experimental program was carried out in the General Electric Low Speed Research Compressor, which provides for investigation at low Mach numbers ($M \leq 0.15$) and large geometric scale. Extensive tuft probing showed that the two-stage, 0.5 radius ratio compressor selected for the test was indeed hub critical. Circumferential groove and baffled wide blade angle slot hub treatments under the stators were tested. Performance measurements were made with total and static pressure probes, wall static pressure taps, flow angle measuring instrumentation and hot film anemometers. Stator hub treatment was not found to be effective in improving compressor stall margin by delaying the point of onset of rotating stall or in modifying compressor performance for any of the configurations tested. Extensive regions of separated flow were observed on the suction surface of the stators near the hub. However, the treatment did not delay the point where flow separation in the stator hub region becomes apparent.

17. Key Words (Suggested by Author(s))	18. Distribution Statement
Compressors Stall Margin Improvement Compressor Hub Treatment Compressor Casing Treatment	Unclassified - unlimited

19. Security Classif. (of this report)	20. Security Classif. (of this page)	21. No. of Pages	22. Price*
Unclassified	Unclassified	93	$ 3.00

* For sale by the National Technical Information Service, Springfield, Virginia 22151

TABLE OF CONTENTS

LIST OF ILLUSTRATIONS

LIST OF ILLUSTRATIONS (Continued)

LIST OF ILLUSTRATIONS (Continued)

LIST OF ILLUSTRATIONS (Concluded)

LIST OF ILLUSTRATIONS (Concluded)

LIST OF TABLES

SUMMARY

Based on the demonstrated success of casing treatment as a means for increasing compressor stall margin for tip sensitive single stages, an experimental program was undertaken to investigate the potential benefits of applying similar treatments to those stages where stall originates in the stator hub region. The program was designed to determine whether hub treatment would delay the onset of any unsteady flow, modify the extent and severity of any unsteadiness, delay the point of onset of rotating stall or modify the performance of the compressor in any other beneficial fashion. A 0.5 radius ratio two-stage Low Speed Research Compressor configuration, which had been used previously for fan distortion investigations and which showed evidence of stall inception in the hub region, was chosen as the test vehicle. This fan configuration was modified by removing the stator hub shrouds and replacing them with rotating hub spools which incorporated stator hub treatment. A smooth spool (baseline) configuration, a circumferential groove treatment configuration and a baffled wide blade angle slot treatment configuration were tested.

Although extensive tuft probing showed that the test vehicle was indeed hub critical, the performance data, obtained for the baseline and the two treatment configurations, showed that stator hub treatment did not modify the fan performance in any discernible fashion. It was suspected that stall might be originating in the rotors rather than the stators. Therefore, the blades and vanes of the test vehicle were restaggered in order to load the stators relative to the rotors. Tuft probing showed that the flow in the stator hub region was then worse than before; however, the fan performance was not modified by the treatment. The blades and vanes were then returned to their original staggers and one-half of the vanes in each stator were removed, raising the stator D-factors by approximately 40%. For this case the flow in the stator hub region was in even worse shape "aerodynamically speaking" with large regions of separation and backflow appearing on the stator suction surfaces. However, just as for the other configurations tested, stator hub treatment did not modify the onset, extent or severity of flow unsteadiness. It did not delay the point of onset of rotating stall, nor did it modify the performance of the compressor in any discernible fashion.

The results of this program should not be used to conclude that hub treatment does not have potential for compressor performance improvement. The fact that it was not effective for the particular vehicle configuration selected for this investigation may point to the fact that a better understanding of rotating stall and the onset of flow instability in turbomachinery is needed prior to further investigation of hub treatment.

INTRODUCTION

Recent applied research (References 1-8) has shown that compressor casing treatment can substantially improve the stall characteristics of fan and compressor stages. Different casing treatment configurations have been identified which provide either significant improvements in extending the stall line with some penalties in efficiency or modest gains in stall margin with no efficiency penalties. The effectiveness of the treatment was judged primarily by its ability to maintain or increase the pressure ratio while decreasing the weight flow below that obtained for a reference solid casing at the stall limit point. This stall limit point was defined as the point of onset of rotating stall or surge.

During the years 1968 to 1970 NASA conducted tests to demonstrate the concept of improving stall margin by use of casing treatment. The program described in Reference 1, for example, showed 7 percent improvement in stall margin for a 2-point sacrifice in efficiency. By the end of 1971, the concept has been firmly established. Osborn, Lewis and Heidelberg (Reference 2) had conducted tests on the following geometrically different porous casings: two perforated casings, three variations of honeycomb, circumferential grooves, axial slots, two variations of skewed slots, and four variations of blade angle slots. Significant stall margin increases were obtained with several of the treatments. The skewed slot configuration gave 20.7 percent increase in stall margin with a 7-point loss in efficiency. The blade angle slot and the circumferential groove configurations gave a 17.5 percent and 13.5 percent increase in stall margin, respectively, with efficiencies as high or slightly higher than those obtained with the reference solid casing. Other investigators (References 3-7) obtained similar beneficial results while continuing to investigate the effect of the geometric parameters associated with the treatment designs. It was learned that most of the benefit came from treating the center 60 percent of the chord projection. Treatment near the leading or trailing edge was generally ineffective. Bailey (Reference 5) showed that increasing the depth of the circumferential grooved treatment resulted in lower near-stall flows. From such information, a number of design rules-of-thumb emerged covering the percent open area in the treated area, the ratio of cavity depth to cavity width, the axial extent of the treatment, etc.

In 1972 Prince, Wisler and Hilvers (Under NASA Contract NAS3-15707, Reference 8) began a detailed investigation into the mechanisms and principles behind the beneficial influences of casing treatment. Analytical modeling of the flow patterns in the casing treatment cavities was carried out in conjunction with an experimental program to test several different treatment configurations. Each configuration tested showed an improvement in stall margin. The circumferential groove treatment yielded a 5.8 percent reduction in stalling flow with no sacrifice in efficiency. The axial-skewed slot treatment yielded a 15.3 percent reduction in stalling flow with a 1.8-point sacrifice in efficiency. The blade angle slot treatment yielded a 15.0 percent reduction in stalling flow with a 1.4-point sacrifice in efficiency. Although these values were consistent with previous casing treatment experience, the tests were conducted at low Mach numbers ($M<0.1$) showing that the stall margin improvements did not require the presence of compressibility effects, such as cavity resonance, to be effective. The improved stall margin correlated well with observations of higher-than-normal

static pressures on the rotor blade pressure surfaces in the tip region, and with increased maximum diffusions on the suction surfaces. Blade surface pressure loadings were found to have shifted toward the trailing edge. Also, extensive tuft surveys and pressure and velocity measurements were made within the treatment cavities.

Since rotor tip casing treatment has been shown to be effective in improving the stall characteristics of fan and compressor stages which are rotor tip critical, a logical next step is to investigate the potential benefits of applying similar treatments to those stages where stall originates in the stator hub region. The program herein reported was designed to examine this potential and to develop an initial understanding of hub treatment effectiveness.

EXPERIMENTAL RESOURCES

Low Speed Research Compressor Facility

The General Electric Low Speed Research Compressor (LSRC) is an experimental facility which is used for testing the aerodynamic characteristics of various compressor and fan designs. It is ideally suited for the exploration of phenomena in which viscous effects, characterized by Reynolds number, play a predominant role but where compressibility effects, characterized by Mach number or density ratio, are relatively unimportant. Since many compressor flow problems are in this category (secondary flows, wall boundary layer breakdowns, leakage effects, etc), this facility has been used extensively during its 13 years of existence.

Even though the blade tip speed employed is low [80 meters per second maximum (260 fps)], the large tip diameter [152.5 cm (60 in.)] allows testing with blade chord Reynolds numbers of about 500,000. This is sufficiently high to be above any critical value known for compressor stages and, in fact, is higher than many smaller engines encounter during altitude operations. The large diameter also makes it possible to study small-scale phenomena, such as secondary flows, without the need for extreme miniaturization of instrumentation.

A cross sectional drawing of the LSRC is presented in Figure 1. The facility is mounted vertically as shown in the photograph of the final build-up, Figure 2. A large flow-straightening screen, which fits over the bell-mouth, was used to insure uniform, disturbance-free flow into the compressor. Significant axial positions are indicated by plane locations as shown in Figure 3. Plane 0.0 marks the flow measuring plane of the calibrated bell-mouth, plane 1.0 indicates the inlet to the first rotor, plane 1.5 marks the first rotor discharge and stator inlet, plane 2.0 marks the first stator discharge and the second rotor inlet. Plane 2.5 indicates the second rotor discharge and the inlet of the second stator. Plane 3.0 marks the discharge of the second stator. The exit of the LSRC is covered with a large movable plate for throttling the flow. The throttle annulus area varies linearly from 0 m^2 to 1.88 m^2 (0 ft^2 to 20.2 ft^2) as the throttle position numbers vary from 0 to 4 422.

The rig is driven from the floor below by a 300 kilowatt (400 HP) steam turbine. Input power is obtained from a strain-gage-type torquemeter and an electronic pulse-counter speed indicator that reads to the nearest 1/10th rpm. Flow is measured in a calibrated bellmouth. This calibration includes the effect of the mushroom-shaped high solidity inlet screen enclosure and flow-straightener assembly (at top of Figure 2) used for performance tests. The screen surface area is 16 times the flow measurement plane area and has a porosity of 25 percent.

Fluid density is deduced from measurements of barometric pressure, ambient temperature, and air moisture content. A first order approximation of the small compressibility effects encountered at low speeds is included in performance computations when precise efficiencies are being sought.

Note: Numbers in Circle are for Identifying Parts in the Subassembly Drawings.

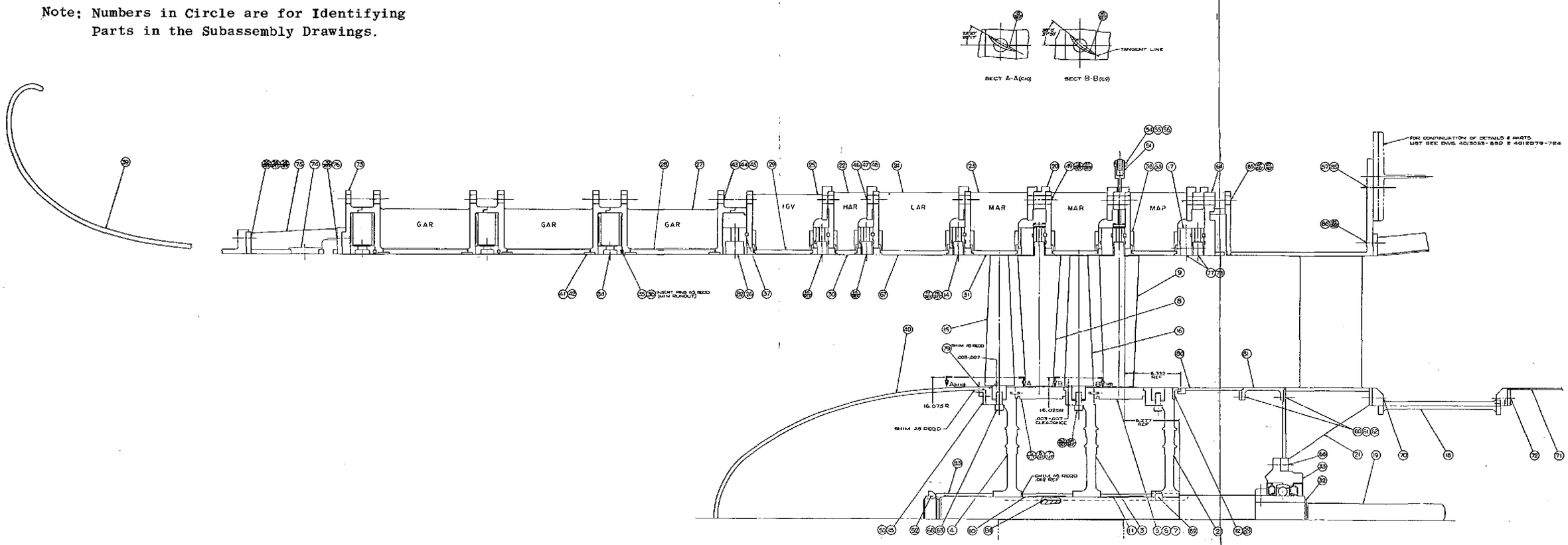

Figure 1. LSRC Hub Treatment Assembly.

FOLDOUT FRAME

REPRODUCIBILITY OF THE ORIGINAL PAGE IS POOR

FOLDOUT FRAME

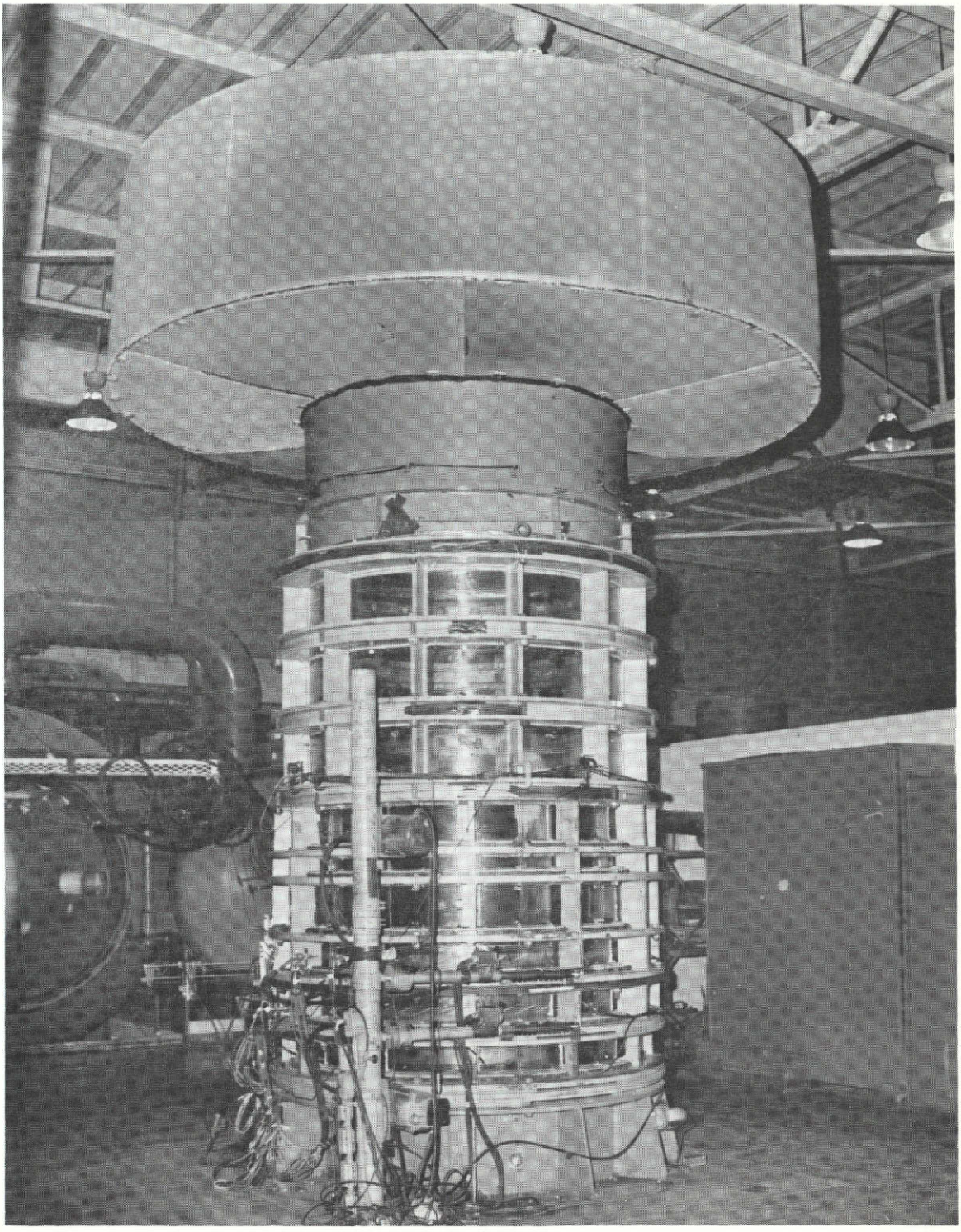

Figure 2. Photograph Showing Low Speed Research Compressor Buildup for Stator Hub Treatment Program.

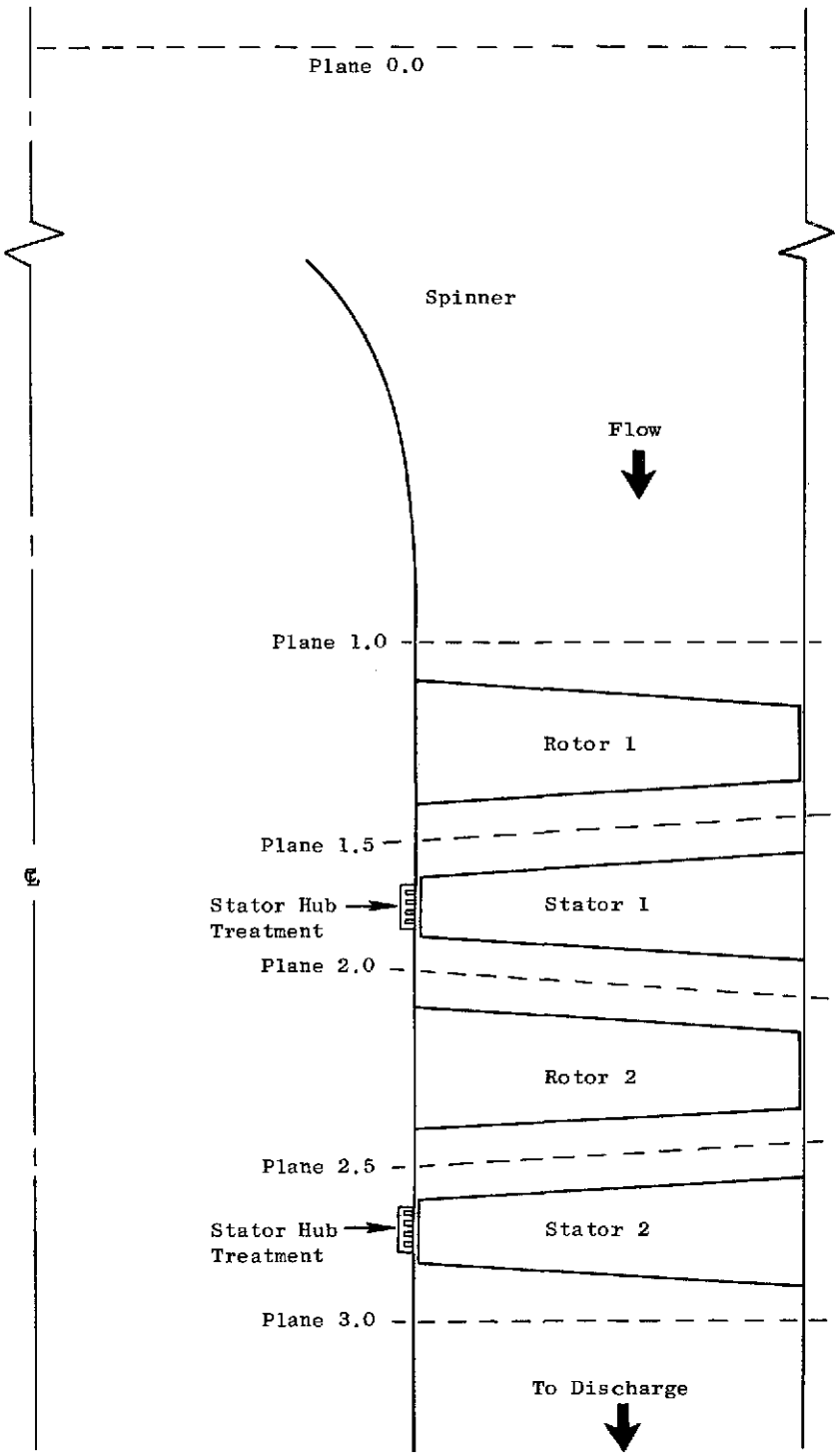

Figure 3. Schematic Low Speed Research Compressor Showing Measurement Planes and Location of Stator Hub Treatment Spools.

In order to keep operation simple and inexpensive, pressures are read on vertical or inclined water manometers. Since it may take an hour or more with the usual two-man test crew to record all desired pressures for one throttle setting, variations in ambient density due to barometer and room temperature variations may be significant. Possible errors are avoided by making frequent slight adjustments to the speed so as to keep a reference gage pressure in the discharge constant. This approach is justified by the similarity laws for low Mach number flow, which say that all gage pressures in the vehicle should remain in the same ratio, independent of speed, except for negligible effects due to the slight Reynolds number variations that result from this procedure. In order to compute accurate efficiency, the torque, speed, and ambient conditions are all read simultaneously two or more times during the pressure data logging process and the results are averaged.

Test Compressor

The test compressor selected for the Stator Hub Treatment Program was the 0.5 radius ratio, two-stage compressor configuration with shrouded stators which had previously been tested in 1971 and which had shown evidence of stall inception in the hub region. The vehicle was modified by removing the stator hub shrouds and using interchangeable rotating spools which incorporated various hub treatment geometries that rotated under the stator hub, as shown in Figure 3. The geometries which were tested were the smooth spool (baseline), the circumferential groove treatment and the baffled wide blade angle slot treatment. The airfoils for the compressor had a modified NACA 65-Series thickness distribution on a circular arc meanline. The blading geometry and other design parameters are given in Tables I and II. For comparison, the blading geometry used in the casing treatment investigation (Reference 8) is included in Table I.

Due to the 0.381 m (1.25 ft) length of the cantilevered stators, there was concern that rotating stall cells might excite resonance and cause the stator to fatigue and fail at the shank. Therefore a bench test was conducted to determine the axial, torsional and flexural resonant frequencies of the stator. A photograph of the blade being tested is presented in Figure 4. The tests showed that the only frequency to be concerned about was first flex at 40 cps, which could be excited by a multisector (four-lobe) stall cell at 600 rpm. Although occurrence of this type of stall cell is unlikely, precautionary measures were taken. The dynamic stress in the stator shanks was evaluated during shakedown testing. This stress was shown to be within limits even in the first stall mode, thus verifying the mechanical integrity of the compressor. However, an agreement was reached with the mechanical people that no testing would be done with the compressor in stall.

The stators of the Low Speed Research Compressor were mounted in rings which could be rotated circumferentially. Thus circumferential surveys to obtain data across a vane pitch were made by keeping the instrumentation fixed and rotating the stators. The casing windows of the LSRC are made from transparent plexiglass, thus allowing good visibility for making tuft surveys. The photograph in Figure 5 shows the observation ports through the casing windows over the rotor tips. Additional photographs in Figure 6 show a partial build-up of the baseline Stator Hub Treatment LSRC configuraton.

Table I. Blading Geometry.

	Hub Treatment Stators Stage #1	Stage #2	Casing Treatment Rotor
Blade Chord	7.95 cm (3.13 in)	8.92 cm (3.51 in)	11.61 cm (4.58 in)
Axially Projected Chord	7.44 cm (2.93 in)	8.46 (3.33 in)	8.46 cm (3.33 in)
Max. tip thickness/chord	0.055	0.050	0.045
Max. tip thickness	0.437 cm (0.172 in)	0.447 cm (0.176 in)	0.523 cm (0.206 in)
Spacing	4.78 cm (1.88 in)	4.52 cm (1.78 in)	8.86 cm (3.49 in)
Number of blades	50	53	54
Stagger	20.8°	18.6°	43.4

Table II. Mechanical and Aerodynamic Design Parameters of the Blading for the Stator Hub Treatment Study.

Blade Row	% Imm.	Solidity	Camber Angle (degrees)	Aspect Ratio	Stagger Angle (degrees)	Lift Coeff.	Work Coeff.	Flow Coeff.	Diff. Factor	Airfoil	Hub Radius Ratio	No. of Blades
R_1	10	1.3637	6.8	3.378	62.1	0.3391	0.4441	0.3679	0.2756	65 series	0.5	55
	50	1.6106	18.2	3.623	52.0	0.5047	0.7797	0.5198	0.3981			
	90	2.0054	47.2	3.968	30.0	0.8278	1.5925	0.7511	0.5265			
S_1	10	1.3403	35.8	3.125	15.9	0.7390	---	0.3491	0.3457			50
	50	1.4536	46.7	3.650	17.1	0.8847	---	0.5238	0.3798			
	90	1.5385	62.1	4.702	19.7	1.1207	---	0.7883	0.4992			
R_2	10	1.2632	4.4	3.448	66.9	0.3084	0.3659	0.3537	0.2321			52
	50	1.5338	10.9	3.597	54.6	0.3441	0.5199	0.5123	0.2796			
	90	1.9060	24.6	3.947	39.2	0.4640	0.9689	0.7960	0.3570			
S_2	10	1.3792	26.9	3.219	17.2	0.5886	---	0.3660	0.2432			53
	50	1.6046	24.3	3.505	16.0	0.5270	---	0.5055	0.2561			
	90	1.8251	35.0	4.202	15.9	0.5464	---	0.7796	0.2870			

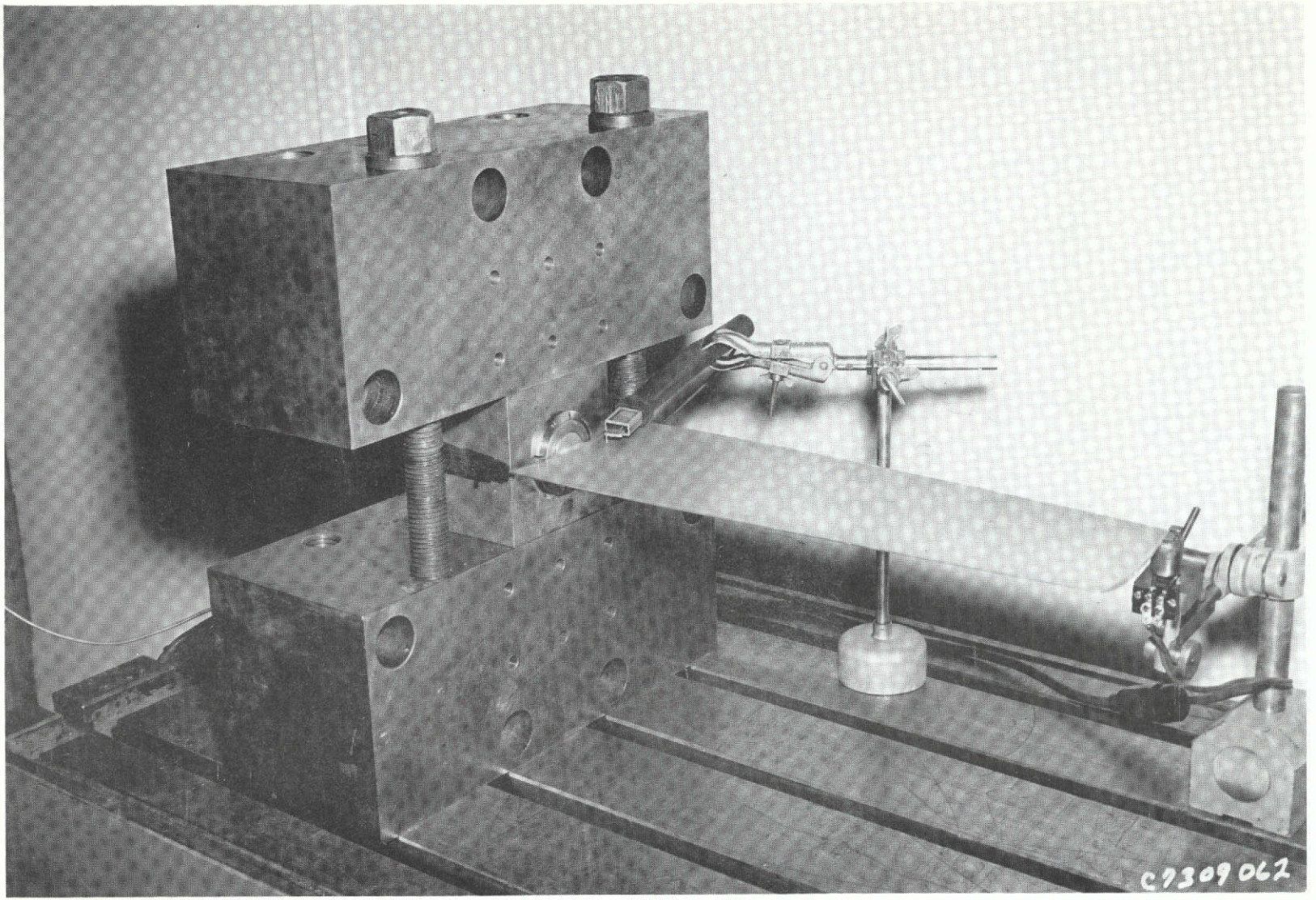

Figure 4. Bench Test Setup to Evaluate Stator Vane Critical Frequencies.

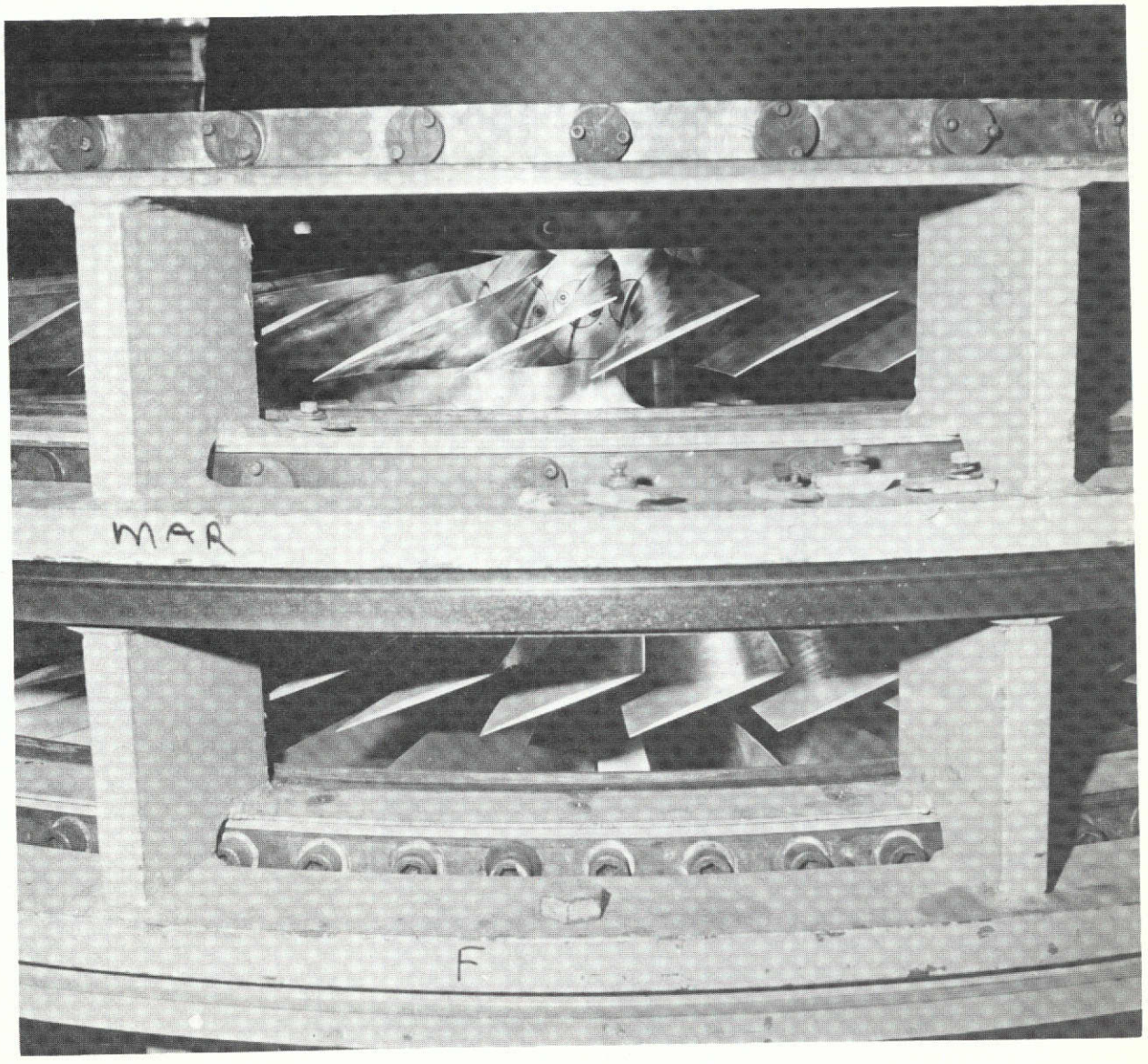

Figure 5. Partial Buildup of the Baseline Stator Hub Treatment LSRC Configuration, Showing Observation Ports.

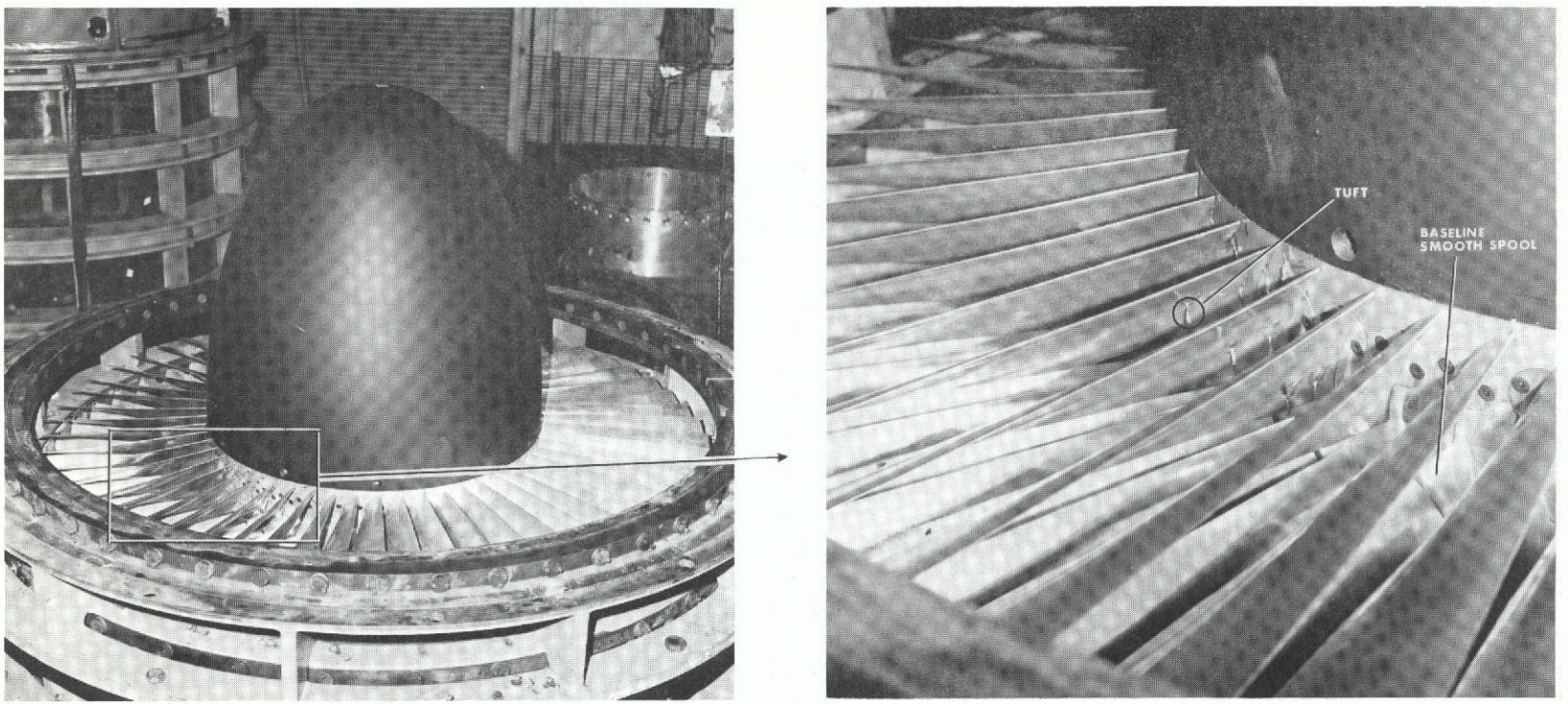

(a) First Stage Rotor and Spinner

(b) Closeup Showing Smooth Spool Rotating Hub and Tufts on First Rotor Pressure Surface

Figure 6. Partial Buildup of the Baseline Stator Hub Treatment LSRC Compressor.

Design of the Stator Hub Treatment

The various experimental programs described in References 1-8 have shown that porous wall casing treatments over axial flow compressor rotor tips can act to postpone the onset of stall and increase the useful operating range of the compressor. However, the geometric parameters associated with the treatment designs can be quite critical. Therefore, the design "rules-of-thunb" that have emerged from the previously successful casing treatment investigations were used. These design "rules-of-thunb" are summarized below.

1. Treatment over the 20% of the meridionally projected rotor chord from either the leading edge or the trailing edge is ineffective. Most, if not all, of the benefits come from treating the center 60% of the chord projection. (References 1-7).

2. The most successful treatments have 65-75% open area in the treated surfaces (References 2, 4). For circumferential grooves this means that the ratio of cavity width to land width should be greater than 2.0 (reference 8). Circumferential grooves with 50% open area (ratio of cavity width to land width equal 1.0) were much less effective than those with open area of 65% or more.

3. The most successful treatments have a cavity depth which is 3 or more times the cavity width (Reference 5).

4. The ratio of the cavity depth to the blade spacing should be greater than 0.15 (Reference 8).

5. Among the slotted treatment configurations, the work input is roughly proportional to the freedom of the flow to recirculate axially. The unbaffled axial-skewed slots allowed considerably greater freedom for recirculation and required considerably greater work input. (Reference 8)

Three different hub treatment spool configurations were designed using the "rules-of-thumb" discussed above and the blading geometry given in Table I. The first was a smooth spool (no treatment) configuration which would serve as a baseline. The second configuration consisted of circumferential grooves. The mechanical designer recommended that a minimum land width of 0.3175 cm (0.125 inches) be used. The cavity width and cavity depth were then determined by using this 0.3175 cm (0.125 inch) land width with design "rules-of-thumb" numbers 2 and 3 respectively. The resulting configuration, which is summarized in Table III and shown in Figures 7a and 8, consisted of six grooves, 0.6985 cm (0.275 inches) wide and 2.032 cm (0.80 inches) deep with 0.3175 cm (0.125 inch) lands between the grooves. The third configuration consisted of baffled wide blade angle slots. The design is based on maintaining the ratio of slot (cavity) width to maximum stator vane tip thickness equal to 1.85 which was the same as that used on the Casing Treatment Program (Reference 8). A land width of 0.3175 cm (0.125 inches) was chosen and the rest of the dimensions were scaled from the Casing Treatment Program geometry. Baffles were incorporated to prevent the flow from recirculating axially.

Table III. Circumferential Grooves (Centered Over Stator).

	Hub Treatment	Suggested Value	Casing Treatment *4
Axial Extent of Treatment	5.78 cm (2.275 in)		5.97 cm (2.35 in)
Axial Extent/Axial Projected Chord	0.728		0.706
Groove (Cavity) Width	0.699 cm (0.275 in)		0.889 cm (0.35 in)
*1 Land Width	0.318 cm (0.125 in)		0.381 cm (0.15 in)
Groove Depth	2.032 cm (0.80 in)		2.54 cm (1.0 in)
Number of Grooves	6		5
*2 Groove Depth/Groove Width	2.91	$\geq$ 3.0	2.86
*3 Groove Depth/Blade Spacing	0.437	> 0.15	0.286
*4 Groove Width/Land Width	2.2	$\geq$ 2.0	2.33
Open Area/Total Area	0.688		0.70

*1 Minimum width recommended by mechanical designer for LSRC testing
*2 Suggested value, NASA TM X-2459, January 1972, Ref. 5
*3 Suggested analytical value, NASA Contract NAS3-15707, Ref. 8
*4 Satisfactory results obtained in NASA Contract NAS3-15707, Ref. 8

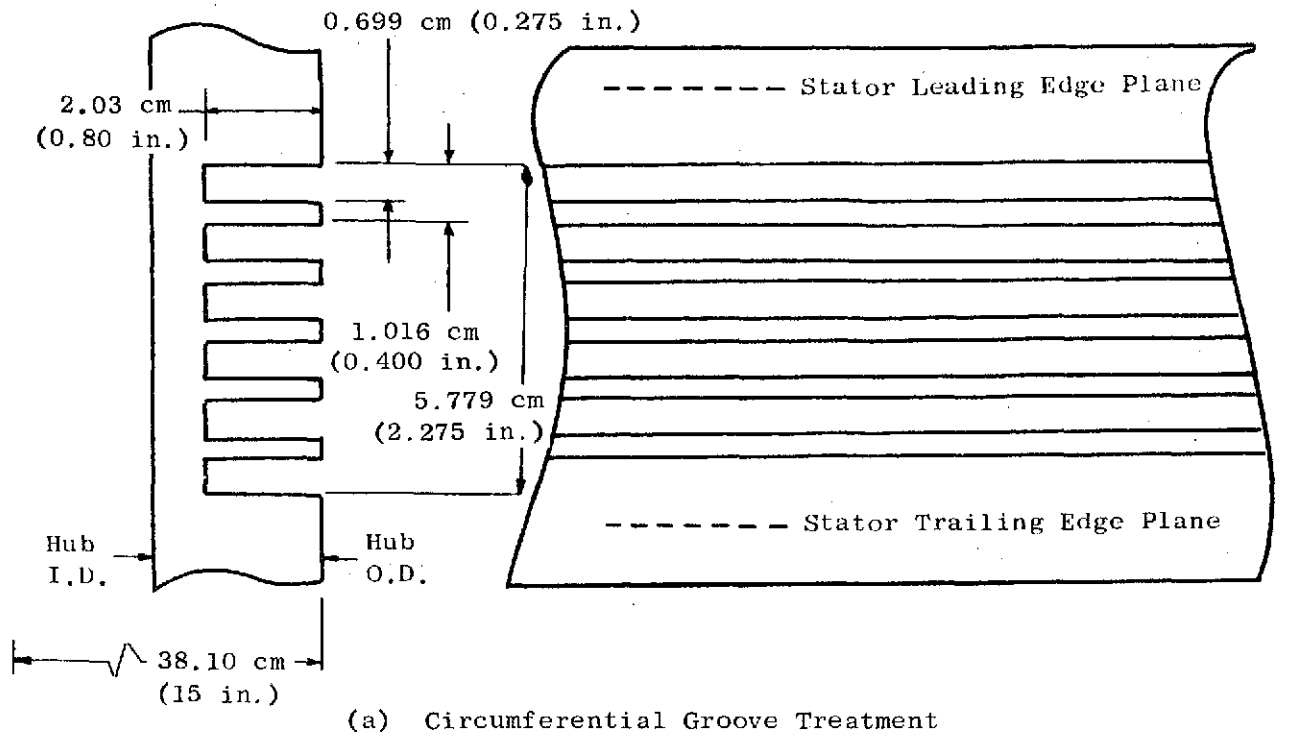

(a) Circumferential Groove Treatment

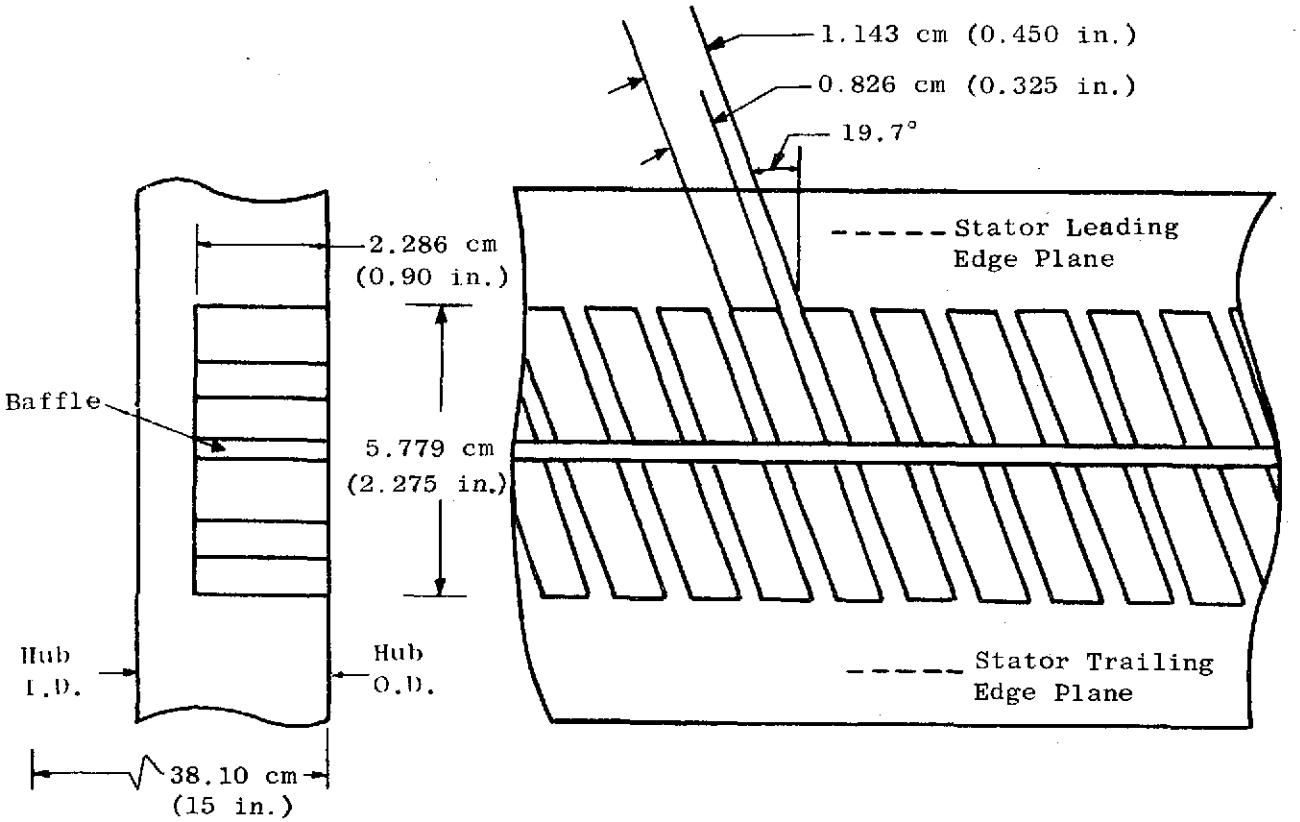

(b) Baffled Wide Blade Angle Slot Treatment

Figure 7. Stator Hub Treatment Configurations.

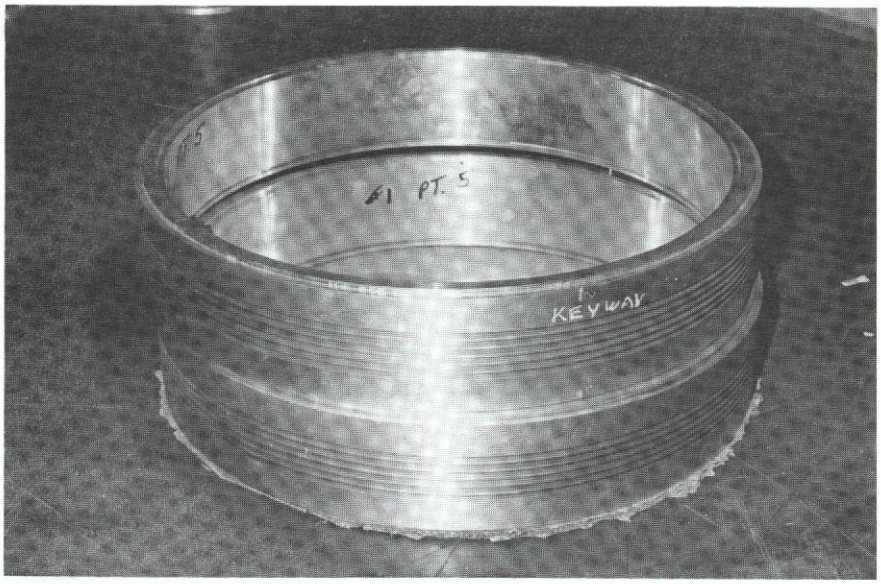

(a) Circumferential Groove Stator Hub Treatment Spools

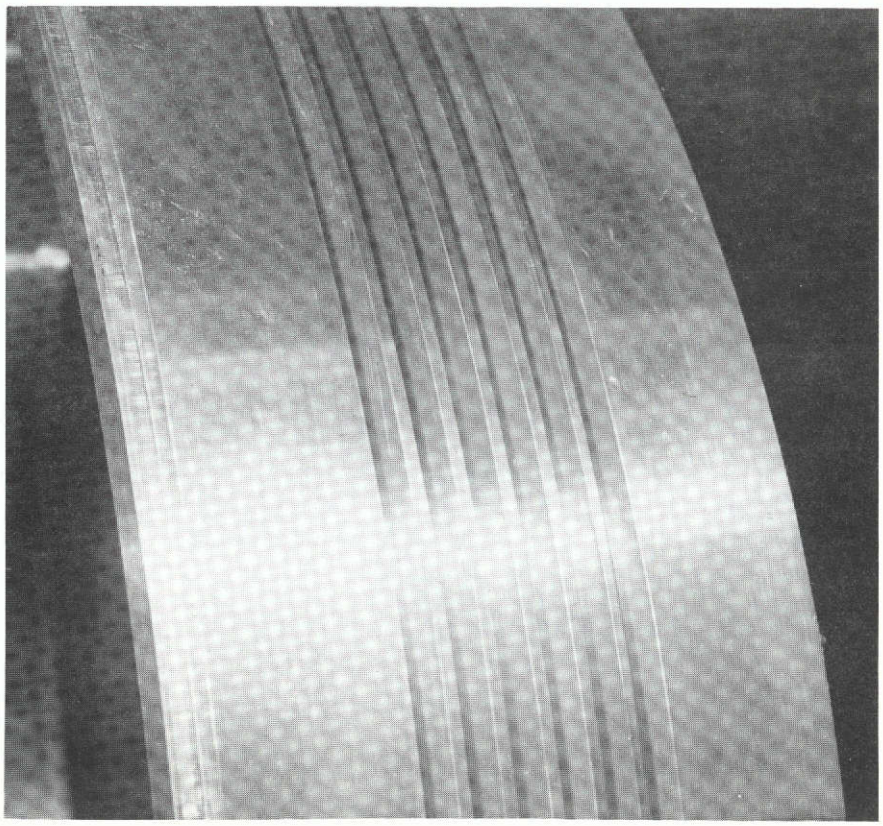

(b) Closeup of Circumferential Grooves

Figure 8. Photograph Showing Circumferential Groove Stator Hub Treatment Spools.

The resulting configuration, which is summarized in Table IV and shown in Figures 7b and 9, consisted of baffled wide blade angle slots 0.8255 cm (0.325 inches) wide and 2.286 cm (0.90 inches) deep with 0.3175 cm (0.125 inch) lands. The slots were inclined at an absolute angle of -19.7 degrees relative to axial direction. This angle was the average of the stagger angles of stage No. 1 and No. 2 stators. It can be seen from Table I that the axially projected chords for stages No. 1 and No. 2 of the hub treatment stators are not very different. For this reason and for ease of manufacture and cost considerations, the first and second stage hub treatment spools were identical.

Consideration was also given to an axial skewed slot configuration. The choice between that and the baffled wide blade angle slot configuration was almost a tossup since they both gave about the same stall margin improvement in the Casing Treatment Program (Reference 8). However, since the wide blade angle slots have a somewhat better efficiency and had not root bending stress problem, they were chosen for test in the Stator Hub Treatment Program.

Instrumentation

The instrumentation for the baseline test, the circumferential groove treatment tests and the wide blade angle slot treatment tests was identical and consisted of:

1) Knitting yarn tufts placed on flow surfaces of the rotors and stators (see Figure 6b), on the rotating hub surfaces and on traversible probes

2) Overall
Wet and dry bulb thermometer, barometer, electronic (digital readout) tachometer, strain gauge torquemeter

3) Flow measurement plane
Eleven casing static pressures-equally spaced - with provision for manifolding

4) Total Pressures
Twelve element total pressure rakes (5%, 10%, 20%, 30%, 40%, 50%, 60%, 70%, 80%, 90%, 95% span from casing) located at planes 1.0, 1.5, 2.0, 2.5, and 3.0

Traversible (radial direction) single-element total pressure probes, as needed

5) Static Pressures
Eleven casing static pressure tape, circumferentially equal spacing, with provision of manifolding, located at planes, 1.0, 1.5, 2.0, 2.5 and 3.0

Freestream traversible (radial direction) static pressure probes at planes 1.0, 1.5, 2.0, 2.5 and 3.0

Table IV. Wide Blade Angle Slots - Baffled (Centered Over Stator).

	Hub Treatment	Suggested Value	Casing Treatment *1
Axial Extent of Treatment	5.78 cm (2.275 in)		5.97 cm (2.35 in)
Axial Extent/Axial Projected Chord	0.728		0.706
Slot (Cavity) Width	0.826 cm (0.325 in)		0.953 cm (0.375 in)
Land Width	0.318 cm (0.125 in)		0.368 cm (0.145 in)
Slot Depth	2.286 cm (0.90 in)		2.54 cm (1.0 in)
*1 Slot Width/Max. Blade Thickness	1.87	>1.5	1.82
Slot Depth/Slot Width	2.77		2.66
Slot Width/Land Width	2.60		2.59
Slot Depth/Blade Spacing	0.492		0.286
*1 Open Area/Total Area	0.722	.6 - .7	0.721
Slot Angle (relative to tip section stagger angle)	0°		+10°
Slot Angle (relative to axial direction)	-19.7°		

*1 Satisfactory results obtained in NASA Contract NAS3-15707, Ref. 8

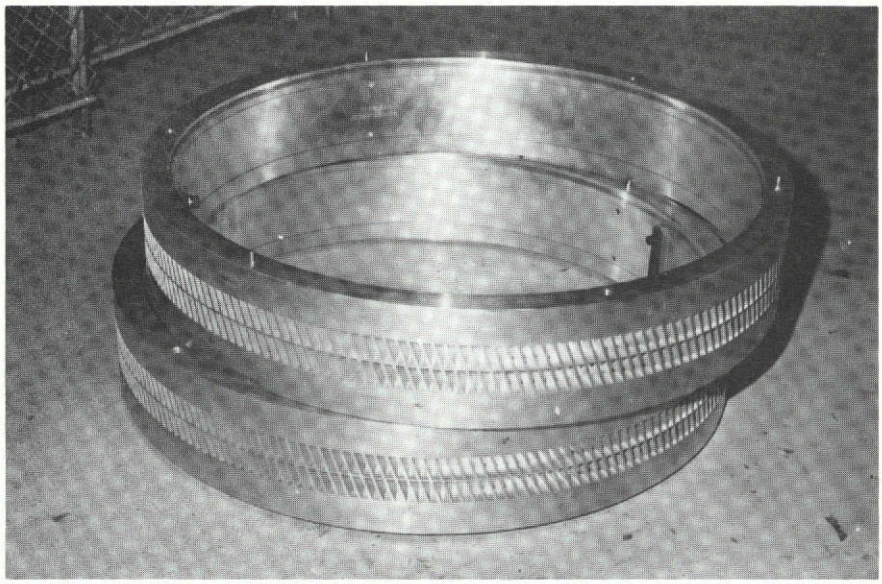

(a) Baffled Wide Blade Angle Slot Stator Hub Treatment Spools

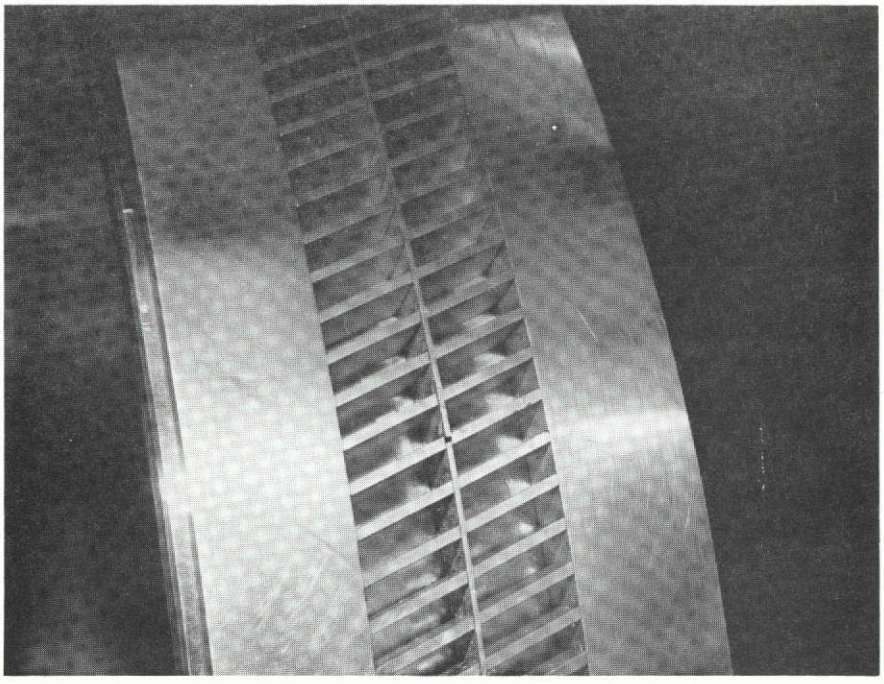

(b) Closeup of Baffled Wide Blade Angle Slots

Figure 9. Photograph Showing Baffled Wide Blade Angle Slot Treatment Spools.

6) Flow Angle
Traversible tufted probe

Automatic angle measuring instrumentation (wedge probe type) as shown in Figure 10 located at planes 1.0, 1.5, 2.0, 2.5 and 3.0,

7) Velocity, Boundary Layer Survey, Rotor Wake Survey
Radially traversible single-element hot film anemometers with both perpendicular and parallel wires were located at planes 1.0, 1.5, 2.0, 2.5 and 3.0.

Test Procedures

Four types of data were taken during the testing phase of the program: Probing Data, Preview Data, Standard Data, and Detailed Traverse Data. A discussion of each of these types of data is presented below. Vehicle schematics are shown in Figures 1 and 3 to aid in describing the measurement planes. The location of the instrumentation was discussed previously in the section entitled Instrumentation.

Probing Data

The Probing Data testing procedure is designed to map separation zones, to determine stall inception location, and to determine extent and frequency of rotating stall cells. These data are obtained by using knitting yarn tufts viewed in both steady and stroboscopic light. Detailed visual probing records are maintained.

Preview Data

The Preview Data testing procedure is designed to obtain a preliminary flow characteristic showing compressor performance based on either casing and/or hub static pressure rise. Efficiency, work coefficient and static pressure coefficient are determined as a function of bellmouth flow coefficient. Preview data for the Stator Hub Treatment Program consisted of the following: (1) determination of the stalling throttle setting from probing data, from audible rotating stall cells and from a sudden decrease in the static pressure rise across the compressor as recorded on an inclined manometer; (2) measurement of hub static pressure (95% immersion) and manifolded casing static pressure at planes 1.0, 2.0 and 3.0 for one circumferential stator position at each throttle setting being tested; (3) measurement of bellmouth static pressures; and, (4) measurement of torque, ambient barometric pressure, dry and wet bulb temperature and rotative speed.

Standard Data

The Standard Data testing procedure is designed to obtain precise flow characteristics showing compressor performance based on mass average total pressure rise. Efficiency, work coefficient, and total pressure coefficient are determined as a function of bellmouth flow coefficient. Standard data

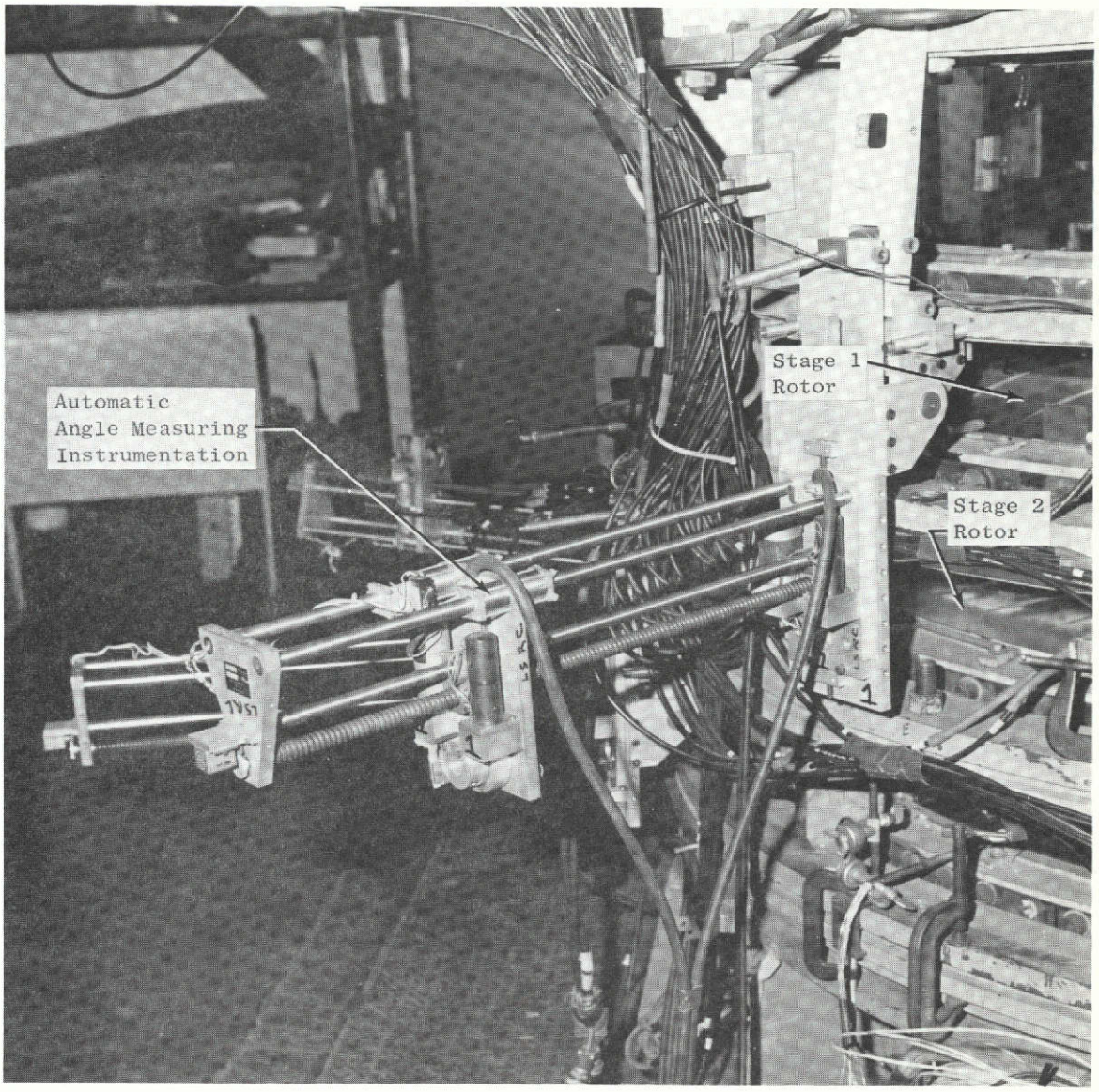

Figure 10. Photograph Showing Instrumentation for Automatic Determination of Flow Angle.

for each of the throttle settings tested in the Stator Hub Treatment Program consisted of the following: (1) measurement of the radial variation of total pressure at planes 1.0 and 3.0 for ten circumferential stator positions; (2) measurement of hub static pressures at planes 1.0, 1.5, 2.0, 2.5 and 3.0 for ten circumferential stator positions; (3) measurement of the radial variation of total pressure at planes 1.5, 2.0 and 2.5 for one nominal circumferential stator position; (4) measurement of bellmouth static pressures; and, (5) measurement of bellmouth static pressures; and, (5) measurement of torque, ambient barometric pressure, dry and wet bulb temperature and rotative speed.

Detailed Traverse Data

The Detailed Traverse Data testing procedure is designed to obtain blade row performance by measuring the radial and circumferential (across one blade pitch) variation of static pressure, total pressure and flow angle. Detailed Traverse Data for each of the throttle settings tested in the Stator Hub Treatment Program consisted of the following: (1) division of the flowfield across a blade pitch into a grid of radial-circumferential measuring stations as shown in Figure 11 where the minimum number of measuring stations is indicated by the solid symbols; (2) measurement of total pressure, static pressure and absolute flow angle at planes 1.0, 1.5, 2.0, 2.5 and 3.0 for each of the measurement stations discussed above; and, (3) measurement of ambient barometric pressure, dry and wet bulb temperature and rotative speed.

Normal rotative speed was chosen to maintain 12.7 cm H_2O (5 inches H_2O) as the value for the normalization parameter $1/2\ \rho\ U_t^2$, based on measurements of the inlet temperature and barometric pressure for the day. The speed was set for the nearest integral rpm, and data were recorded only when speed was within one rpm. For a nominal tip speed of 45.7 m/sec (150 ft/sec) this represents a precision of $\pm 0.2\%$. Holding $1/2\ \rho\ U_t^2$ constant simplified the normalization procedure and allowed rapid comparison of raw data. The Reynolds number varied $\pm 2\%$ by this procedure, which is considered to be insignificant for Reynolds number effects.

A standard series of throttle settings was chosen for convenience in making comparisons between treatment configurations. Three of these throttle settings, the near stall, peak efficiency and wide open settings, were of primary importance. The "near-stall" throttle setting is the most clearly defined and represents the setting at which the compressor operation is stable but just on the verge of rotating stall. The "peak efficiency" setting is self explanatory. The "wide open" throttle setting is the setting at which the highest flow was achieved. Other throttle settings were then selected in order to complete the performance characteristic. Throughout the experimental program and this report, the term stall is used to indicate rotating stall with pulsating pressures, rotating stall cells, etc.

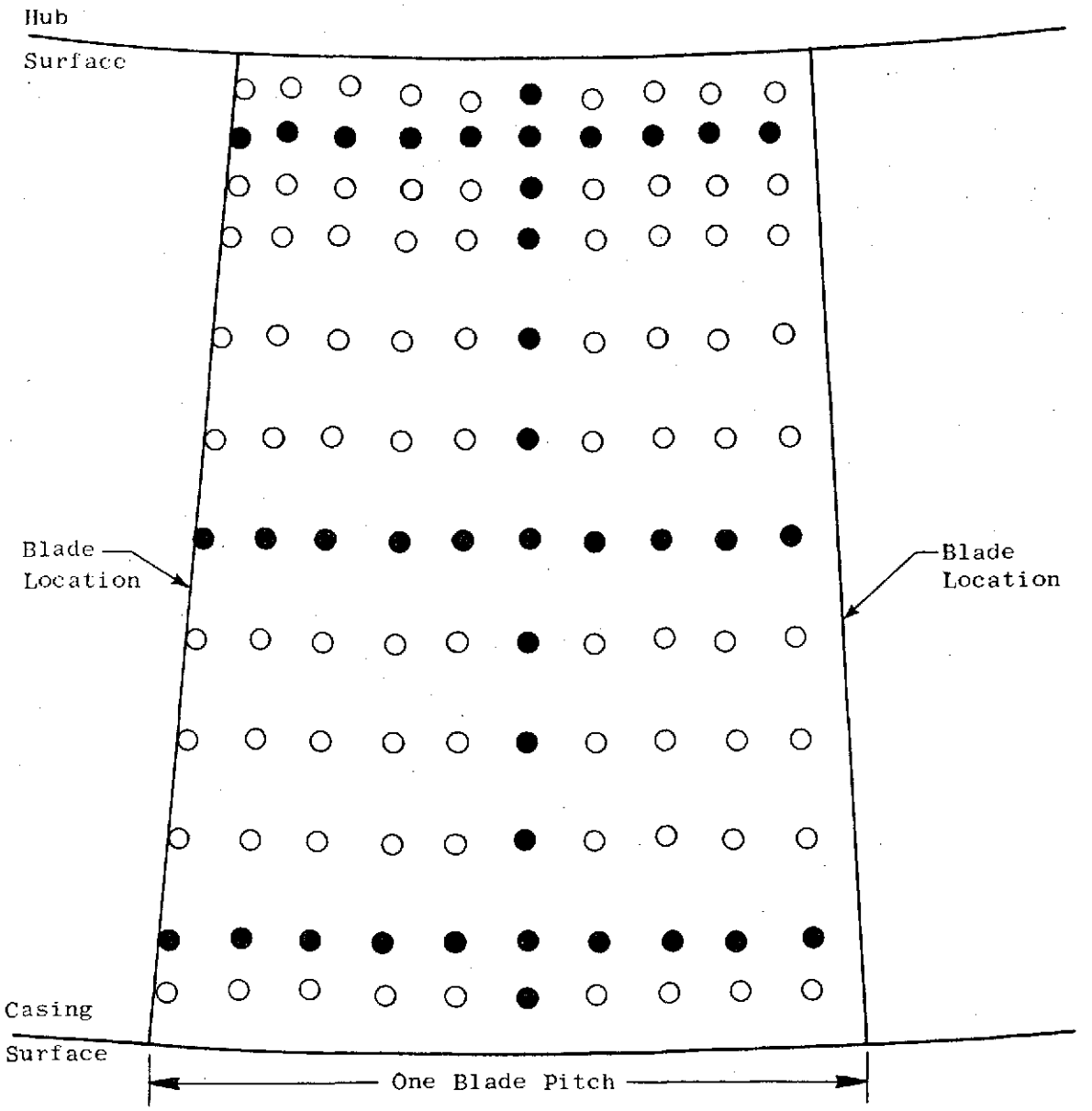

Figure 11. Schematic Showing Relative Measuring Locations at Which Detailed Traverse Data were Obtained.

EXPERIMENTAL RESULTS

The experimental program was designed to investigate the potential benefits of applying hub treatment to those compressors and fans which are stator hub critical. Three different Low Speed Research Compressor (LSRC) configurations were tested. The first, Configuration No. 1, consisted of the 0.5 radius ratio compressor with the interchangeable spools as described in the section entitled Test Compressor. The smooth spool (baseline), the circumferential groove treatment spool and the baffled wide blade angle slot treatment spool were tested using Configuration No. 1. Configuration No. 2 was the same as Configuration No. 1 except that the blades and vanes were restaggered in order to load the stators relative to the rotors. The smooth spool (baseline) and the baffled wide blade angle slot treatment spool were tested in this restaggered configuration. Configuration No. 3 was obtained by returning the blades and vanes to their original stagger and removing one-half of the stators in each stage. The smooth spool (baseline) and the baffled wide blade angle slot treatment spool were then tested in Configuration No. 3. The LSRC test configurations are summarized below:

LSRC Configuration	Buildup	Treatment Spools Tested
No. 1	Two-stage, unshrouded stators, 0.5 radius ratio	Smooth, circumferential grooves, baffled wide blade angle slots
No. 2	Restagger	Smooth, baffled wide blade angle slots
No. 3	Reduced solidity, original stagger	Smooth, baffled wide blade angle slots

Configuration No. 1

Smooth Spool Baseline Performance

The baseline performance of the compressor was demonstrated by using smooth spools under the stator tips. Probing Data, Preview Data, Standard Data and Detailed Traverse Data were obtained for various throttle number setings from wide open to near stall. The correlation of throttle number setting with flow coefficient, ϕ, is shown in Figure 12. This throttle curve will be useful in interpreting the throttle number settings discussed in the report.

Schematic representations of the tuft probing measurements are presented in Figure 13. The data in Figure 13a show that the flow was smooth and steady at all axial, radial and circumferential positions from wide open throttle setting 422 (ϕ = 0.472) to throttle setting 240 (ϕ = 0.437). As the compressor was throttled further toward stall, the tufts near the hub on stator 1 and on rotors 1 and 2 began to show evidence of unsteady flow.

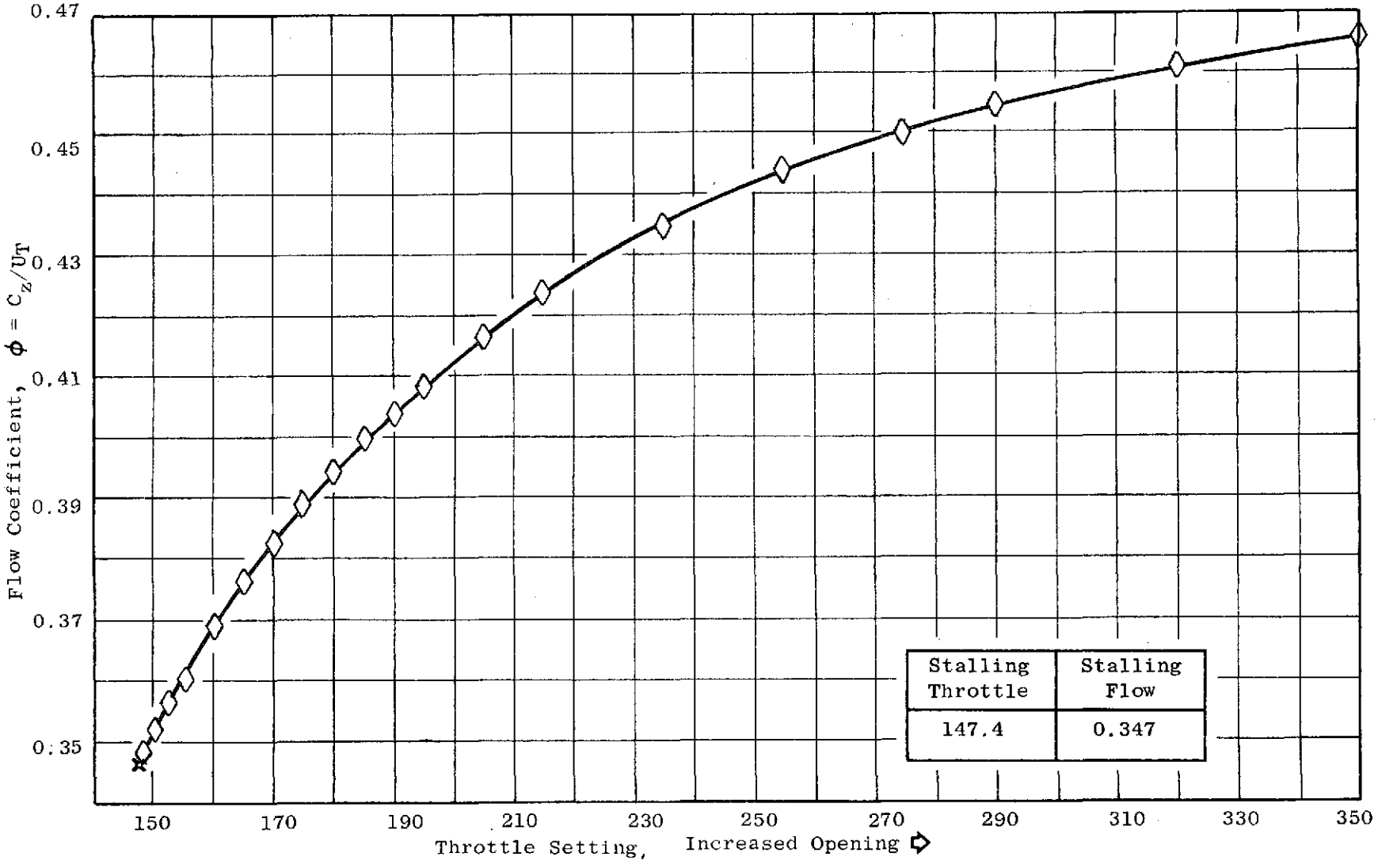

Figure 12. Flow Coefficient Versus Throttle Setting, Smooth Spool (Baseline) Configuration No. 1.

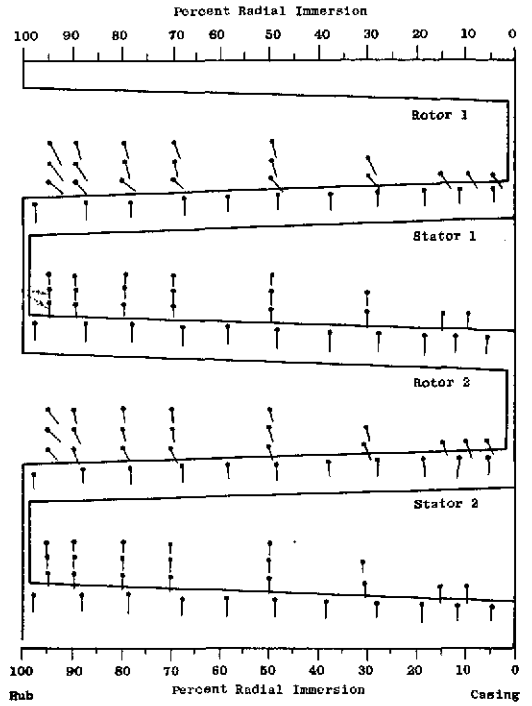

(a) ϕ = 0.437, Throttle 240

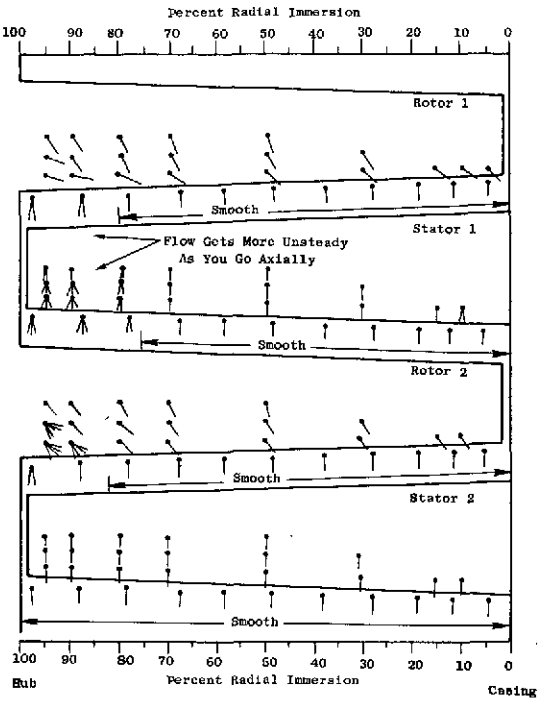

(b) ϕ = 0.394, Throttle 180

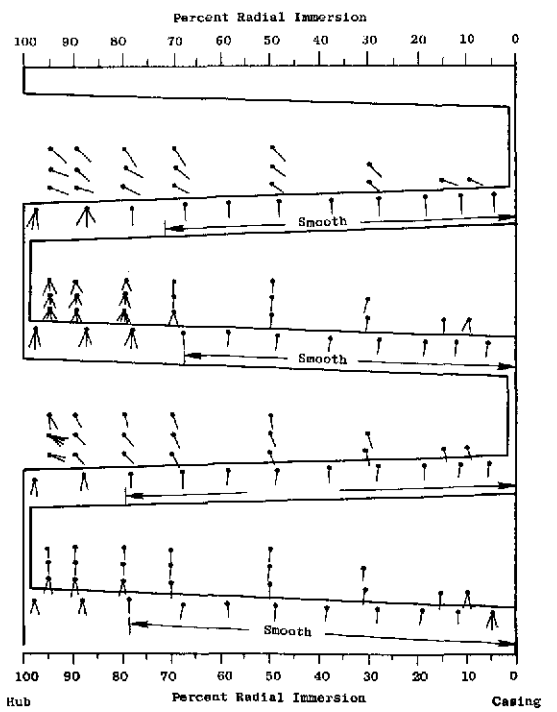

(c) ϕ = 0.369, Throttle 160

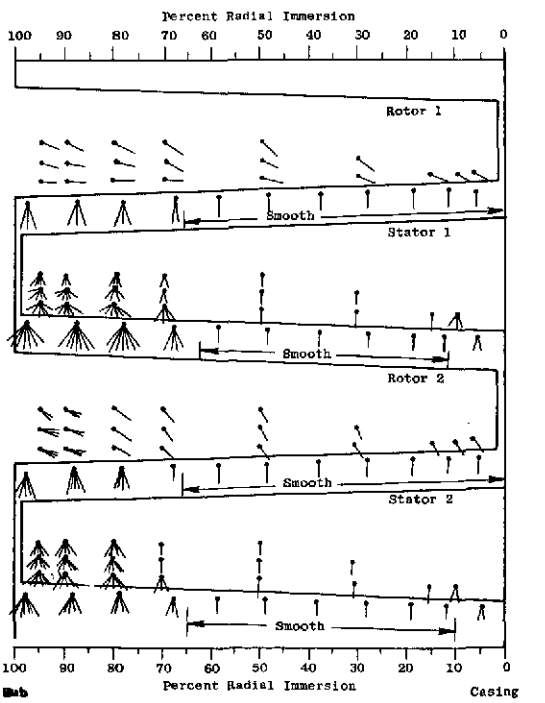

(d) ϕ = 0.347, Throttle 147.5

Figure 13. Schematic Representation of the Tuft Probing Measurements for Various Flow Coefficients, Smooth Spool Baseline Configuration No. 1, U_t = 45.7 m/sec (150 ft/sec).

This region of rough flow progressed radially, extending from 100 percent to 80 percent immersion at throttle setting 180 (ϕ = 0.394) as shown schematically in Figure 13b. At this throttle setting the tufts near the trailing edge of rotor 1 pointed almost radially outward, indicating flow separation and the dominance of centrifugal force on the tuft. Tufts mounted on the rotor 1 hub near the trailing edge showed a random motion, flipping at all angles through 360°, indicating very unsteady flow and separation. The tufts on stator No. 1 showed that unsteady flow is present to about 80 percent immersion. This unsteady motion extended circumferentially across the pitch. The tufts on rotor No. 2 indicated unsteady motion near the hub trailing edge. The flow over stator No. 2 was smooth. The hub continued to deteriorate as the compressor was throttled below 180 toward stall. At about throttle setting 160 (ϕ = 0.369) stator No. 2 showed the first evidence of unsteady flow near the hub, Figure 13c. At throttle setting 147.5 (ϕ = 0.347, two-tenths count out of stall), the entire hub region from 70 percent to 100 percent immersion was very unsteady and separated. The violent tuft motion near the hub is shown schematically in Figure 13d. Closing the throttle to 147.3 produced full span rotating stall. These data indicate that Configuration No. 1 showed evidence of being hub critical and therefore was a good candidate for demonstrating the potential benefits of stator hub treatment.

Preliminary performance of the Smooth Spool (Baseline) Configuration No. 1 is presented in Figure 14. This performance is shown as average stage casing static pressure coefficient, average stage hub static pressure coefficient, average stage work coefficient and torque efficiency all plotted as functions of flow coefficient. The term "average stage" is used here to indicate that the overall performance parameters, based on the compressor inlet-to-discharge conditions, are divided by the number of stages to get an average value. The torque efficiency is based on casing static pressure and is defined as pressure coefficient divided by work coefficient. It can be seen that the casing static pressure coefficient continued to increase with little rollover until stall was reached (ϕ = 0.347), while the hub static pressure coefficient peaked at a flow coefficient of 0.353 and then dropped slightly as the compressor was throttled to stall. Peak efficiency was reached at a flow coefficient of 0.37. These data served as a baseline for comparison of the circumferential groove and the baffled wide blade angle slot performance data. The additional data obtained for the baseline tests will be presented in the following sections.

Performance Comparisons (Smooth Spool, Circumferential Groove Treatment, Baffled Wide Blade Angle Slot Treatment)

The smooth spools under the stator hubs were replaced with the circumferential groove treatment spools and with the baffled wide blade angle slot treatment spools. Comparisons of the data obtained using these spools are presented in this section.

Stalling throttle settings and stalling flow coefficients for the various spools tested are shown below:

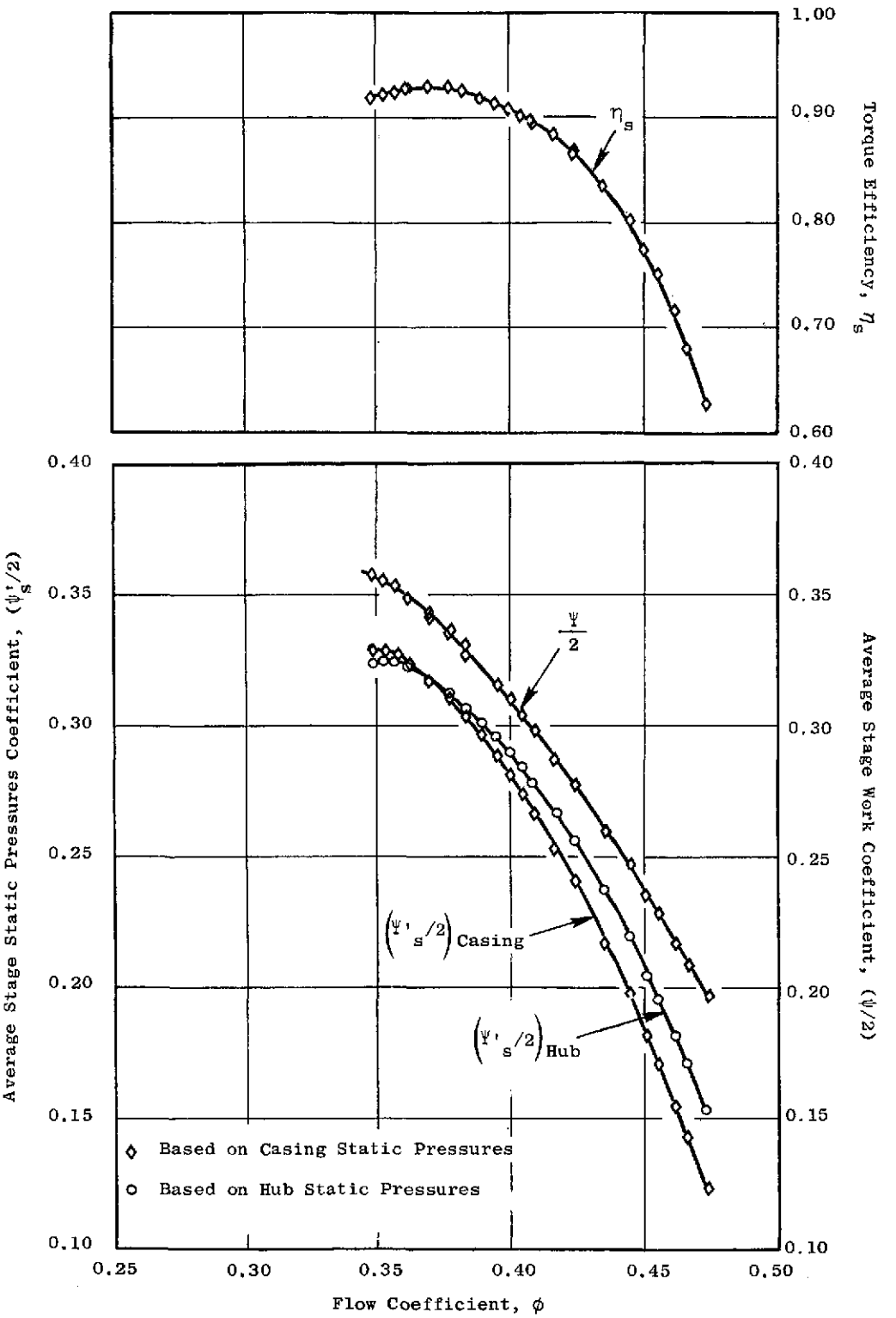

Figure 14. Overall Performance of the Smooth Spool (Baseline) Configuration No. 1, Based on Preview Data, U_t = 45.7 m/sec (150 ft/sec).

Configuration	Stalling Throttle Settings	Stalling Flow Coefficient
Smooth Spool (Baseline)	147.4	0.347
Circumferential Groove	149.1	0.350
Baffled Wide Blade Angle Slots	147.4	0.347

There is clearly no appreciable difference in stalling throttle settings or stalling flow coefficient between the baseline, the circumferential groove treatment and the baffled wide blade angle slot. In addition, the Probing Data obtained for the various treatment spools were quantitatively the same as that presented in Figure 13. There were no observed differences in the onset of the unsteady flow or in the extent and severity of the unsteadiness.

An overall performance comparison, based on casing and hub static pressure measurements (Preview Data), is presented in Figures 15 and 16 for the baseline and treatment configurations. The average stage hub static pressure coefficient shown in Figure 15 is replotted in Figure 16 for clarity, particularly near stall. There were very small differences in the pressure coefficients between the treated and untreated configurations, but these differences are almost within the experimental resolution of the Preview Data. A more accurate evaluation of any performance difference can be obtained by comparing the Standard Data shown in Figure 17. The Standard Data are based on total pressure radial surveys at the inlet and discharge of the compressor. These data clearly show negligible difference in pressure coefficient, work coefficient or torque efficiency between the treated and the untreated configurations. In addition, a comparison of the circumferential and radial variation of normalized total pressure, Figures 18 and 19 respectively, shows negligible differences between the treated and untreated configurations. There were no data taken for the Circumferential Groove Treatment Configuration No. 1 at throttle setting 422.

Measured absolute air angles for the smooth spool (baseline) are presented in Figure 20. Symbols do not appear on the figure to avoid clutter of the stator exit plane data and because of the averaging process used to obtain the curves. This averaging process can be described by referring to Figure 11. A radial survey of the absolute air angle was made at mid-pitch (indicated by the radial row of black dots in Figure 11). This determined the general shape of the radial variation. To fix the magnitude more accurately a circumferential average of flow angle was obtained at 10, 50 and 90 percent radial immersions, as indicated by the three circumferential rows of black dots. The curve giving the general shape of the radial variation was then shifted until it passed through the values indicated by the circumferential average. For the absolute air angles obtained in this manner, there was negligible difference between the treated and the untreated spools.

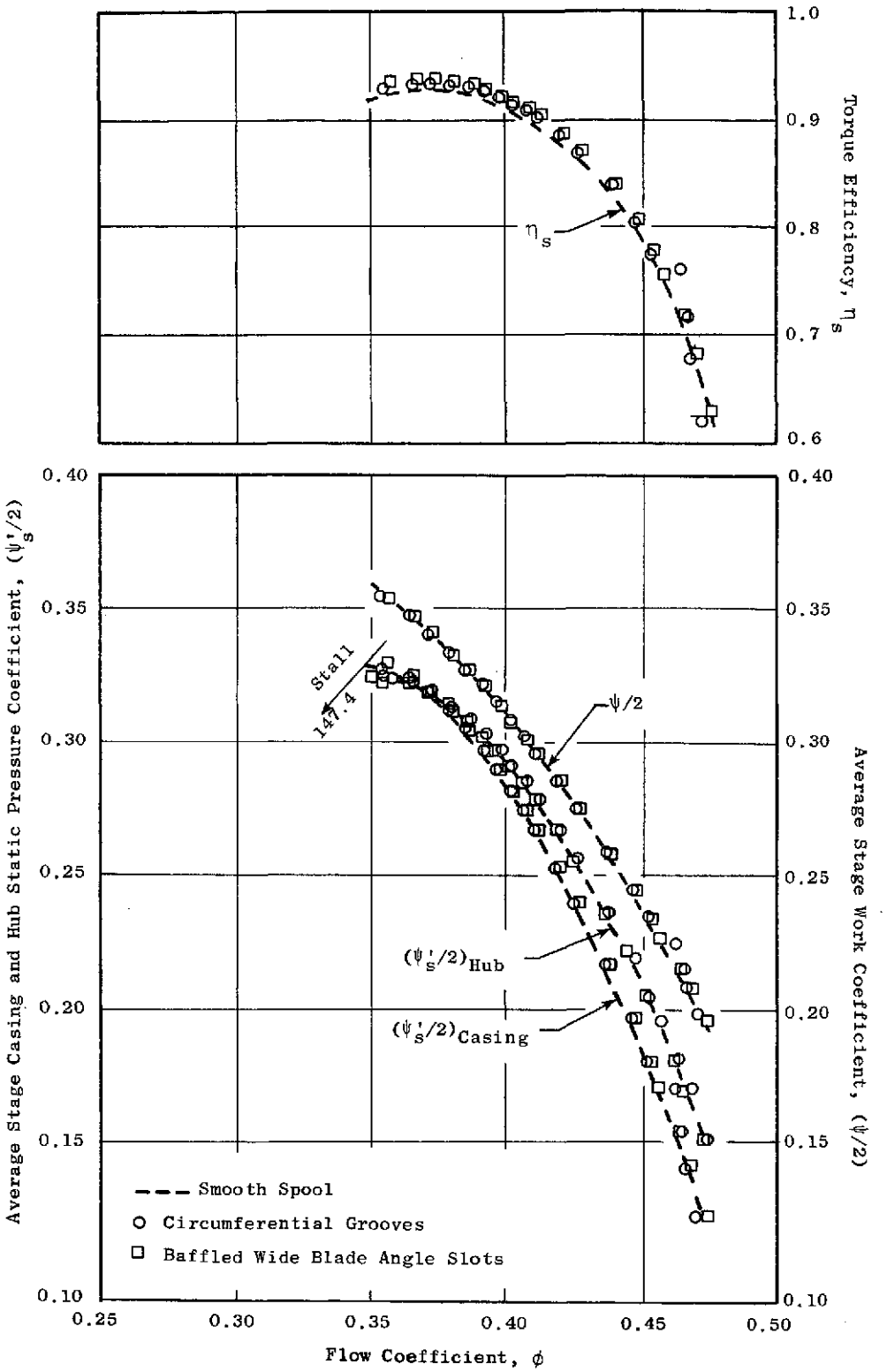

Figure 15. Overall Performance Comparison of Smooth Spool, Circumferential Groove and Baffled Wide Blade Angle Slot Treatment Configuration No. 1, Based on Preview Data, U_t = 45.7 m/sec (150 ft/sec).

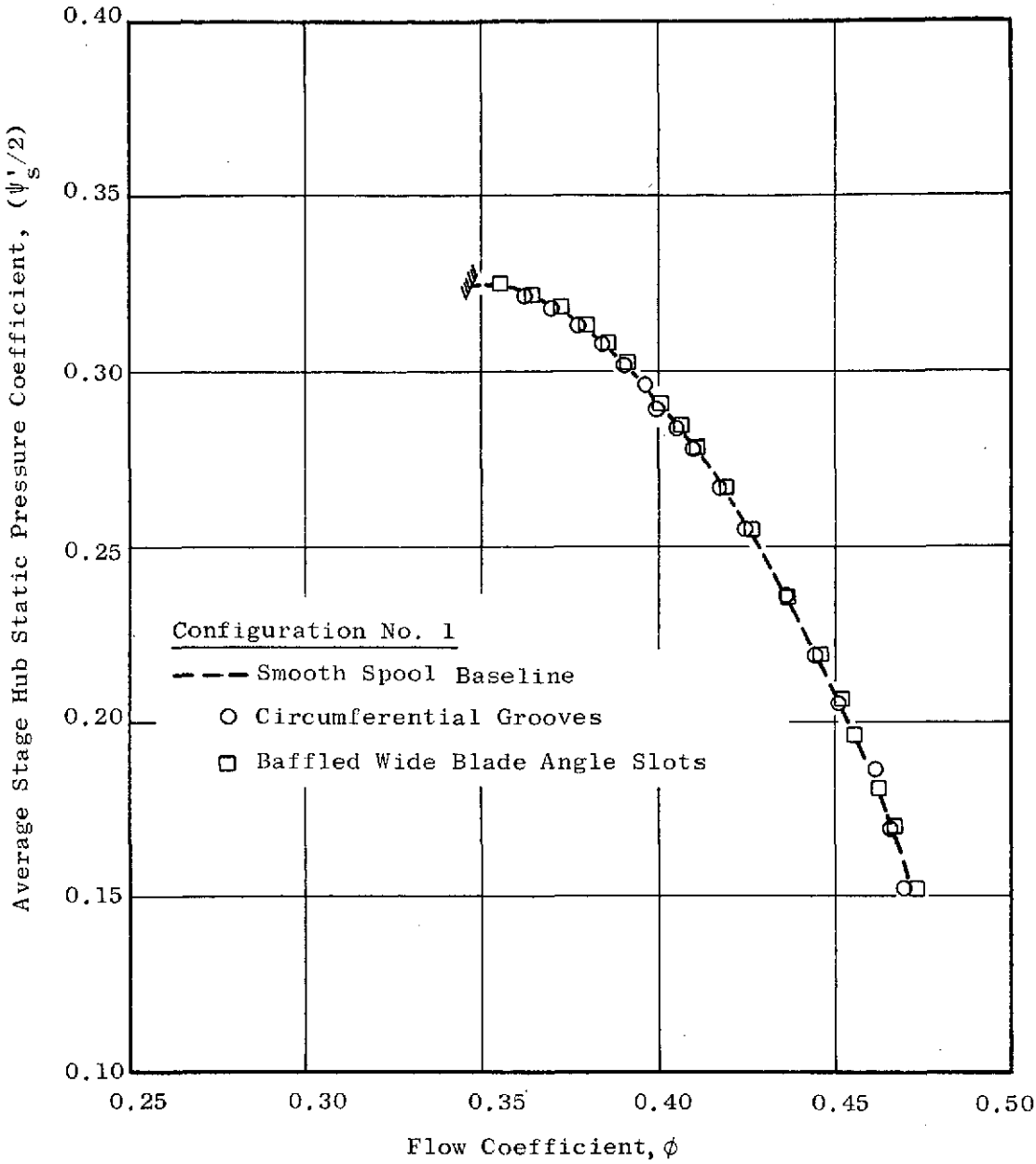

Figure 16. Overall Hub Performance Comparison of the Smooth Spool Baseline, Circumferential Groove and Baffled Wide Blade Angle Slot Treatment Configurations No. 1, Based on Preview Data, U_t = 45.7 m/sec (150 ft/sec).

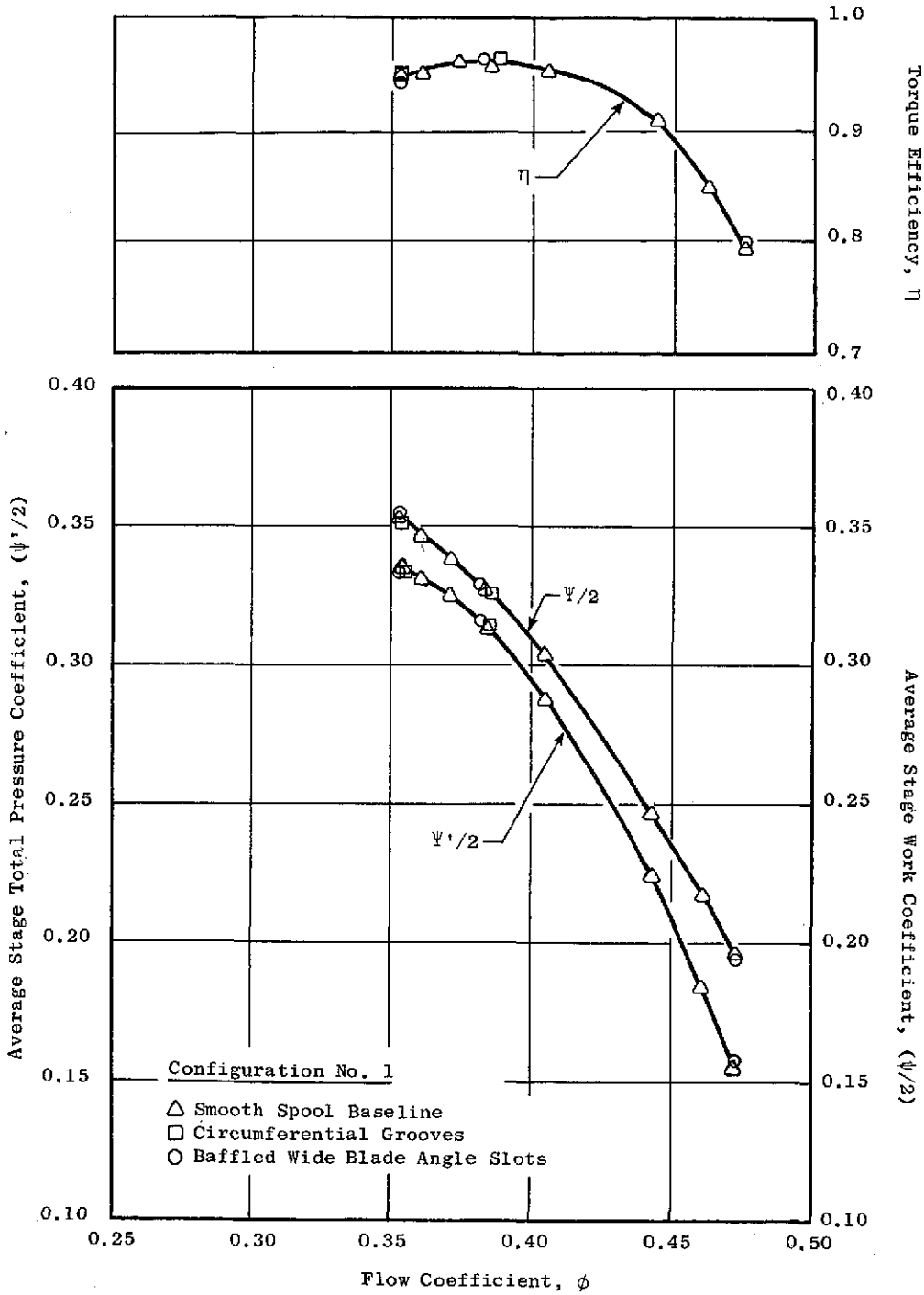

Figure 17. Performance Comparison of Smooth Spool Baseline, Circumferential Groove and Baffled Wide Blade Angle Slot Treatment Configurations No. 1, Based on Standard Data, U_t = 45.7 m/sec (150 ft/sec).

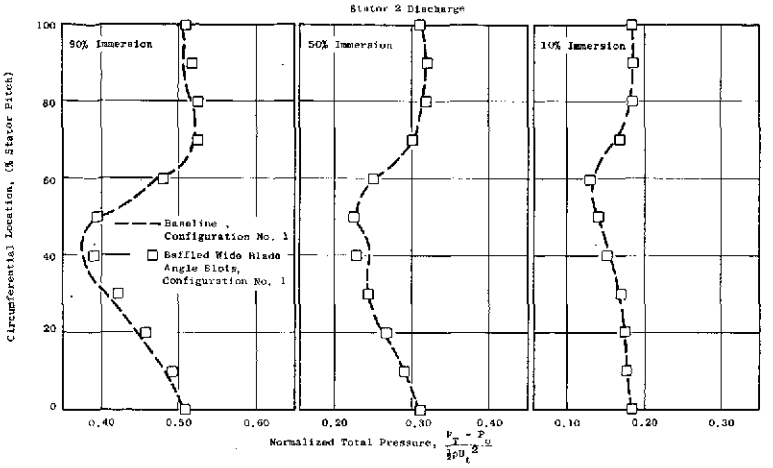

(a) ϕ = 0.472, Throttle 422

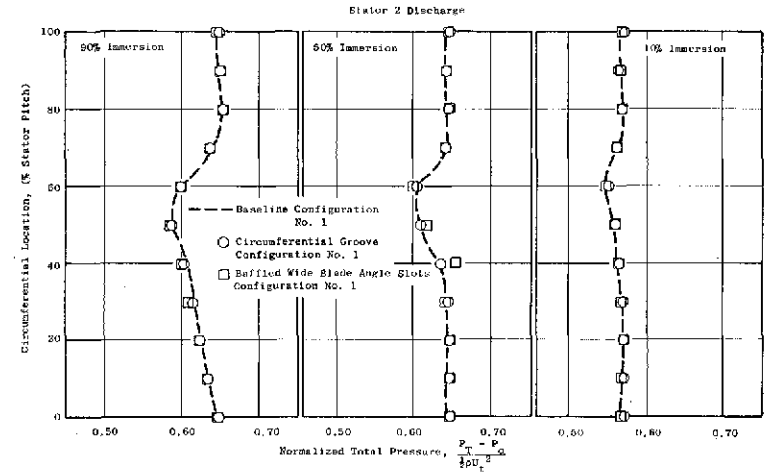

(b) ϕ = 0.383, Throttle 170

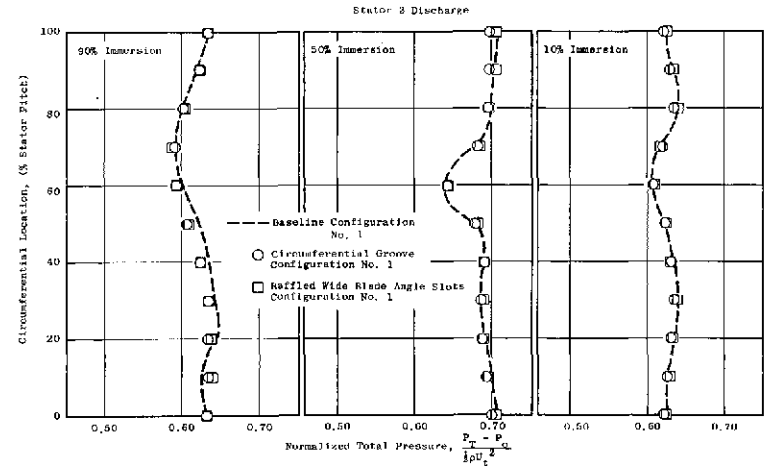

(c) ϕ = 0.352, Throttle 150

Figure 18. Comparison of the Circumferential Variation Across the Blade Pitch of Normalized Total Pressure for the Smooth Spool Baseline, Circumferential Groove and Baffled Wide Angle Slot Treatment Configurations No. 1, U_t = 45.7 m/sec (150 ft/sec).

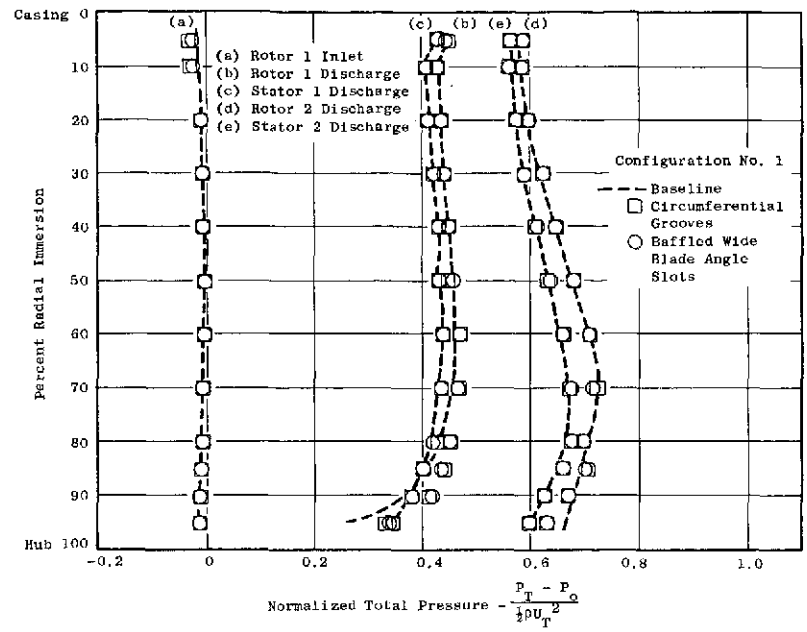

(a) ϕ = 0.383, Throttle 170

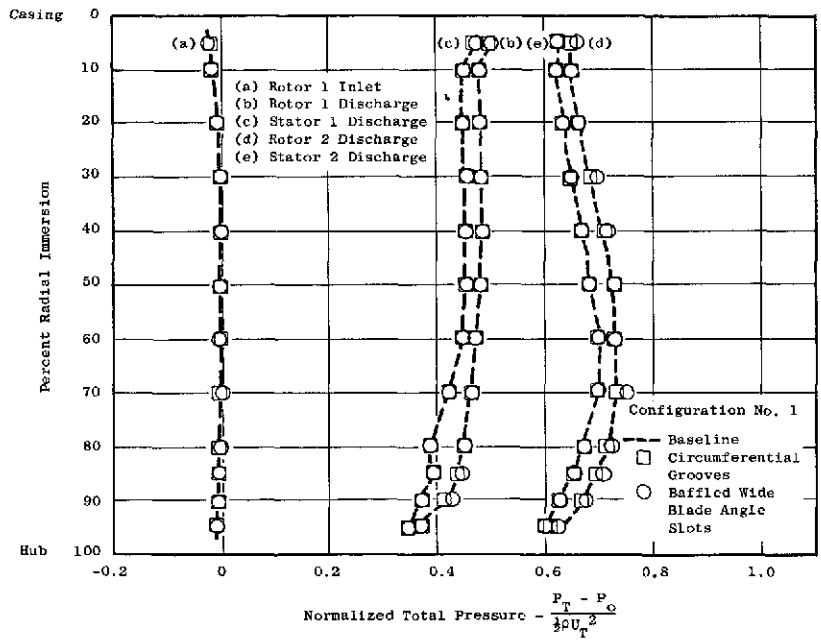

(b) ϕ = 0.353, Throttle 150

Figure 19. Comparison of the Radial Variation of Normalized Total Pressure for the Smooth Spool Baseline, Circumferential Groove and Baffled Wide Blade Angle Slot Treatment Configurations No. 1, U_t = 45.7 m/sec (150 ft/sec).

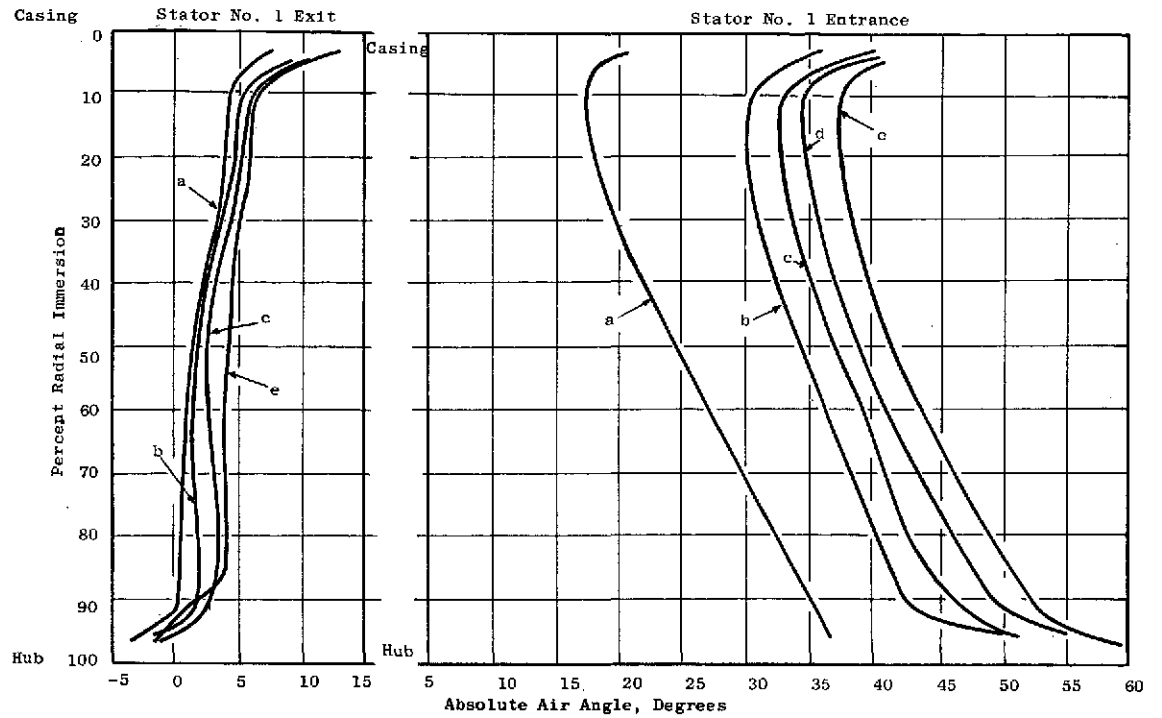

(a). First Stage Stator Entrance and Exit Absolute Air Angles.

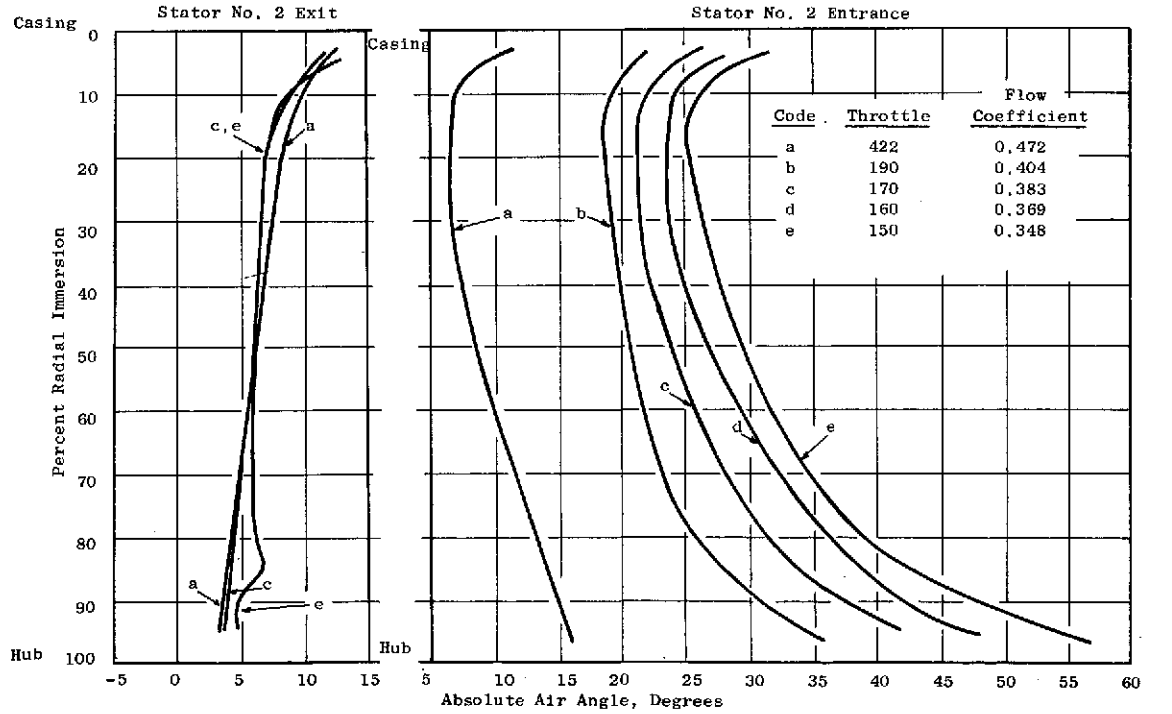

(b). Second Stage Stator Entrance and Exit Absolute Air Angles.

Figure 20. Measured Absolute Air Angles Versus Percent Immersion for Various Flow Coefficients, Baseline Configuration No. 1, U_t = 45.7 m/sec (150 ft/sec).

In order to detect any radial shifts in flow caused by the treatment, the compressor annulus was divided into twelve concentric rings and the local flow coefficient in each ring was determined as shown in Figure 21. The local flow coefficient for the smooth spool (baseline) is nearly constant radially at the compressor inlet, although a slight decrease is observed near the casing. As the compressor is throttled, the general shape of the radial distribution is preserved as the level of local flow coefficient decreases. At the compressor discharge a large radial shift in local flow coefficient is observed for the smooth spool (baseline). For the wide open throttle setting, the local flow coefficient in the hub region is nearly 75 percent larger than the value near the casing, suggesting a strong hub. As the compressor is throttled toward stall, there is a rapid decrease in local flow coefficient near the hub. This is evidence of the increased hub blockage near stall. However as before, the treated and the untreated spool configurations gave the same results, although there is an unexplained discrepancy between the treated and untreated test results near the casing for the wide open throttle setting in Figure 21a. This discrepancy is not apparent at the discharge in Figure 21b.

Performance comparisons for each stage of the compressor, presented in Figure 22, were made to determine whether the treatment changed the relative stage loading. Although it is clear from the magnitude of the pressure rise that the first stage was more highly loaded than the second, it is equally clear that the treatment had no measurable influence on the relative performance.

Based on the information presented above, it is concluded that, for Configuration No. 1, hub treatment was not effective in improving compressor stall margin or in modifying the compressor performance in any discernible fashion.

Half-Speed Performance Comparisons

The influence of Reynolds number on the performance of the compressor was investigated by conducting tests at one-half the full rotative speed. The results for the Smooth Spool (Baseline) Configuration No. 1, presented in Figure 23, show that Reynolds number effects are insignificant. At the start of the program, it was planned that half-speed performance testing would be conducted with the treated as well as the untreated spools. However, in view of the disappointing results obtained with hub treatment at full-speed and in view of the fact that the half-speed and full-speed results were identical for the baseline configuration, it was decided that no further half-speed testing would be conducted. Instead, modifications to the compressor were undertaken in order to find a configuration which was more suitable for investigating hub treatment influences. These modifications will be discussed later in the report.

Rotor Wake Measurements and Boundary Layer Surveys

In the Casing Treatment Study (Reference 8), the rotor blade wakes and casing wall boundary layers were modified by the presence of casing treatment.

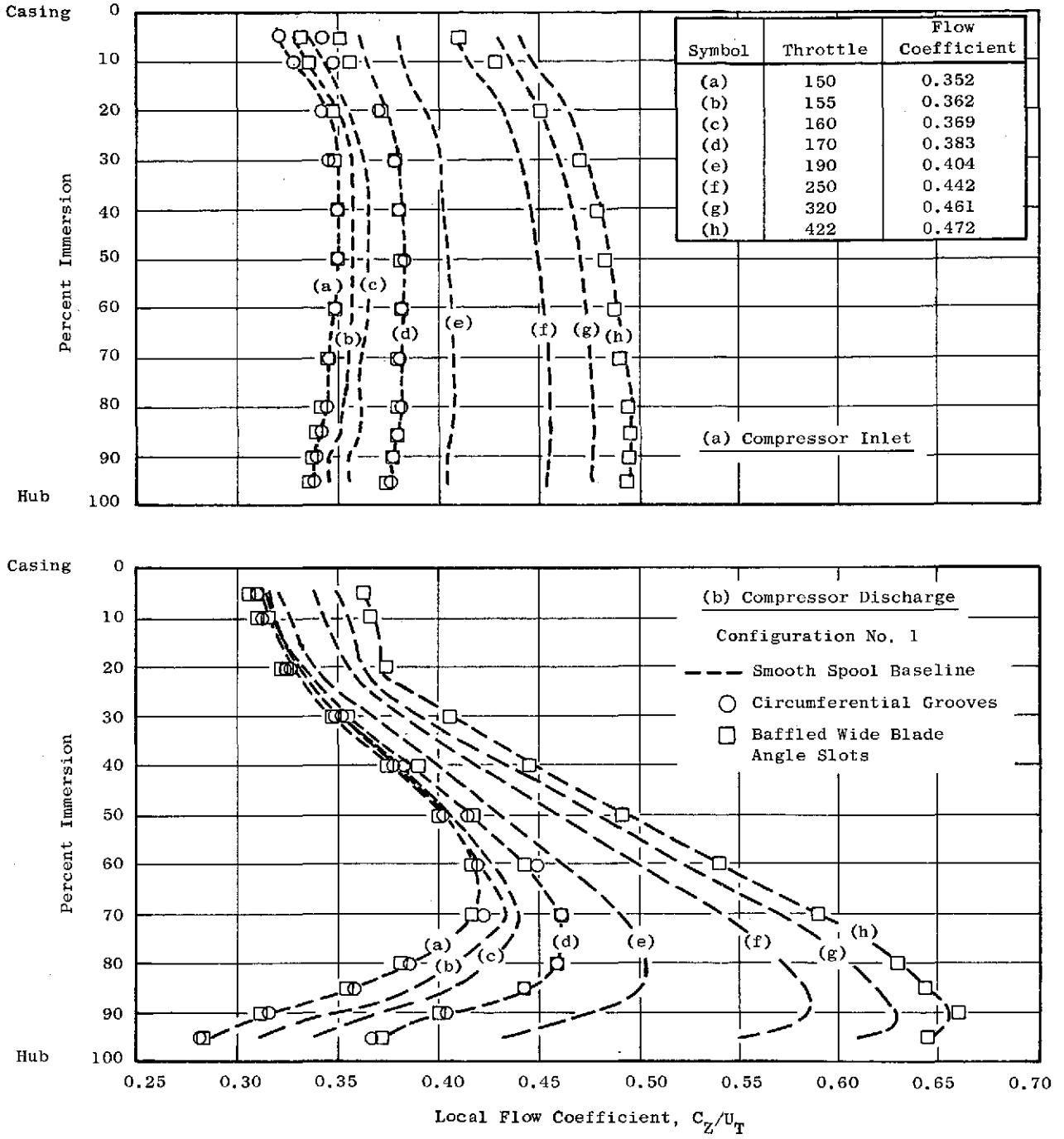

Figure 21. Comparison of the Radial Variation of Local Flow Coefficient for the Smooth Spool Baseline, Circumferential Groove and Baffled Wide Blade Angle Slot Treatment Configurations No. 1, U_t = 45.7 m/sec (150 ft/sec).

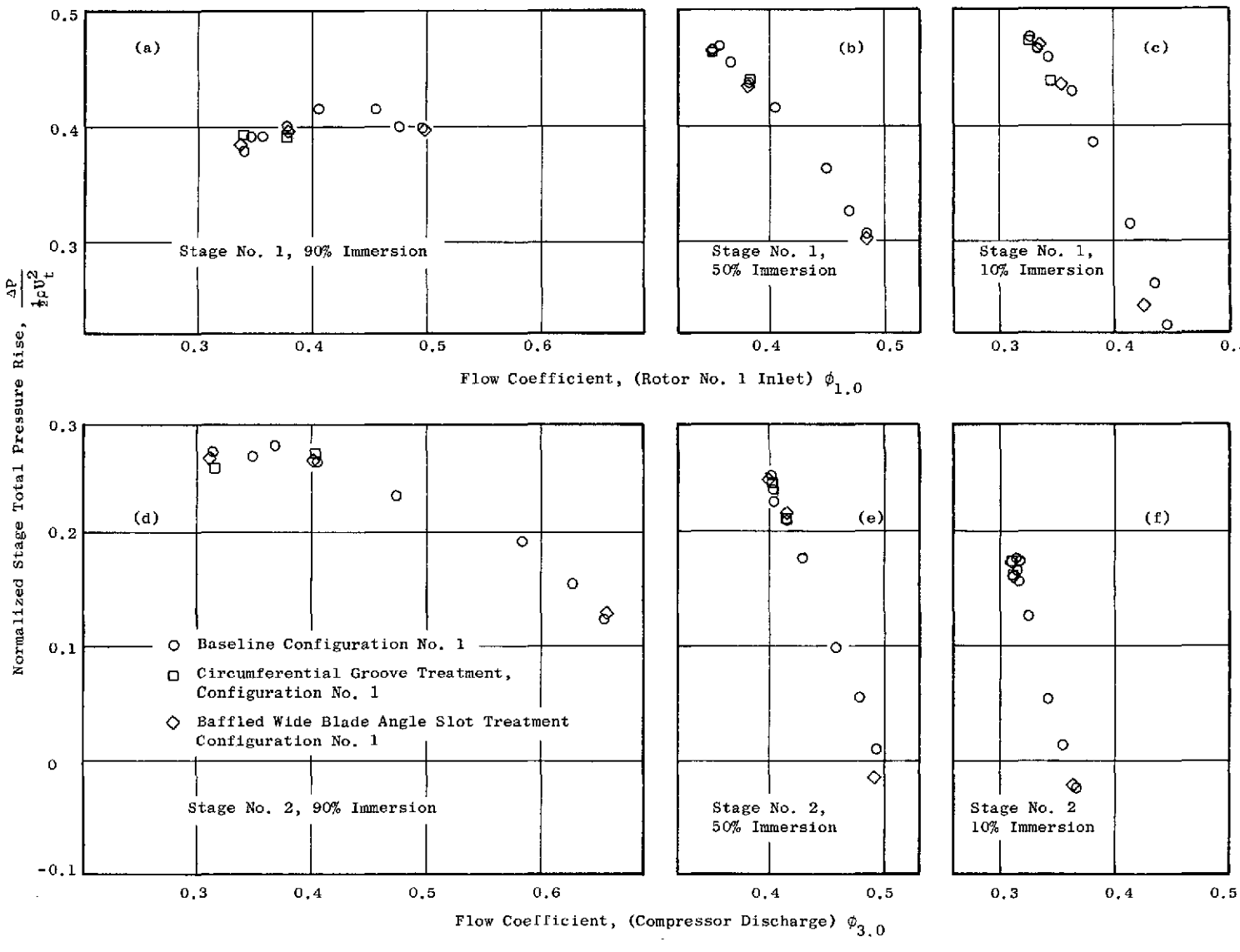

Figure 22. Stage Performance Comparison for the Baseline, Circumferential Groove and the Baffled Wide Blade Angle Slot Treatment Configurations No. 1, U_t = 45.7 m/sec (150 ft/sec).

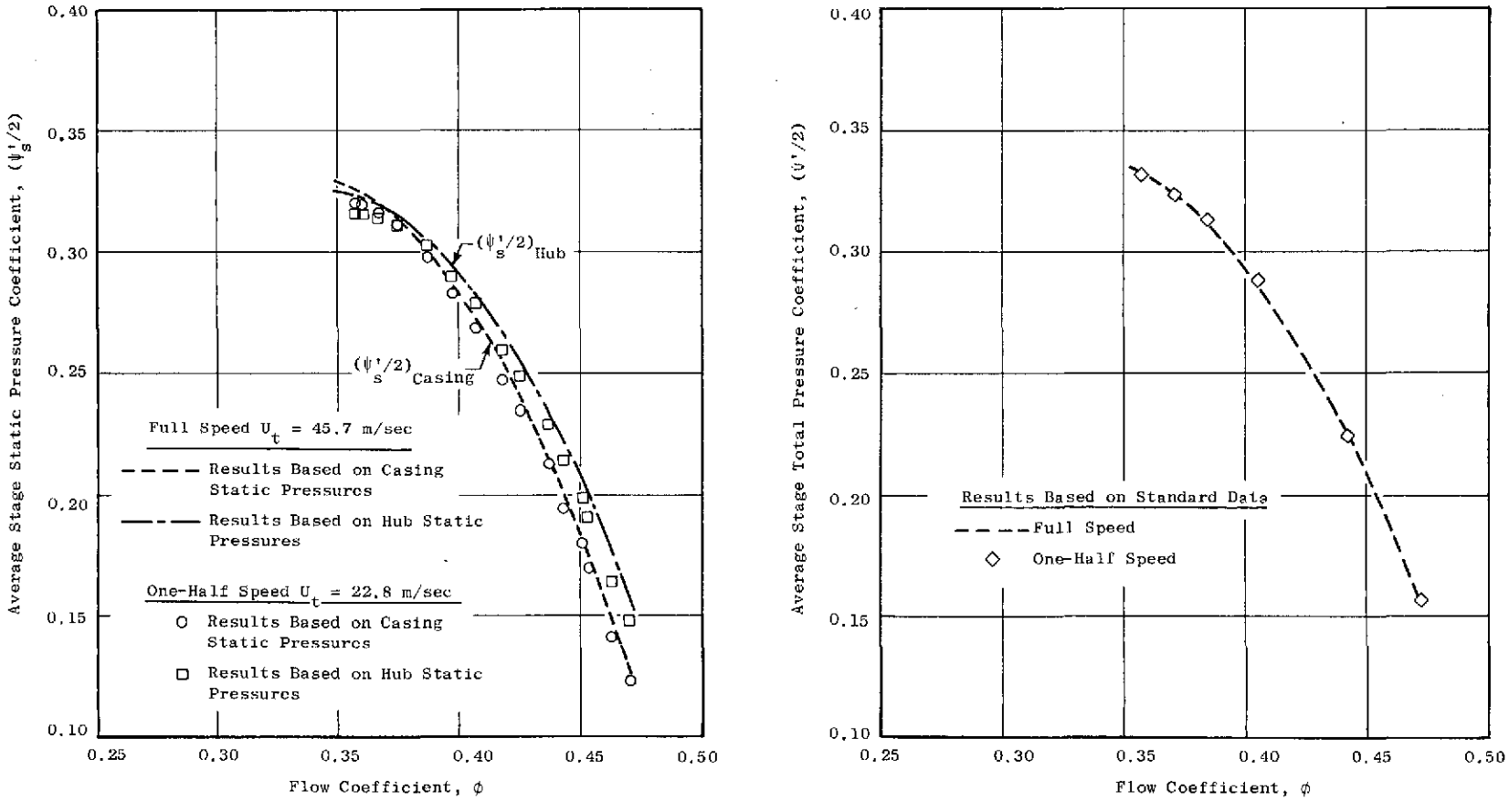

(a) Results Based on Preview Data

(b) Results Based on Standard Data

Figure 23. Comparison of the Full-Speed and Half-Speed Performance for the Baseline Configurations No. 1.

At the start of the Hub Treatment Program, it was anticipated that similar modifications might result with hub treatment. Therefore, rotor blade wake surveys and boundary layer surveys were obtained for the Baseline Configuration No. 1 using hot film anemometers. These results are presented for record in Figures 24-27. The wake surveys show a thickening of the rotor wakes as one traverses radially from the casing to the hub (Figures 24 and 25). The thickening of the rotor one hub wake as the flow is reduced from the wide open throttle setting to the near stall throttle setting is not too pronounced (Figure 26). In fact the variation from wake-to-wake is greater than the variation with flow. The hub wall boundary layer profiles presented in Figure 27 show a thickening of the boundary layer at the rotor No. 1 inlet plane as stall is approached (compare Figures 27a, f, k). Also the boundary layers at the stator exit planes are considerably thicker than those at the rotor exit planes. This is due to the fact that the rotors are re-energizing the flow.

It was originally planned to take rotor wake measurements and boundary layer surveys using the treatment spools; however, due to the cost and time considerations involved in the above-mentioned modifications, no further rotor wake measurements and boundary layer surveys were taken.

Blade and Vane Element Data

Vector diagram analyses were carried out using the experimental data in order to obtain blade and vane element characteristics and to develop a "model" compressor. Primary input to the vector diagram analysis, in addition to the stage geometry, consisted of static pressures measured on the casings before and after blade rows, and the total pressure profiles obtained before and after the rotors and after the last stator. The absolute air angle profiles before and after the rotor were also used as measures of the tangential momentum change and work input. The results are presented in Figures 28-31 as incidence angle, deviation angle, diffusion factor and the loading parameter, $\Delta P/Q$, plotted as functions of the flow coefficient. The increase in incidence angle and loading as the compressor was throttled toward stall is clearly seen in these figures. Also, the hub region was quite a bit more heavily loaded than the tip region as can be seen by comparing the diffusion factors and the loading parameter, $\Delta P/Q$. This loading parameter is defined as the loss in relative total pressure across the blade (absolute total pressure for the vane) divided by the relative dynamic pressure of the flow entering the blade (absolute dynamic pressure for the vane).

Configuration No. 2 (Restagger)

Based on the information presented in the previous section, it was concluded that, for Configuration No. 1, hub treatment was not effective in improving compressor stall margin or in modifying compressor performance. In view of this, a redirection of the program was considered necessary and those steps which would make the stators the limiting item in the compressor were evaluated. Two approaches were considered. The first approach was to change the blade and vane stagger angle to load the stators while keeping the rotor

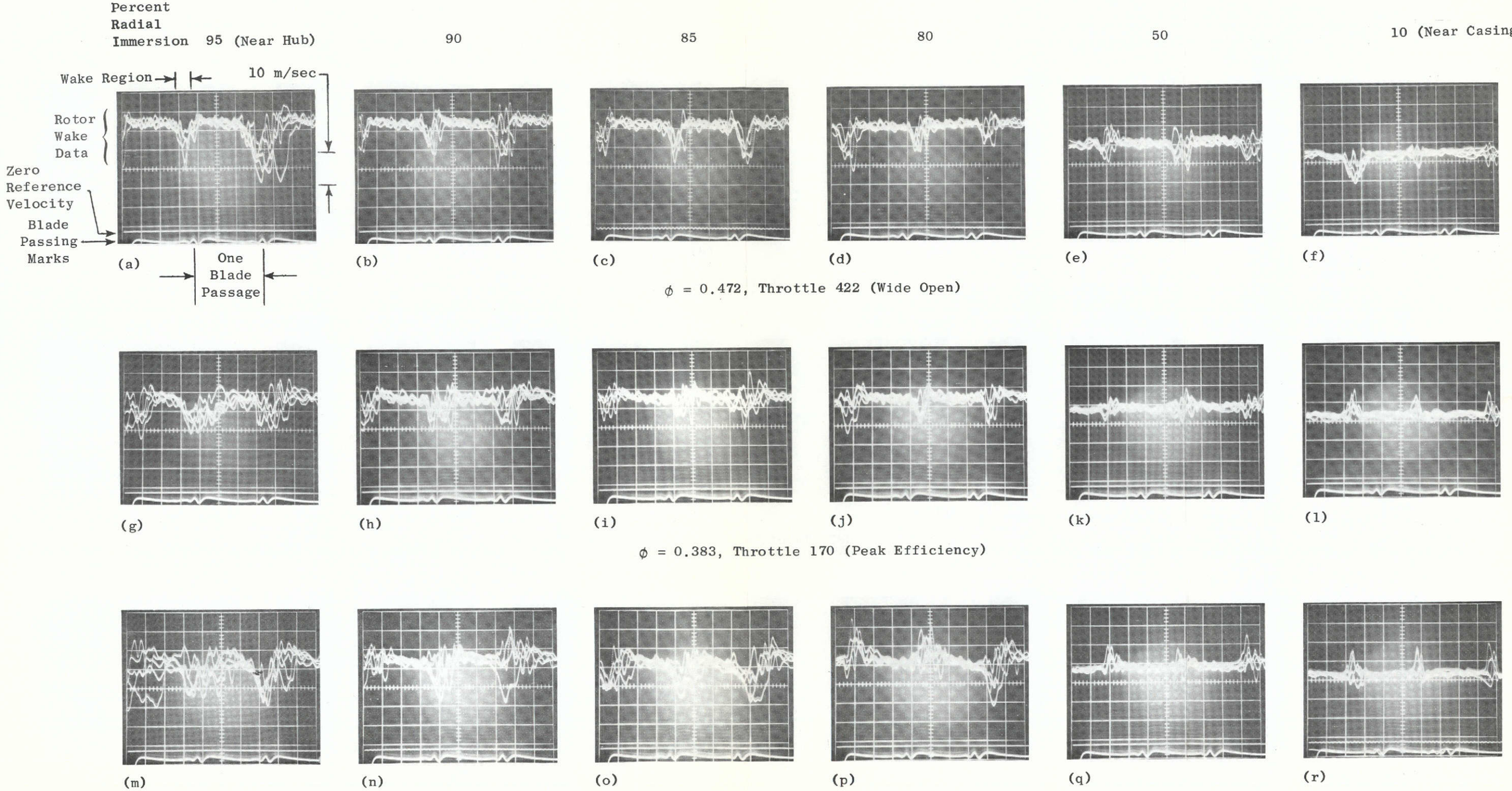

Figure 24. Typical Oscillograms Showing the Output of a Single Parallel Element Hot Film Anemometer Located at Rotor One Exit Plane, Smooth Spool Baseline Configuration No. 1, U_t = 45.7 m/sec (150 ft/sec).

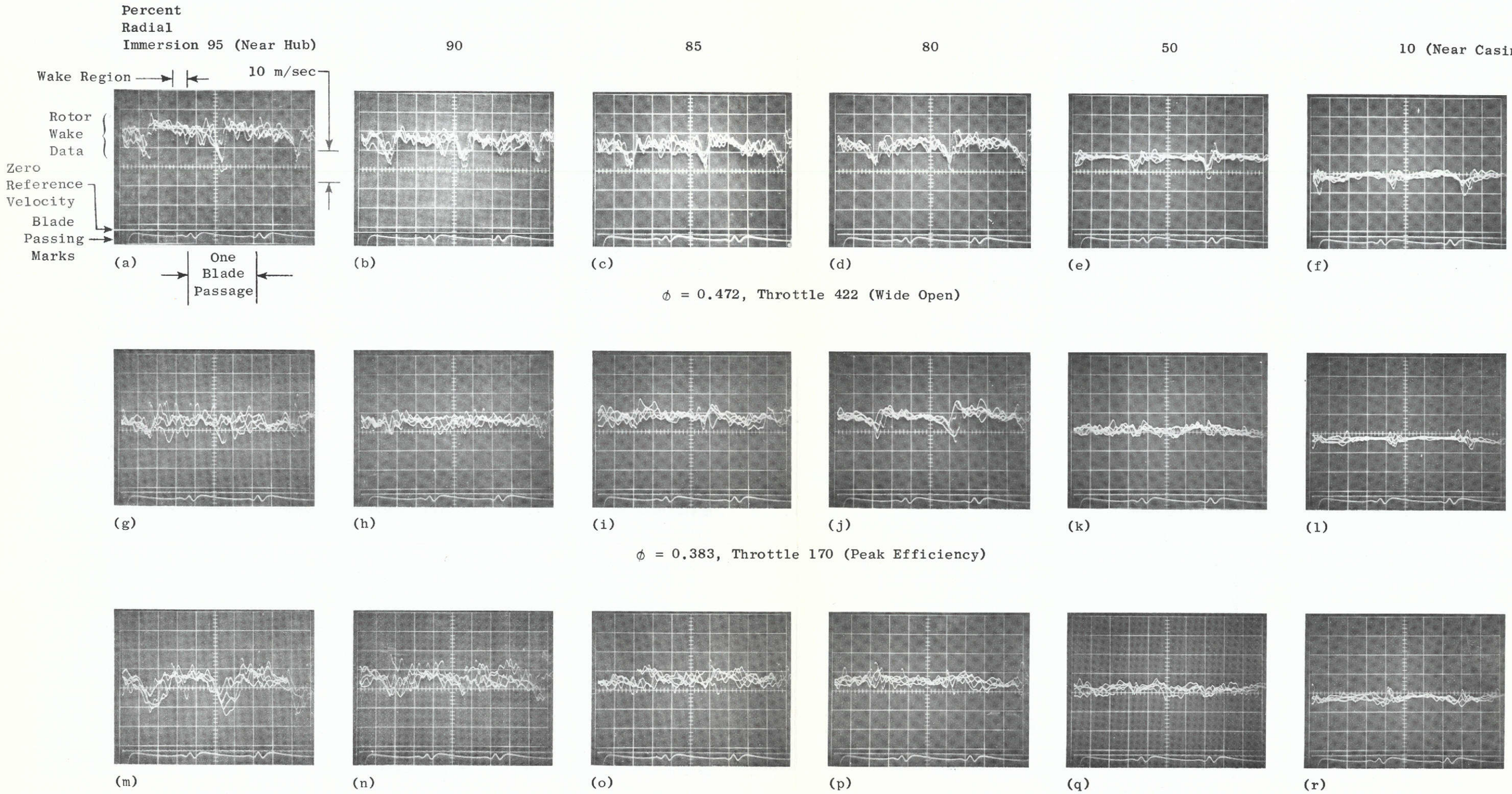

Figure 25. Typical Oscillograms Showing the Output of a Single Parallel Element Hot Film Anemometer Located at Rotor Two Exit Plane, Smooth Spool Baseline Configuration No. 1, U_t = 45.7 m/sec (150 ft/sec).

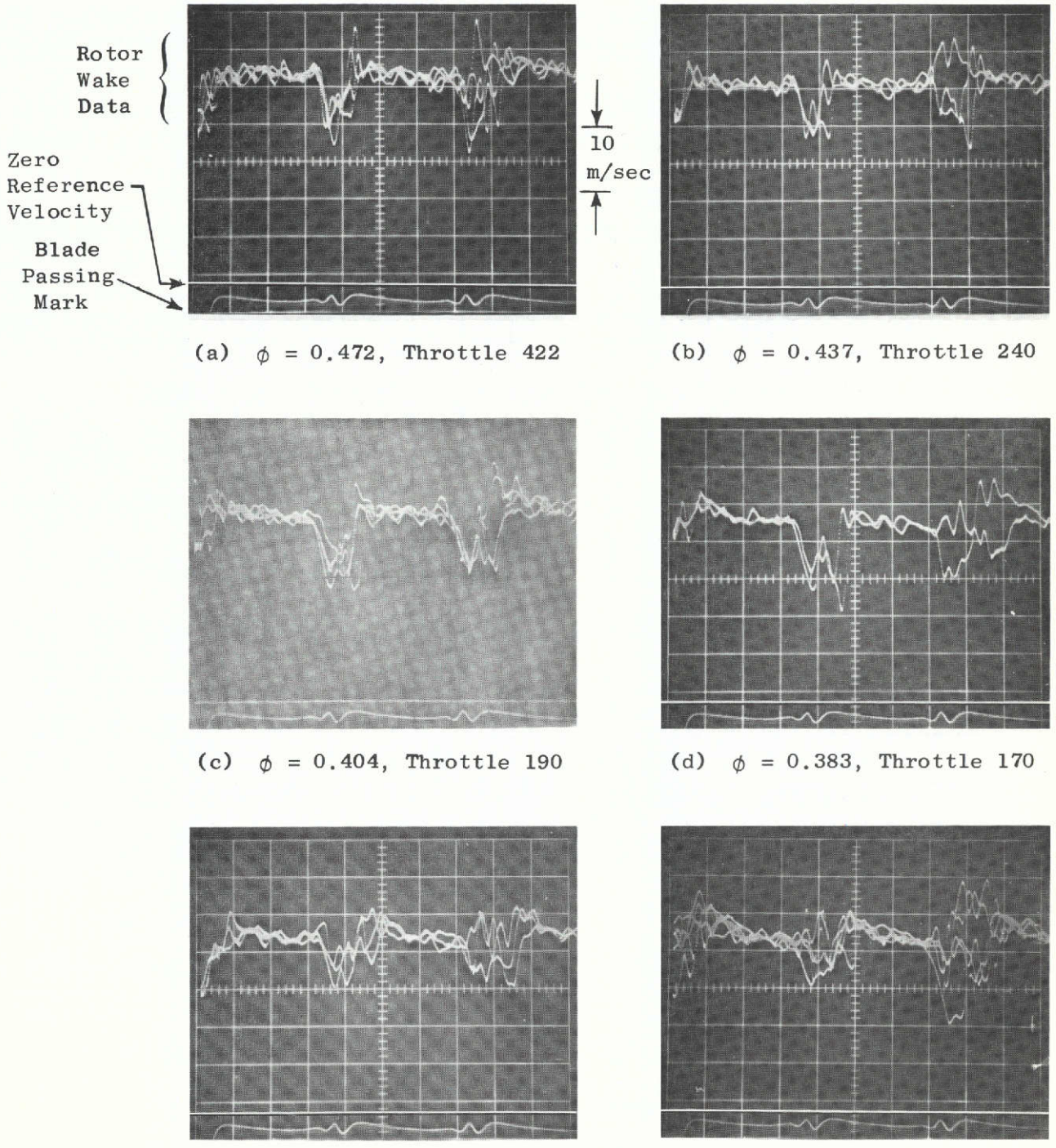

(a) ϕ = 0.472, Throttle 422

(b) ϕ = 0.437, Throttle 240

(c) ϕ = 0.404, Throttle 190

(d) ϕ = 0.383, Throttle 170

(e) ϕ = 0.369, Throttle 160

(f) ϕ = 0.352, Throttle 150

Figure 26. Typical Oscillograms Showing the Output of a Single Parallel Element Hot Film Anemometer Located at Rotor One Exit Plane, 90% Radial Immersion, Smooth Spool Baseline Configuration No. 1, U_t = 45.7 m/sec (150 ft/sec).

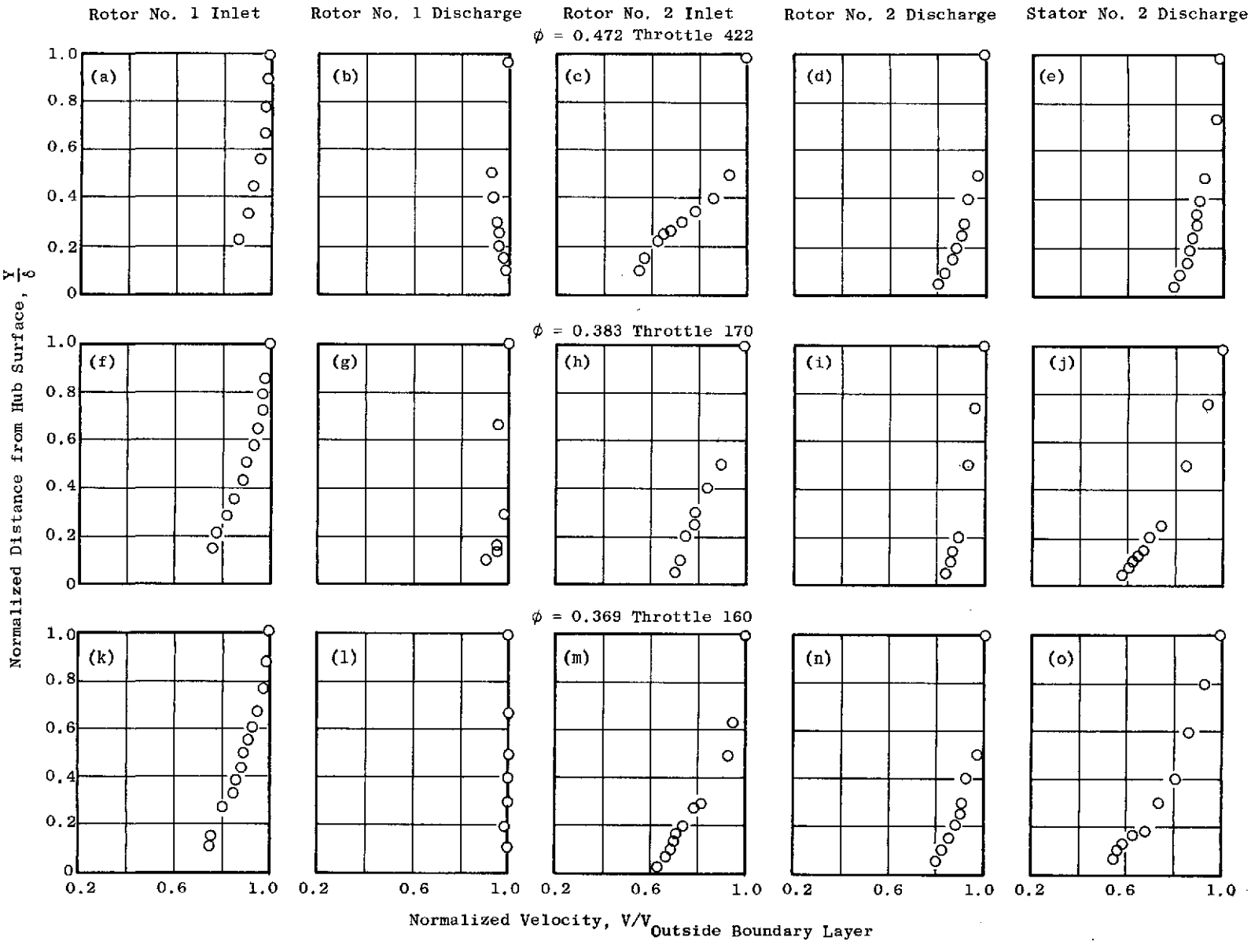

Figure 27. Hub Wall Boundary Layer Profiles.

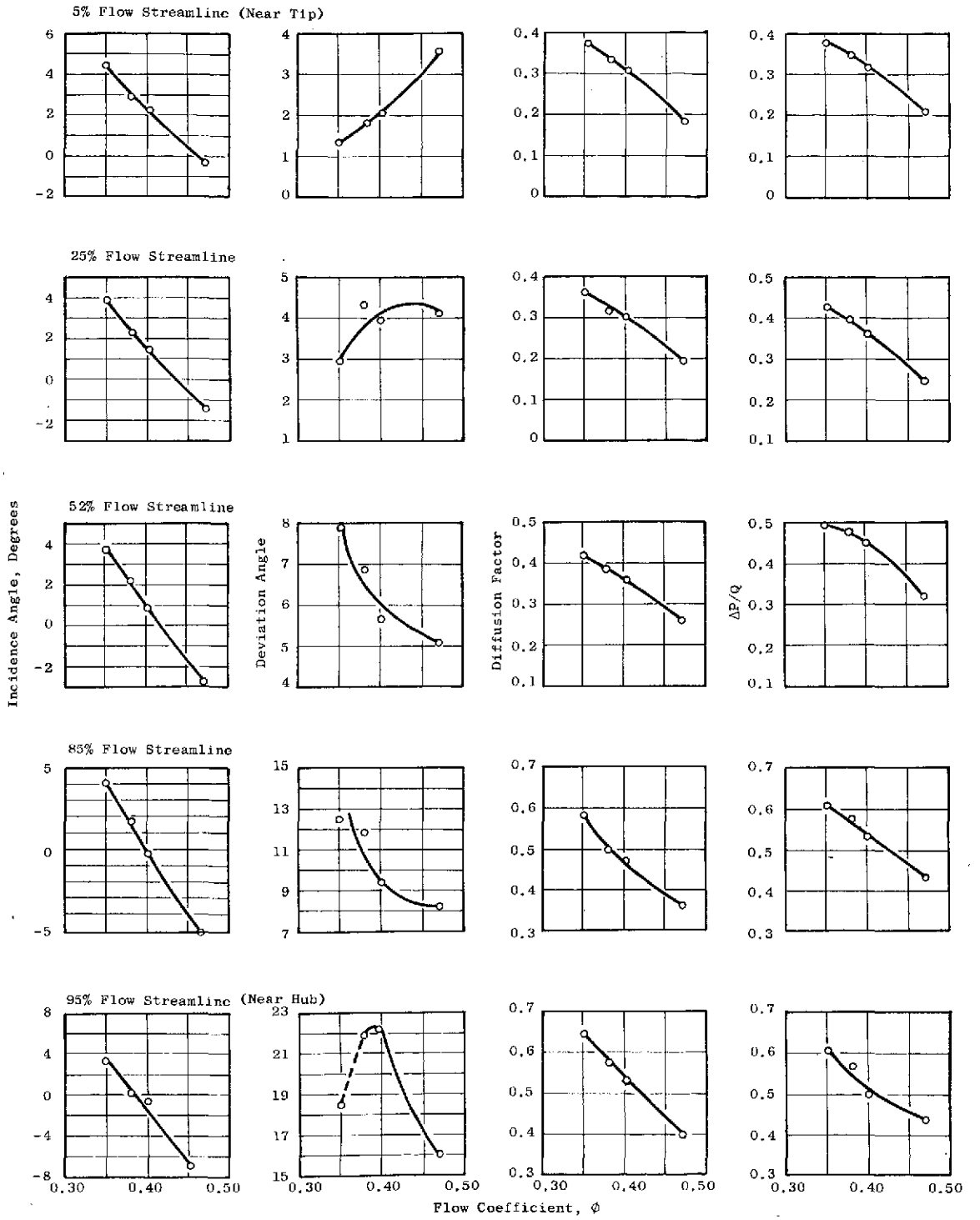

Figure 28. Rotor No. 1 Blade Element Data from Vector Diagram Analysis.

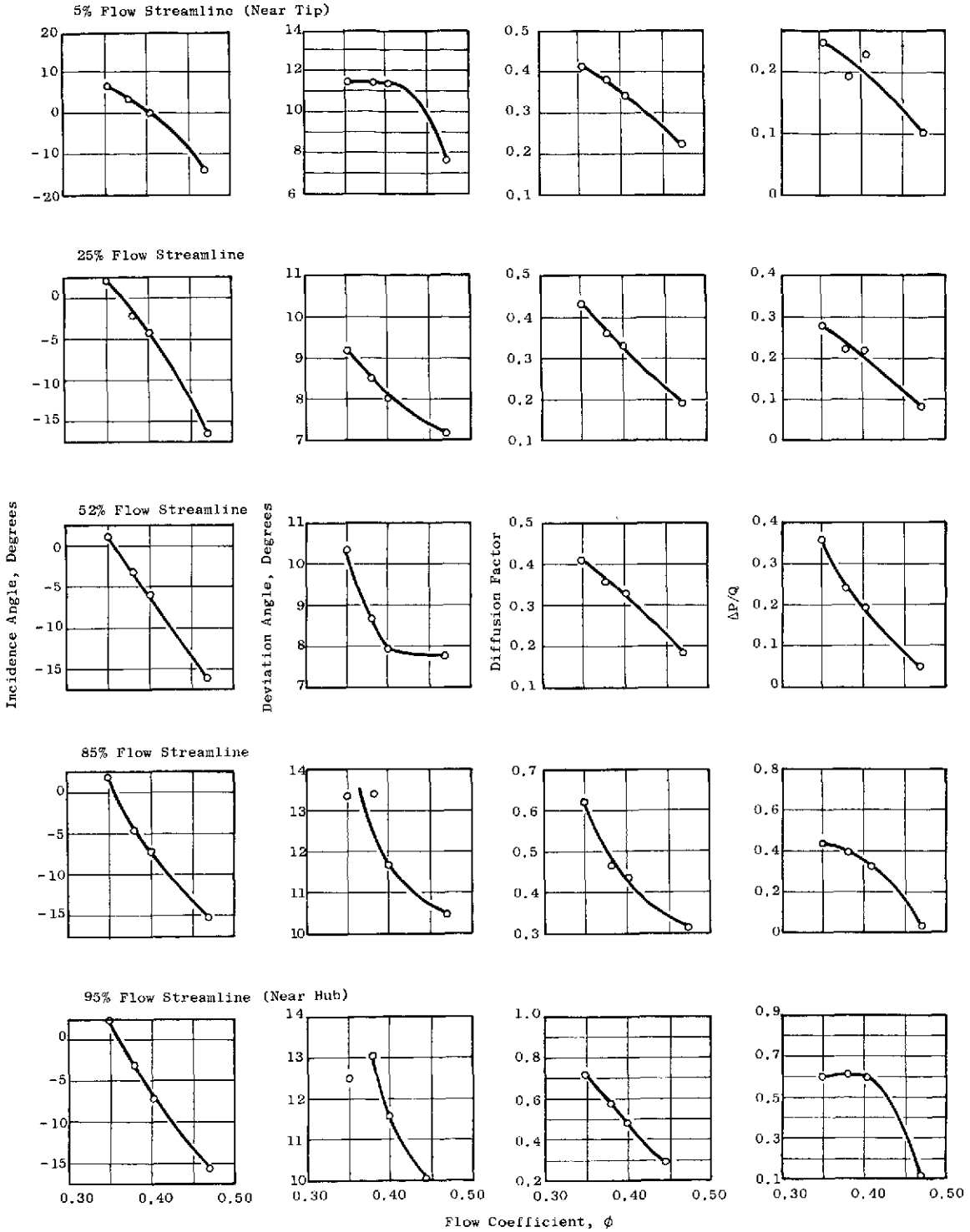

Figure 29. Stator No. 1 Vane Element Data from Vector Diagram Analysis.

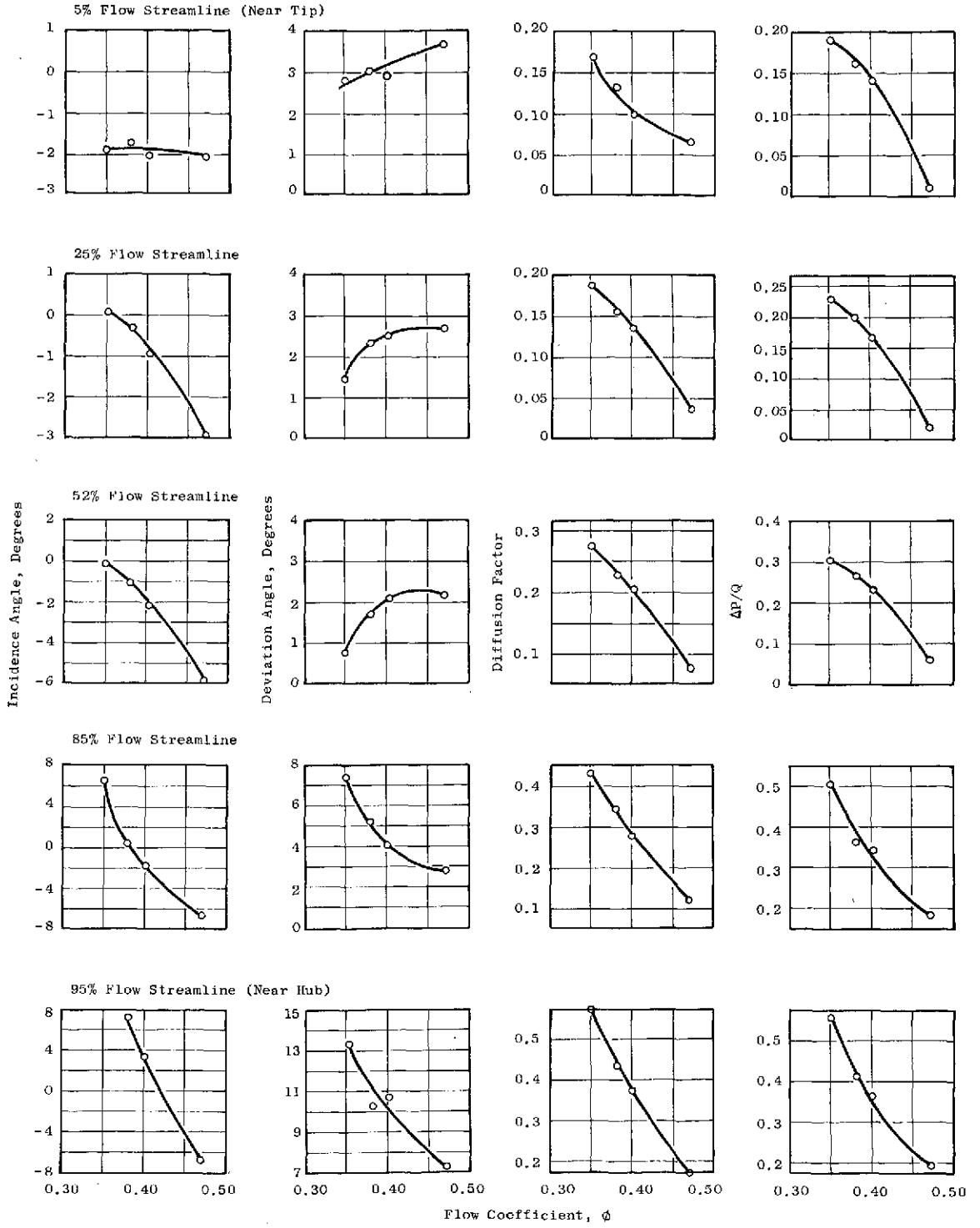

Figure 30. Rotor No. 2 Blade Element Data from Vector Diagram Analysis.

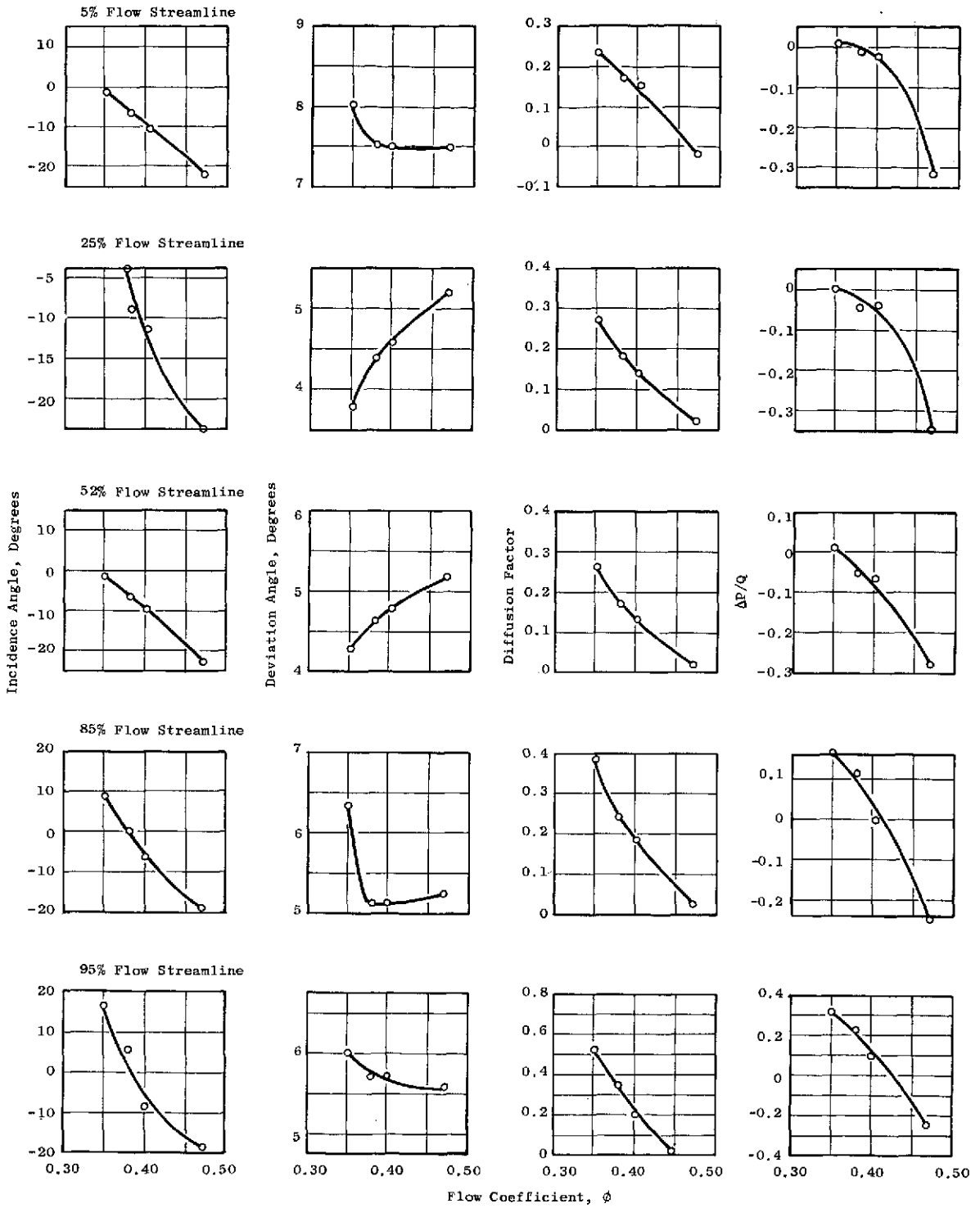

Figure 31. Stator No. 2 Vane Element Data from Vector Diagram Analysis.

loading unchanged. This resulted in Configuration No. 2. The second approach was to lower the solidity of the stators and thus increase their loading, resulting in Configuration No. 3, which is discussed later in this report.

Analytical Predictions

An analytical prediction of the variation in the diffusion factor (D-factor) and incidence angle with a change in blade and vane stagger angle was made. This prediction was obtained by first developing a "model" compressor using the experimental data for the baseline configuration as discussed in the previous section and then by varying the stagger angle on the "model" and predicting the performance based on a solution of the radial equilibrium equation. Typical results of this analysis are presented in Figures 32 and 33. With a stagger angle change in which rotor No. 1 is unchanged, stator No. 1 is opened 8°, rotor No. 2 is closed by 4°, and stator No. 2 is opened 8°, it can be seen from Figure 32 that both rotor D-factors remain unchanged relative to the original stagger case, while stator No. 1 shows a slight increase in loading. The effects, however, are not dramatic. For the same stagger angle change of 0°, +8°, -4°, +8°, the effects on incidence angle are more dramatic as seen in Figure 33. The rotor incidence angles remain unchanged, while stator No. 1 incidence angle is significantly increased. It was felt that this increased incidence angle would tend to make stator No. 1 the limiting item. The blades and vanes of the test compressor were then restaggered in accord with this analytical prediction.

Smooth Spool Baseline Performance

The baseline performance of the restaggered compressor was determined by using the smooth spools under the stator hubs and taking Probing Data and Preview Data. The new throttle curve is compared with that obtained for Baseline Configuration No. 1 in Figure 34. For any given throttle setting, the flow in Configuration No. 2 was reduced by about 5 or 6 percent relative to the flow in Configuration No. 1. This decrease in flow resulted from a higher stator blockage as shown by the increased D-factors and incidence angles in the stage No. 1 stators.

The suction surface tuft probing measurements for the Smooth Spool (Baseline) Configuration No. 2 are shown schematically in Figure 35 for various flow coefficients. As the compressor was throttled from wide open throttle toward stall, the tufts near the hub on stator No. 1 began to indicate unsteady flow as seen in Figure 35a. This region of unsteady flow progressed toward the leading edge and grew radially, extending from 100 percent to 75 percent radial immersion at a flow coefficient of 0.337 (see Figure 35b). At about this same throttle setting, a radially inward flow component (from the casing to the hub) was observed in stator No. 1 near the suction surface trailing edge. This flow is indicated by the dashed arrows in Figure 35. The flow in the hub region continued to deteriorate as the compressor was throttled until backflow developed along the suction surface as shown in Figure 35d. Evidently the stator No. 1 incidence angles were so large that the hub region was badly separated, creating a large blockage and region of reverse flow. This region of reverse flow and low static pressure was fed through the boundary layer,

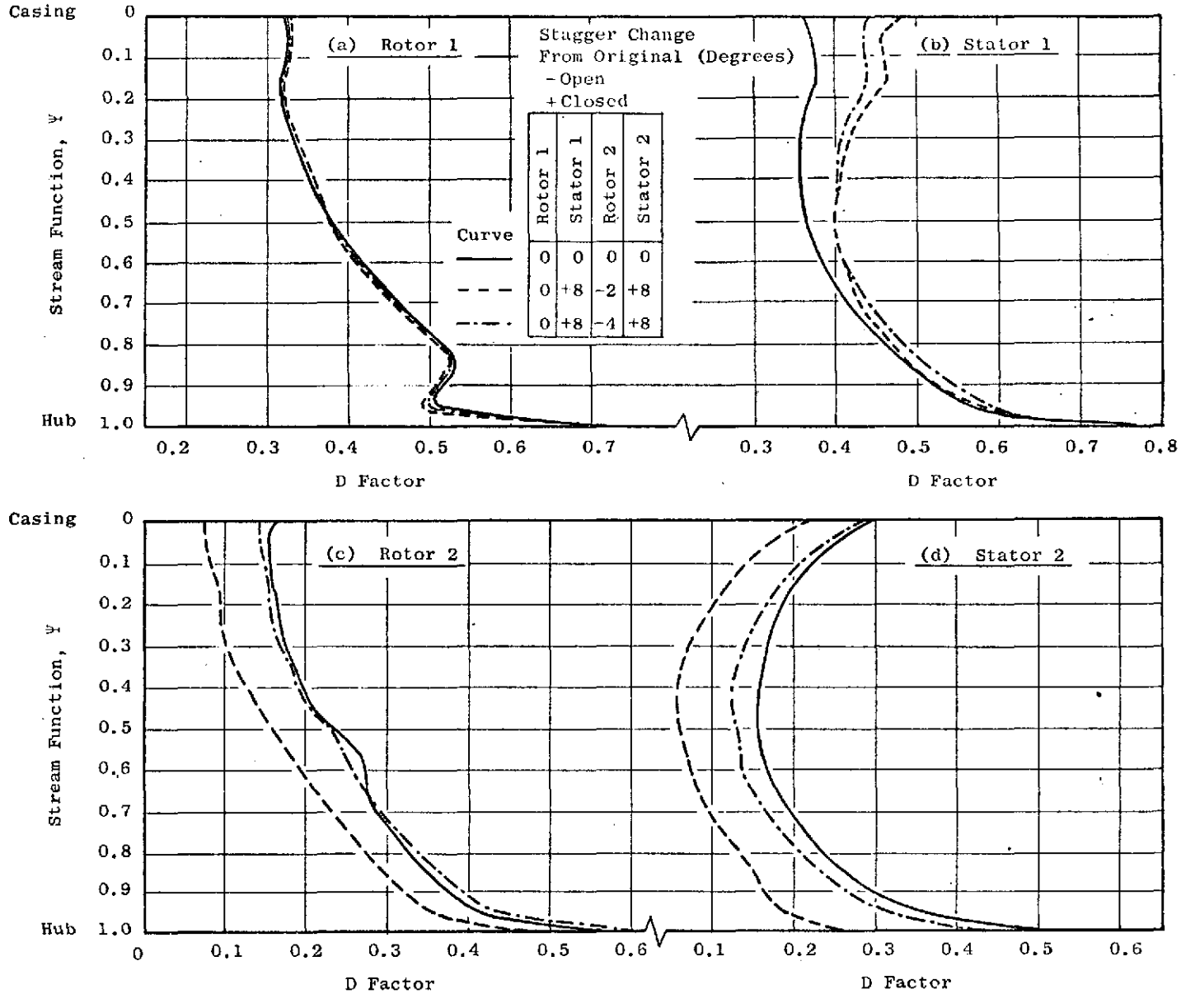

Figure 32. Analytical Prediction of the Variation in D Factor with a Change in Blade and Vane Stagger Angle, Throttle 170, ϕ = 0.383.

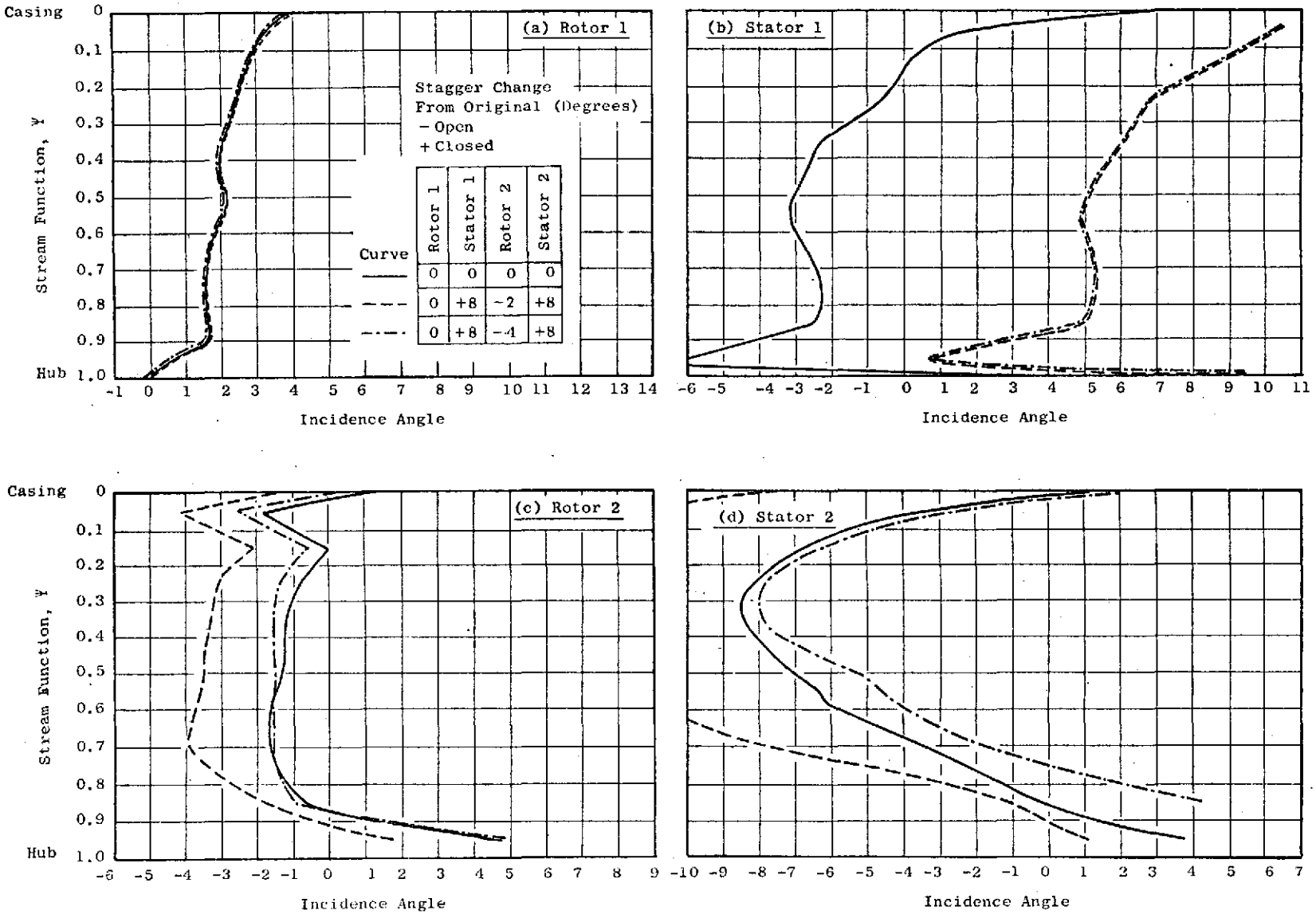

Figure 33. Analytical Prediction of the Variation in Incidence Angle With a Change in Blade and Vane Stagger Angle, Throttle 170, ϕ = 0.383.

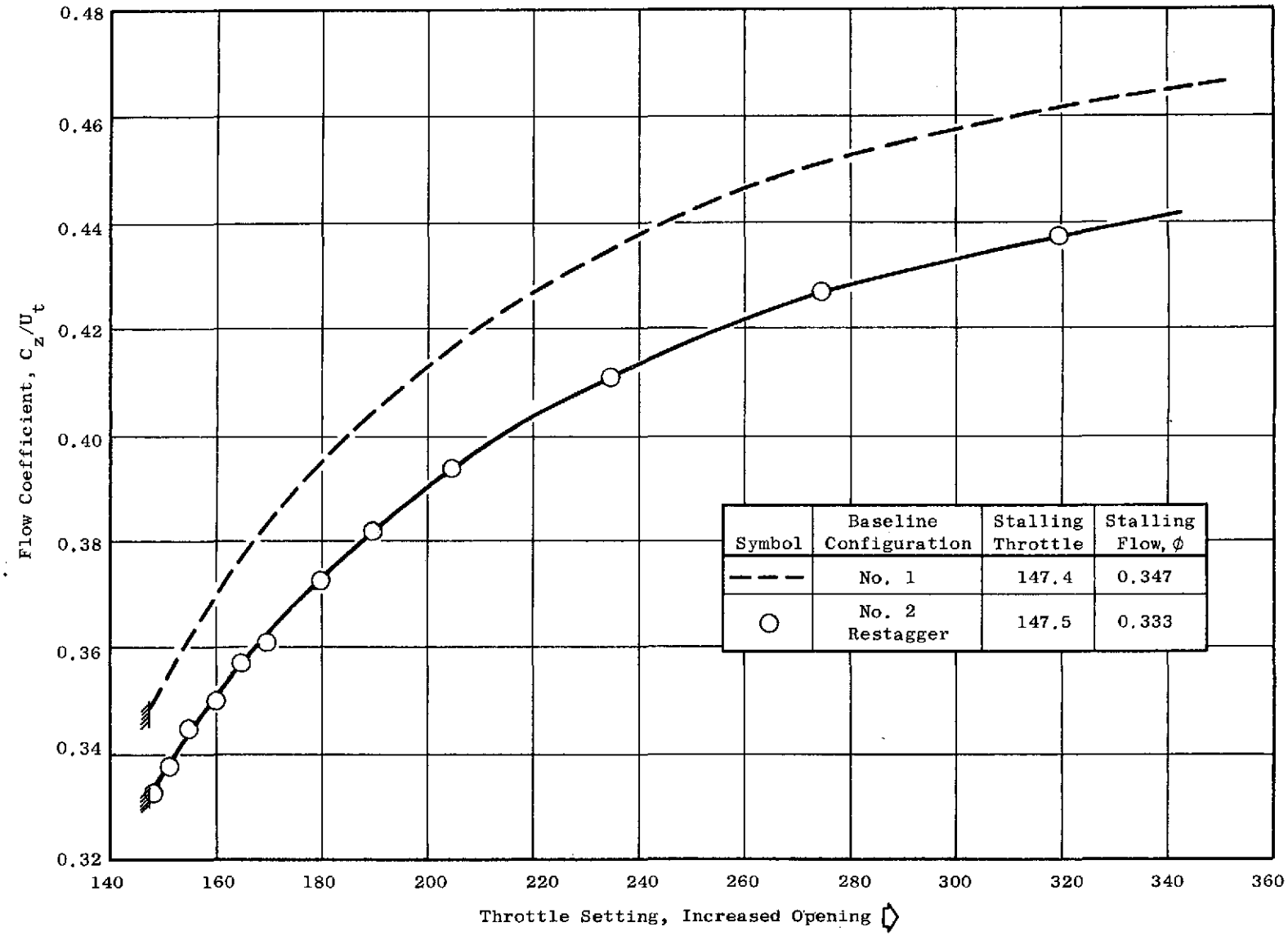

Figure 34. Flow Coefficient Versus Throttle Setting, Smooth Spool (Basline) Configurations Nos. 1 and 2, U_t = 45.7 m/sec (150 ft/sec).

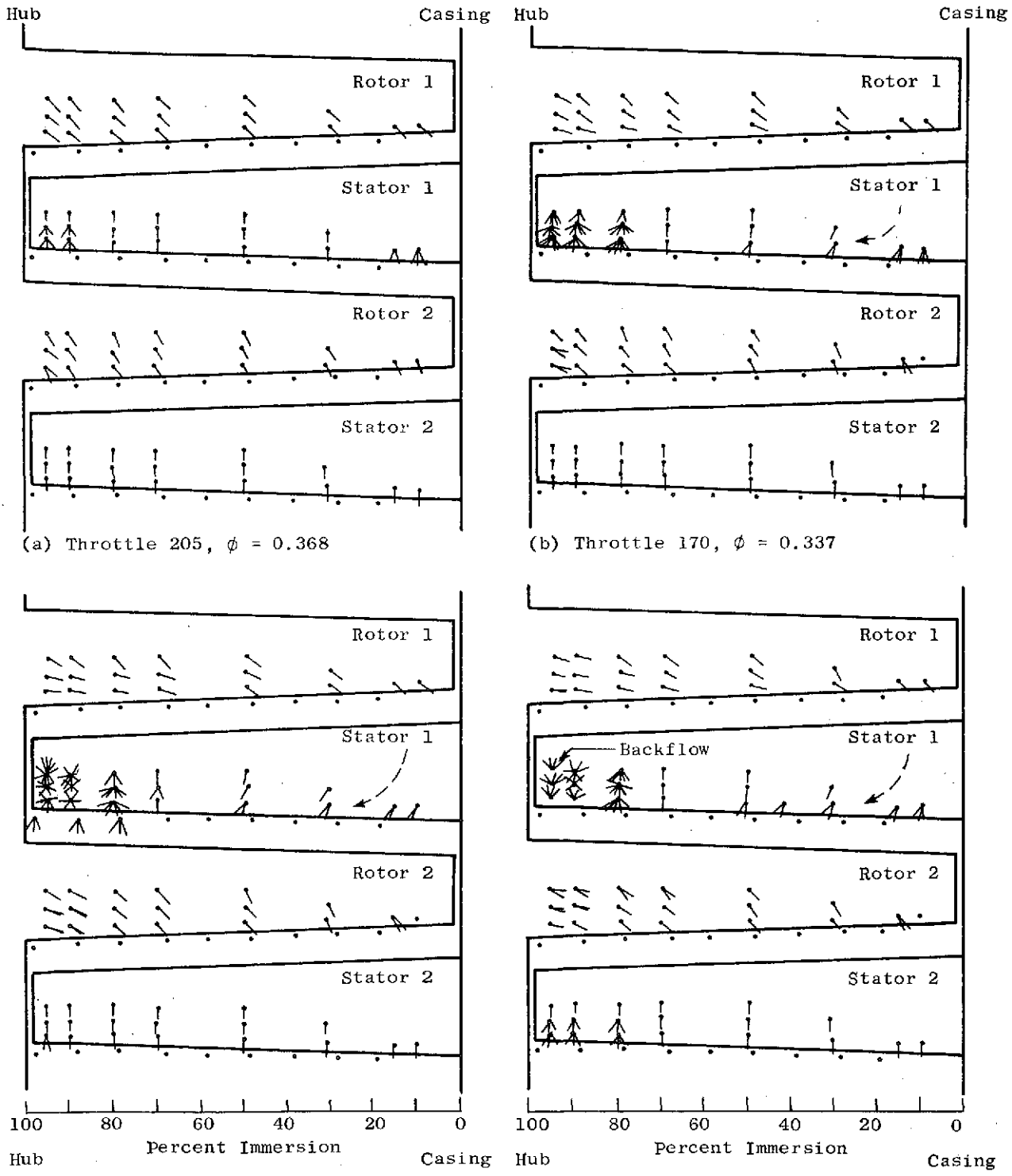

Figure 35. Schematic Representation of the Tuft Probing Measurements, Baseline Configuration No. 2, Restagger 0°, +8°, -4°, +8°, U_t = 45.7 m/sec (150 ft/sec).

causing the radially inward component of flow near the suction surface trailing edge. This type of backflow was not observed during the tufting measurements made with Configuration No. 1. The tufts on stator No. 2 showed smooth flow until about the stalling throttle as indicated in Figure 35d. The tufts in the vicinity of the hub and the trailing edge of both rotors pointed almost radially near stall, indicating flow separation and dominance of centrifugal force on the tuft.

The overall performance comparison between the Smooth Spool (Baseline) Configurations No. 1 and No. 2 is presented in Figure 36. For each configuration, the relative performance of the casing and the hub pressure characteristics was about the same; however, Configuration No. 2 gave considerably less pressure rise than Configuration No. 1. A significant reduction in efficiency was also apparent.

Performance Comparisons (Smooth Spool, Baffled Wide Blade Angle Slot Treatment)

Performance comparisons between the treated and the untreated Configuration No. 2 are based on Preview Data. The treatment made virtually no difference in the stalling throttle or in the stalling flow coefficient, as shown below.

Configuration No. 2	Stalling Throttle	Stalling Flow Coefficient	Stagger Angle Change-Degrees			
			R1	S1	R2	S2
Smooth Spool	146.3	0.331	0	+8	-4	+8
Baffled Wide Blade Angle Slots	147.5	0.333	0	+8	-4	+8

The overall performance comparison of the smooth spool (baseline) and the baffled wide blade angle slot treatment is shown in Figure 37. Again, there was no measurable difference between the treated and the untreated cases. Tuft probing measurements of these two cases were also identical. Since the baffled wide blade angle slot treatment was not effective in modifying compressor performance, it was felt that the circumferential groove treatment would not be effective either. Therefore, the circumferential groove spools were not tested.

Configuration No. 3 (Decreased Solidity)

In view of the above discussed experimental data, it was concluded that stator hub treatment had no beneficial effect on the compressor stall margin or compressor performance for the restaggered LSRC test Configurations No. 2. Therefore, it was decided to proceed with a second modification of the LSRC. This modification utilized reduced solidity as a means of further increasing the stator loading and was identified as Configuration No. 3.

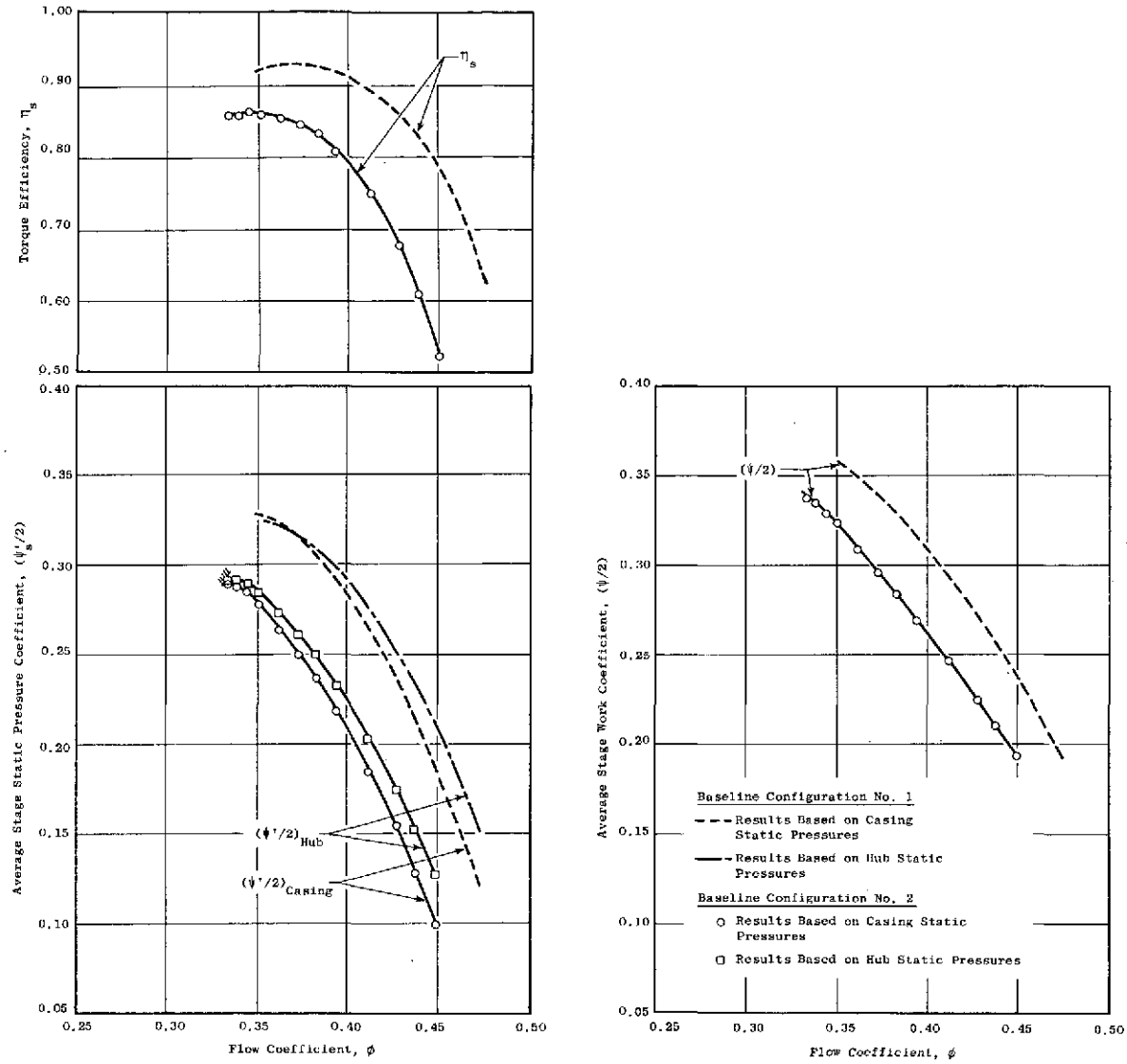

Figure 36. Overall Performance Comparison of the Smooth Spool Baseline Configuration No. 1 and the Smooth Spool Baseline Configuration No. 2, Restagger 0°, +8°, -4°, +8°, Based on Preview Data, U_t = 45.7 m/sec (150 ft/sec).

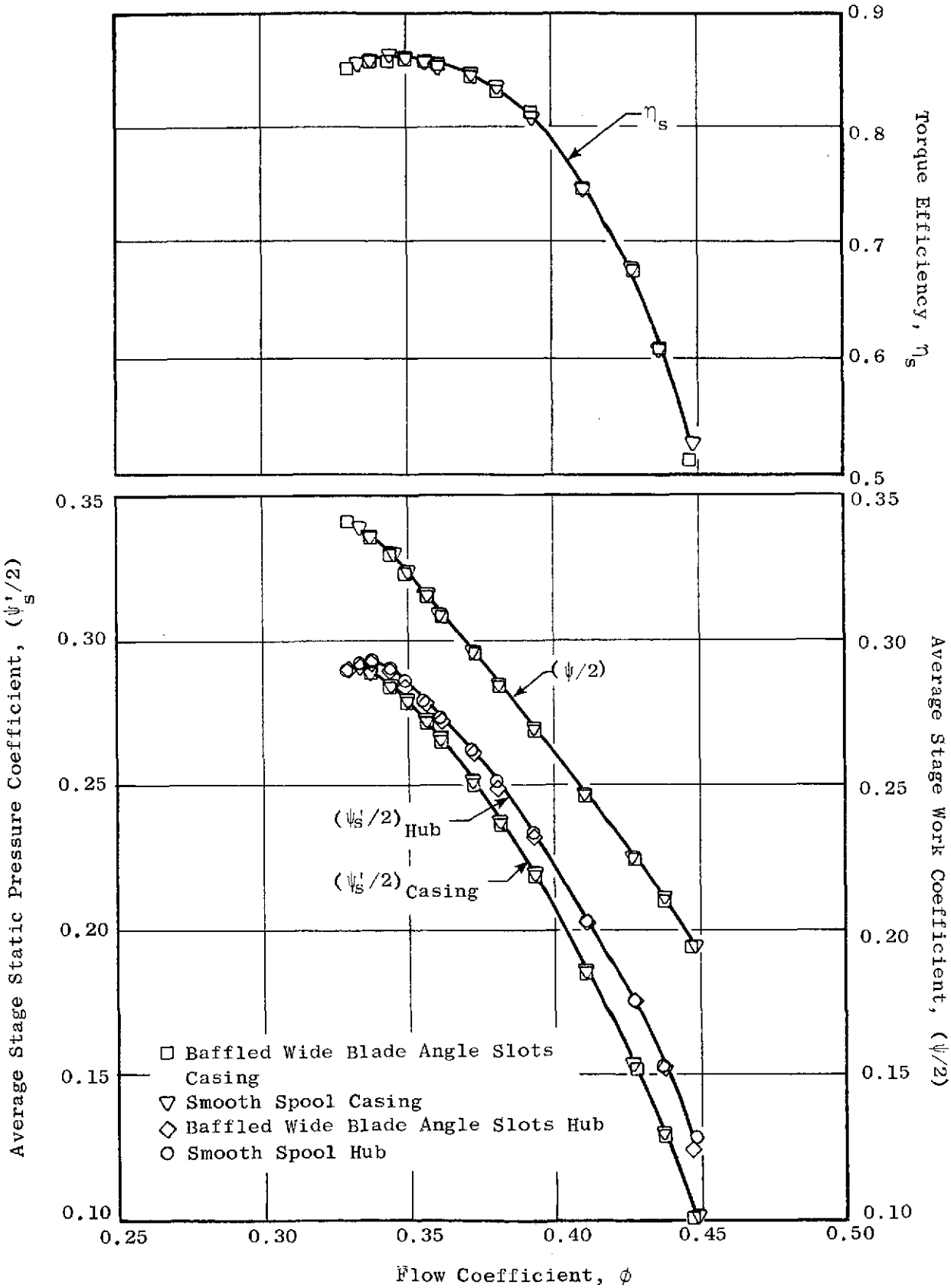

Figure 37. Overall Performance Comparison of the Smooth Spool Baseline Configuration No. 2 and the Baffled Wide Blade Angle Slot Treatment Configuration No. 2, Based on Preview Data, Restagger 0°, +8°, -4°, +8°, U_t = 45.7 m/sec (150 ft/sec).

Analytical Predictions

The effect on stator loading of varying the cascade solidity was analytically evaluated. The D-factor is a measure of such loading and can be computed from

$$D = \left(1 - \frac{V_2}{V_1}\right) + \frac{\Delta C_u}{2\sigma V_1} \qquad (1)$$

where: V_1 = absolute velocity entering the stator
V_2 = absolute velocity leaving the stator
C_u = change in absolute tangential velocity
σ = solidity = chord/spacing

Using equation (1) and the vector diagram information obtained from the experimental baseline data, the change in D-factor when one-half of the stator vanes are removed (i.e. solidity reduced by a factor of 2) was evaluated. The results are shown in Table V.

All of the blades and vanes were returned to their original Configuration No. 1 stagger. Then 25 of the 50 stator vanes were removed from stage No. 1 and 26 of the 53 stator vanes were removed from stage No. 2. This configuration was identified as Configuration No. 3.

Smooth Spool Baseline Performance

The baseline performance of the Configuration No. 3 lower solidity compressor was determined with the smooth spools under the stator hubs by taking Probing Data, Preview Data and Standard Data. The new throttle curve presented in Figure 38 shows that at any throttle setting the flow was reduced by about 9 percent (near stall) below the Baseline Configuration No. 1 flow.

The suction surface tuft probing measurements for the Smooth Spool (Baseline) Configuration No. 3 are presented in Figures 39 and 40. As reported for other configurations, when the compressor was throttled from wide open throttle toward stall, the tufts near the hub on stator No. 1 showed the first indication of unsteady flow in this case for a flow coefficient of $\phi = 0.395$ (throttle setting 250), see Figure 39a. As the compressor was throttled to a flow coefficient of $\phi = 0.368$ and then to $\phi = 0.359$ (throttle settings 200 to 190), the unsteady flow region around the hub of stator No. 1 grew and the hub region of rotor No. 2 and stator No. 2 showed beginnings of unsteady flow, Figures 39b and 39c respectively. Further throttling to $\phi = 0.350$ (throttle setting 180), Figure 39d, produced a backflow region in the hub of stator No. 1. The radially inward flow component, discussed earlier and presented in Figure 35, appeared again in this probing series and is indicated by the dashed arrows. Throttling to $\phi = 0.340$ and then to $\phi = 0.326$ (throttle settings 170 to 160) produced a further deterioration of the flow in the hub region,

Table V. Predicted Change in Stator D-Factor When One-Half of the Stators Are Removed.

	Percent Immersion	D-Factor (no vanes removed)	D-Factor (1/2 of vanes removed)	Condition
1st Stage	95	0.699	0.948	Near Stall
	85	0.583	0.809	Near Stall
	95	0.579	0.806	Peak Efficiency
	85	0.442	0.643	Peak Efficiency
2nd Stage	95	0.524	0.735	Near Stall
	85	0.351	0.509	Near Stall
	95	0.357	0.504	Peak Efficiency
	85	0.216	0.331	Peak Efficiency

On the average, a forty (40) percent increase in D-factor was predicted if one-half of the stators were removed from each stage.

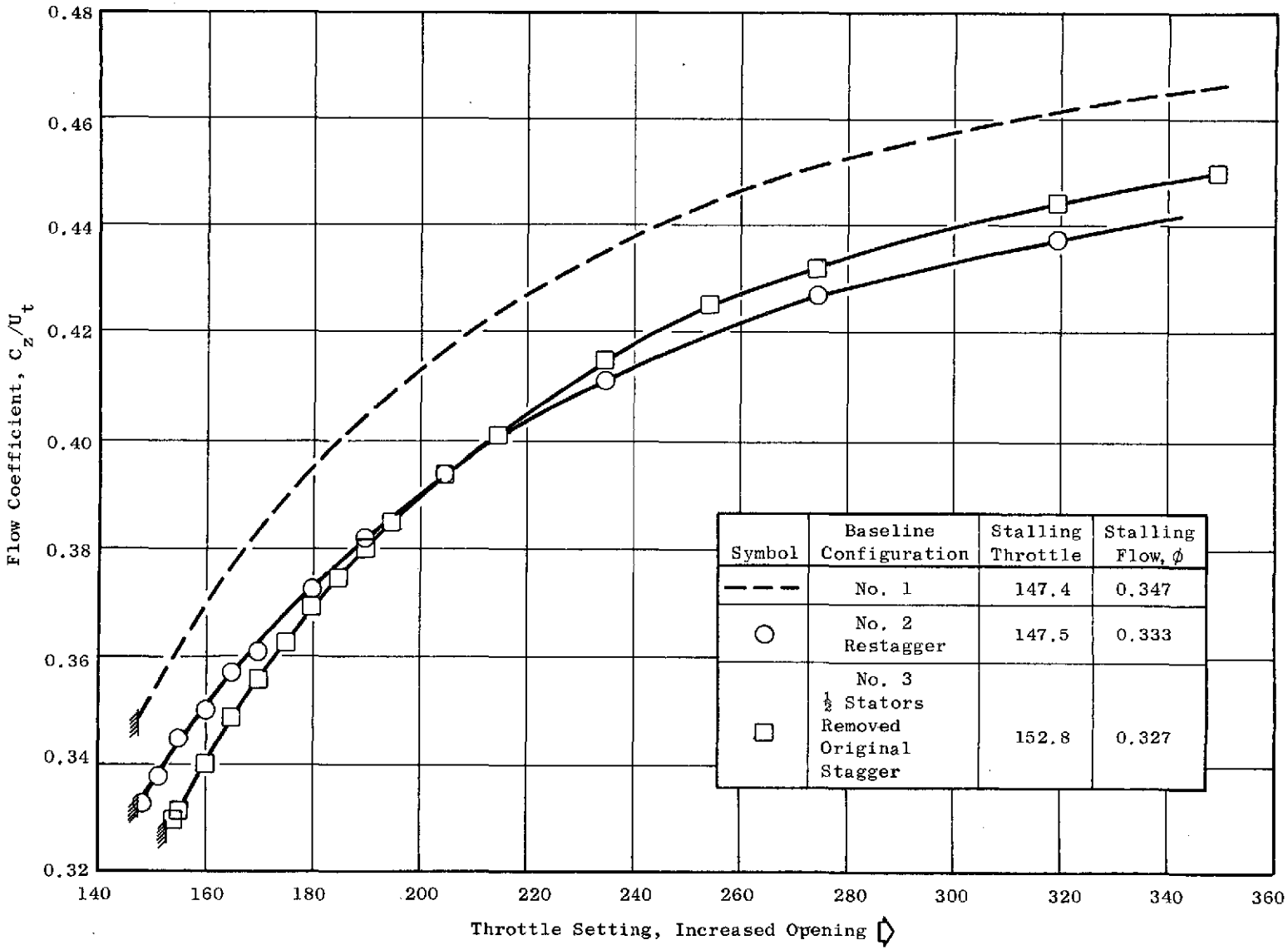

Figure 38. Flow Coefficient Versus Throttle Setting, Smooth Spool (Baseline) Configurations Nos. 1, 2 and 3, U_t = 45.7 m/sec (150 ft/sec).

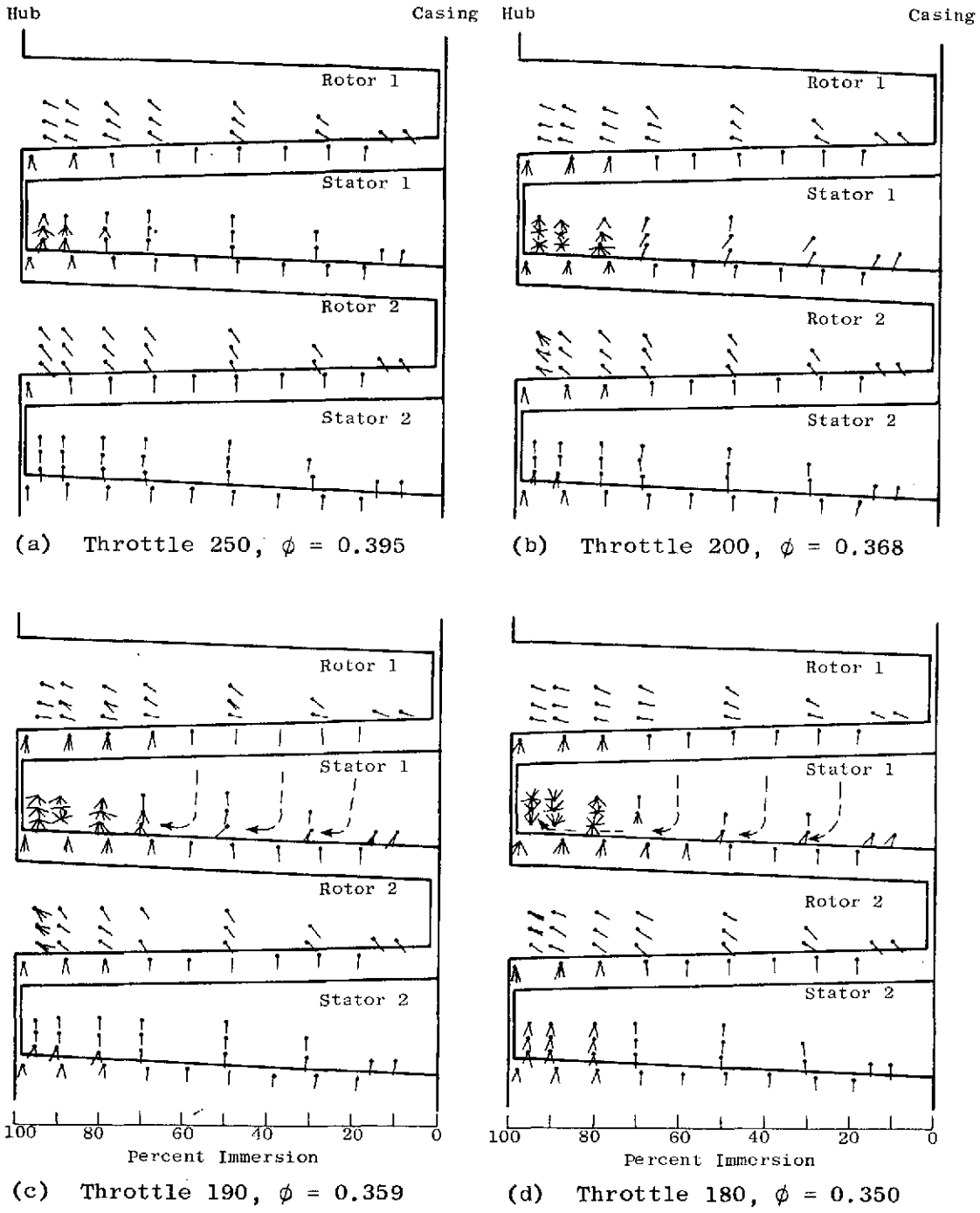

Figure 39. Schematic Representation of the Tuft Proving Measurements, Smooth Spool Baseline Configuration No. 3 with One-Half of the Stators Removed, U_t = 45.7 m/sec (150 ft/sec).

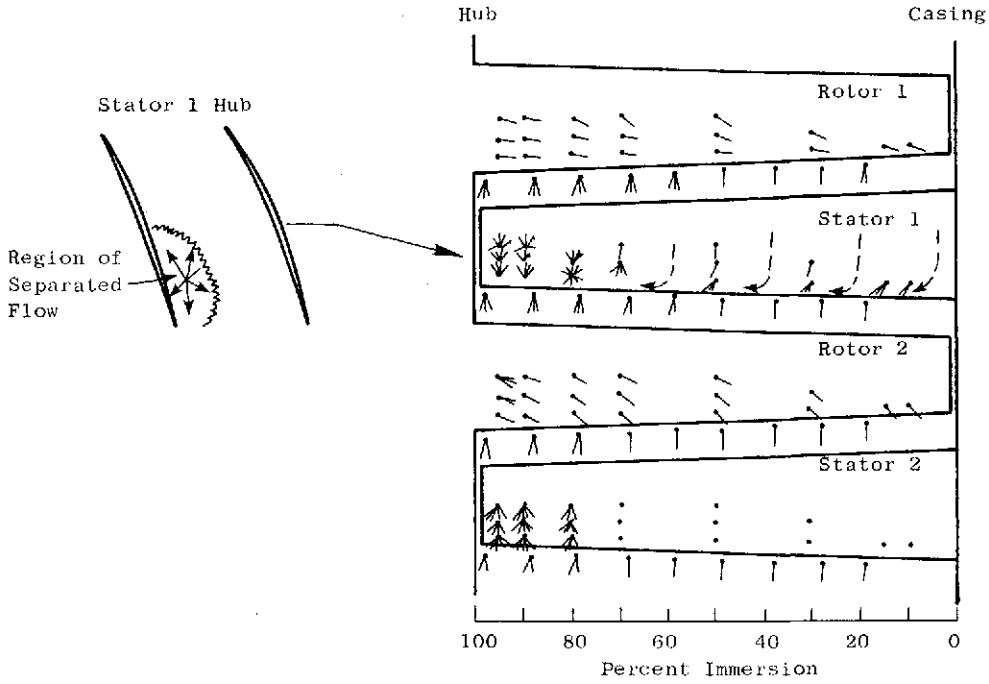

(a) Throttle 170, ϕ = 0.340

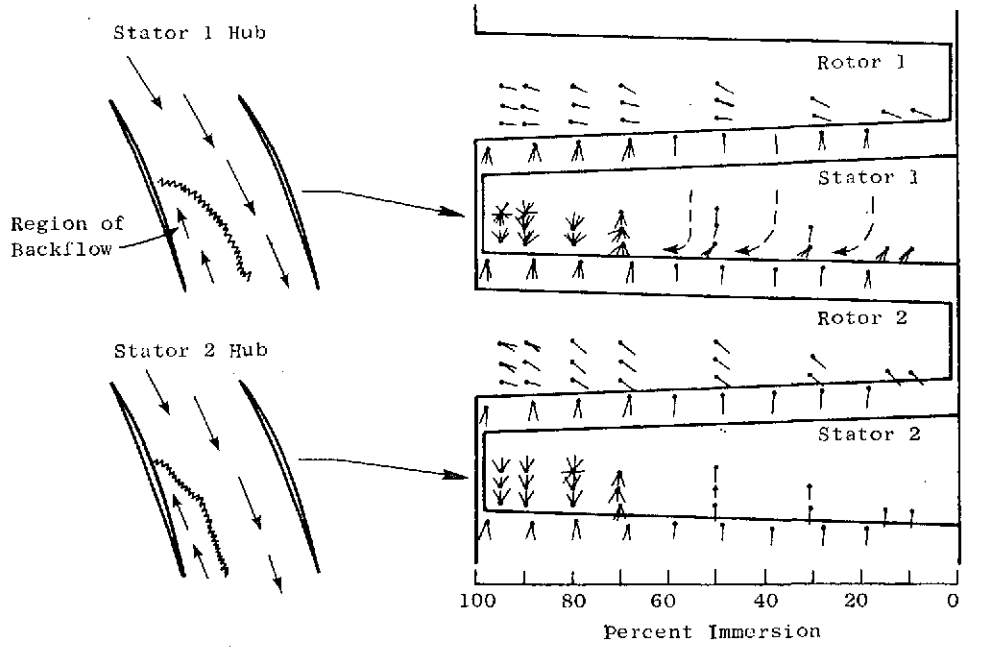

(b) Throttle 160, ϕ = 0.326

Figure 40. Schematic Representation of the Tuft Probing Measurements, Smooth Spool Baseline Configuration No. 3 with One-Half of the Stators Removed, U_t = 45.7 m/sec (150 ft/sec).

particularly in stator No. 2 as shown in Figures 40a and 40b, respectively. The insert showed the region of reverse flow in both stators. As before, the tufts on the rotors indicated the dominance of centrifugal force near stall. The tufting survey showed that both stages of stators were highly separated in the hub region near stall. In fact the separated flow and the reverse flow were more severe for this configuration than for any other configuration tested in this program.

The overall performance of the Smooth Spool (Baseline) Configuration No. 3 is presented in Figure 41 and is compared with the overall performance of the original Baseline Configuration No. 1 in Figures 42 and 43. The hub characteristic shows significantly more rollover for Configuration No. 3 (Figure 42). Using the performance based on total pressure (Figure 43), it is seen that removing one-half of the stator vanes resulted in a loss of 2 points in efficiency and a 17 percent decrease in peak pressure coefficient. Generally the data are shifted downward and toward lower flow coefficients.

Performance Comparisons (Smooth Spool, Baffled Wide Blade Angle Slot Treatment)

A comparison of the stalling throttles and stalling flow coefficients is presented below.

It shows, as before, that there is virtually no difference in stalling throttle or stalling flow coefficient between the treated and the untreated spools.

Configuration No. 3	Stalling Throttle	Stalling Flow Coefficient	Stagger Angle Change-Degrees			
			R1	S1	R2	S2
Smooth Spool Baseline	152.8	0.327	0	0	0	0
			(1/2 stators removed)			
Baffled Wide Blade Angle Slots	153.8	0.329	0	0	0	0
			(1/2 stators removed)			

The overall performance comparison of Figure 44, which is based on Preview Data, shows no really significant difference between the treated and the untreated spools. There was a small difference in pressure coefficient between the two configurations. However, a much more accurate evaluation of any performance difference is obtained by comparing Standard Data which is based on radial surveys of total pressure. These data are presented in Figure 45 and show no difference in pressure coefficient, work coefficient or torque efficiency between the treated and the untreated Configuration No. 3 with one-half of the stators removed.

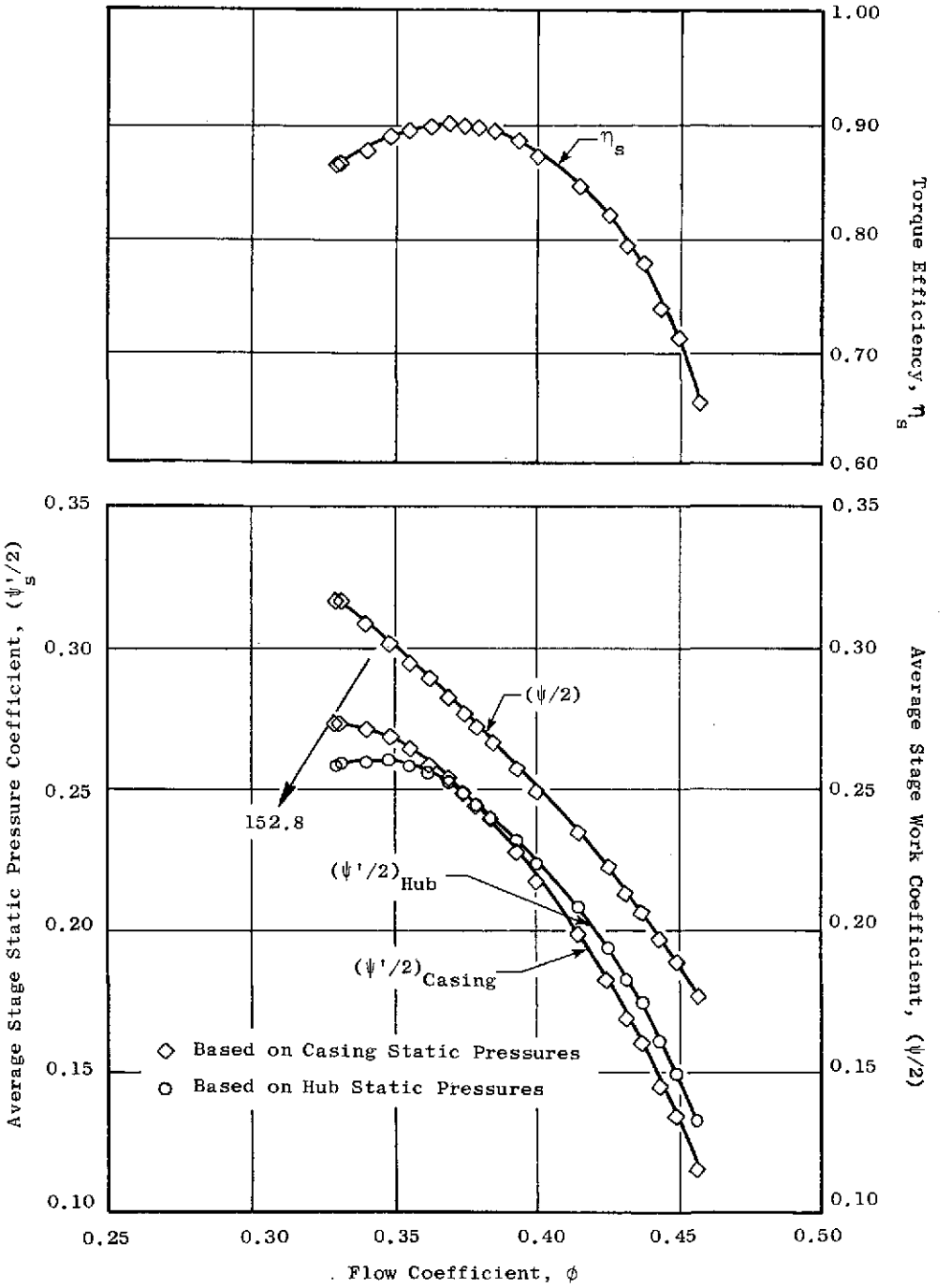

Figure 41. Overall Performance of the Smooth Spool Baseline Configuration No. 3, One-Half of the Stators Removed, Based on Preview Data, U_t = 45.7 m/sec (150 ft/sec).

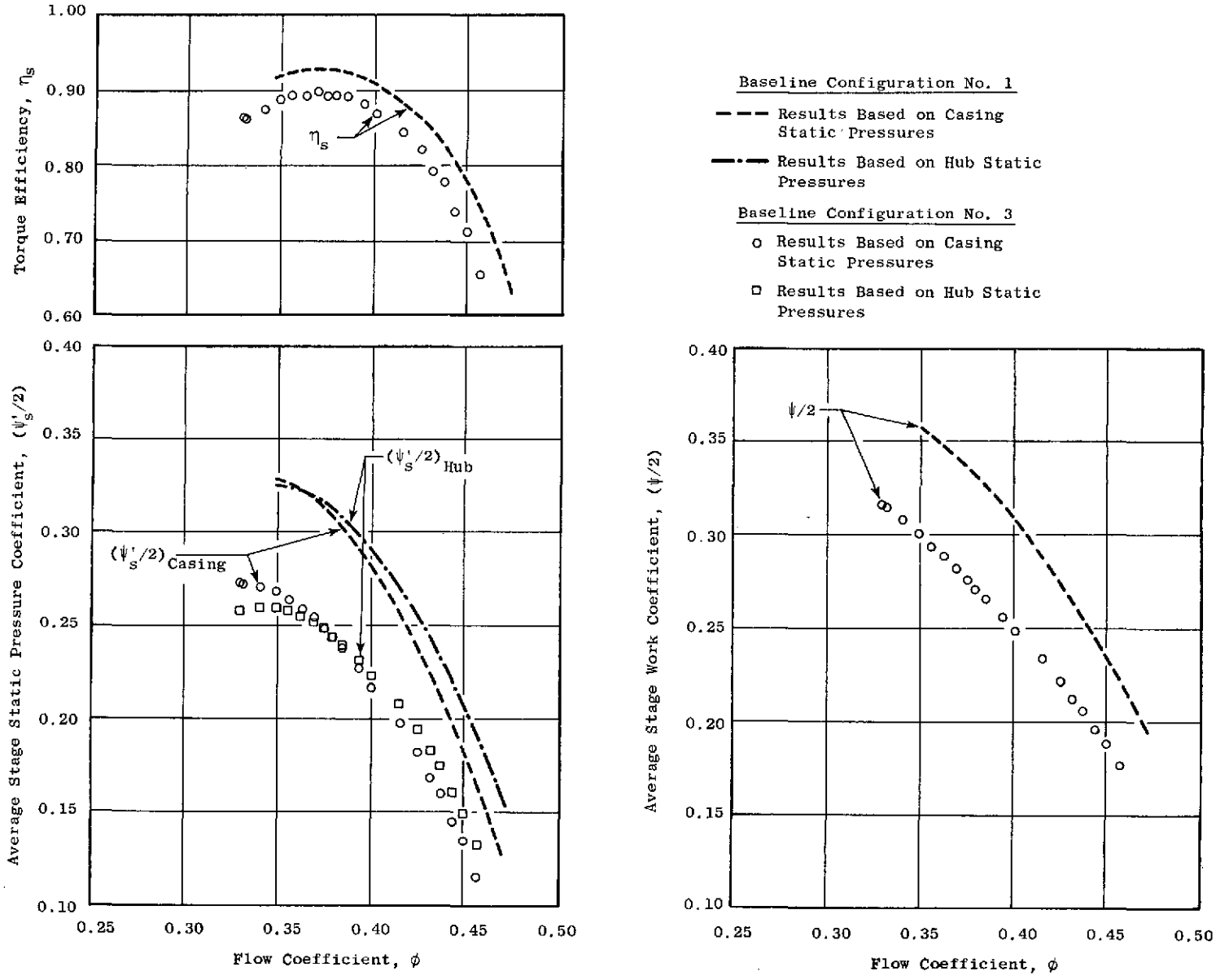

Figure 42. Overall Performance Comparison of the Smooth Spool Baseline Configuration No. 1 and the Smooth Spool Baseline Configuration No. 3 with One-Half of the Stators Removed, Based on Preview Data, U_t = 45.7 m/sec (150 ft/sec).

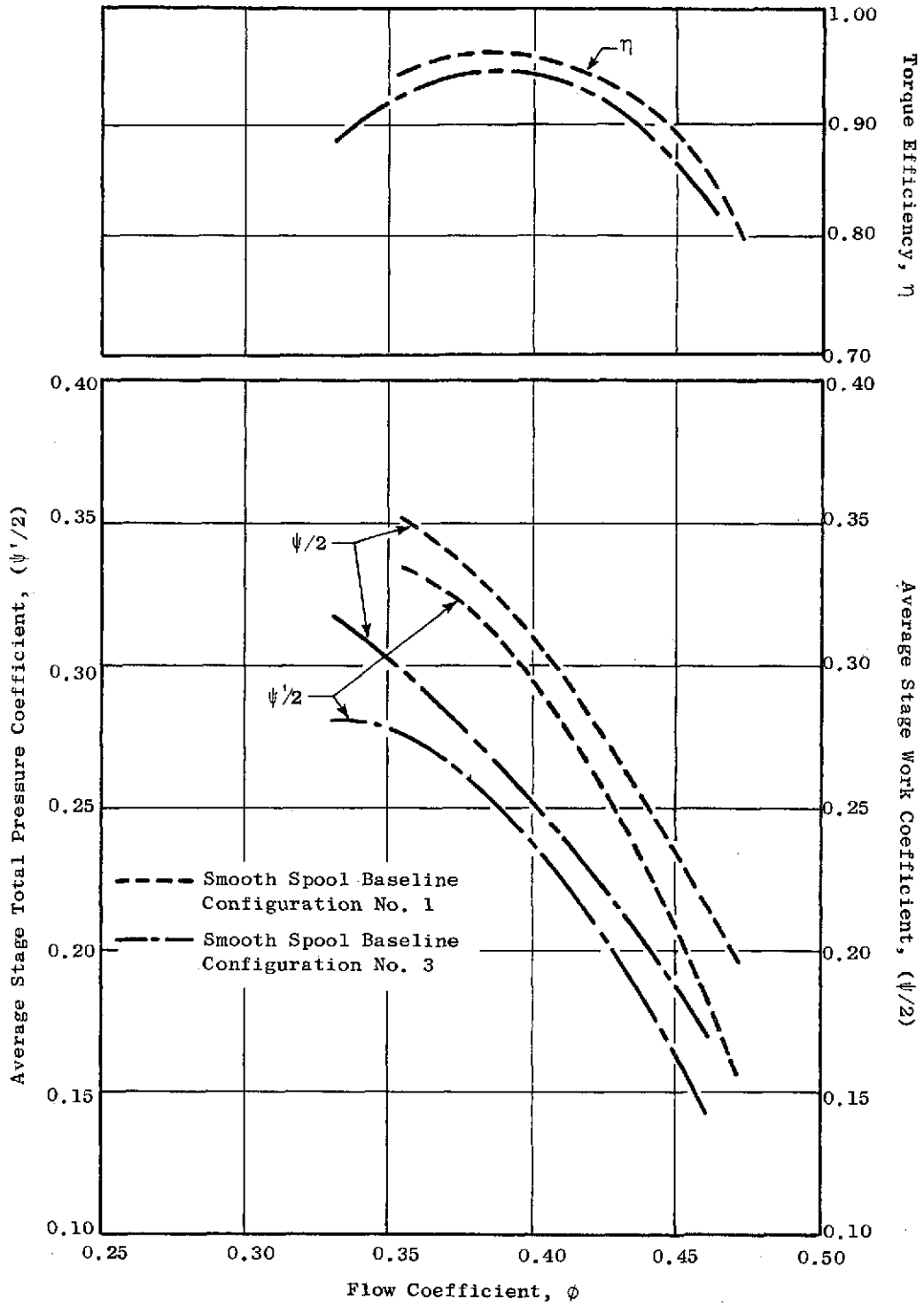

Figure 43. Performance Comparison of the Smooth Spool Baseline Configuration No. 1 and the Smooth Spool Baseline Configuration No. 3, Based on Standard Data, U_t = 45.7 m/sec (150 ft/sec).

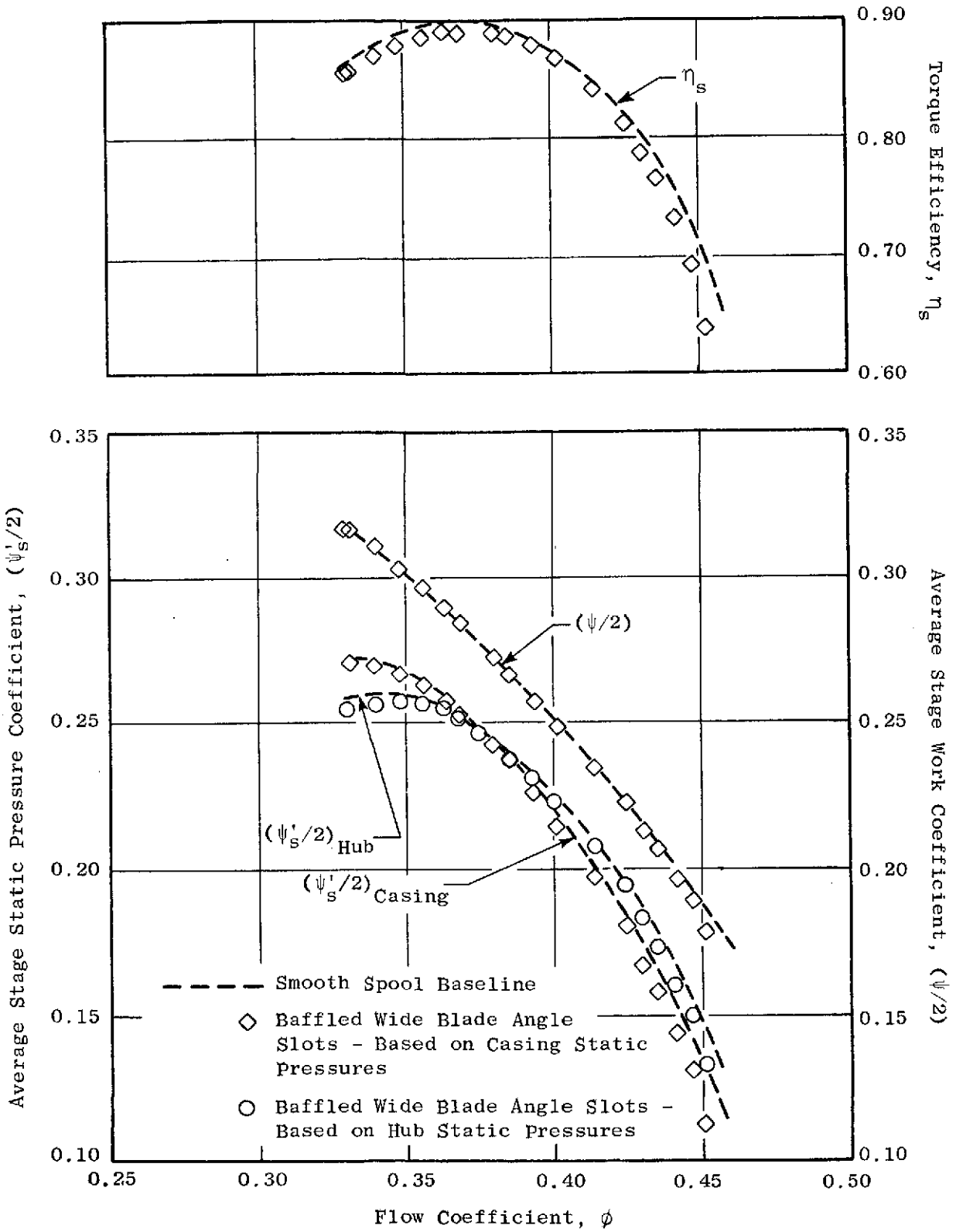

Figure 44. Overall Performance Comparison of the Smooth Spool Baseline and Baffled Wide Blade Angle Slot Treatment Configurations No. 3, Based on Preview Data, One-Half of the Stators Removed, U_t = 45.7 m/sec (150 ft/sec).

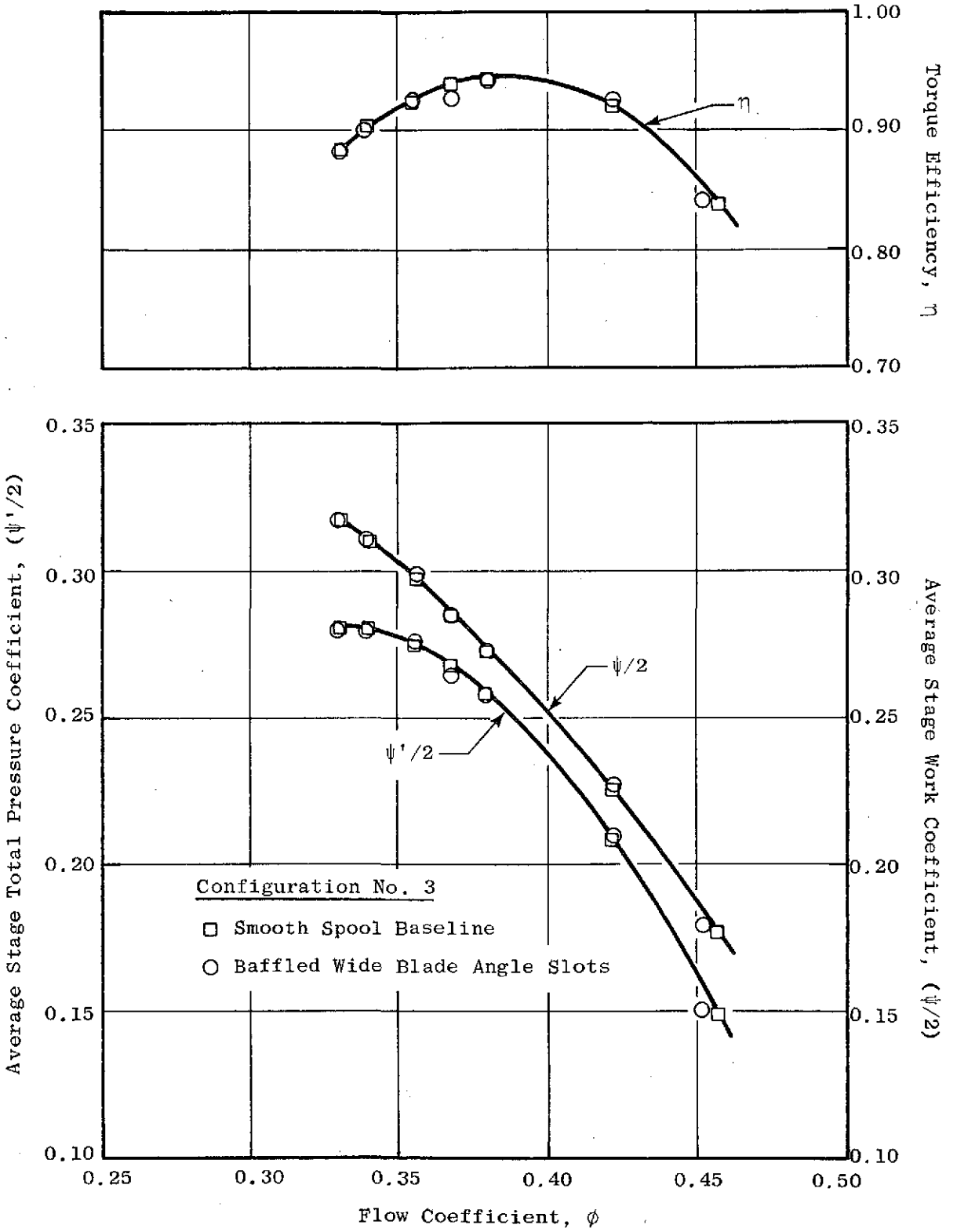

Figure 45. Performance Comparison of the Smooth Spool Baseline and the Baffled Wide Blade Angle Slot Treatment Configurations No. 3, Based on Standard Data, One-Half of the Stators Removed, U_t = 45.7 m/sec (150 ft/sec).

Comparisons of the circumferential and radial variations of normalized total pressure, presented in Figures 46-48, show no significant difference. It is believed that the apparent differences in measured total pressure for the stator 1 discharge 90 percent immersion case, Figure 46, are due to the fact that the probe was located in a highly separated, reverse flow environment. The measurements are therefore suspect. However, reasonable agreement is achieved in the nonwake region. Also, no difference is seen in the radial variation of normalized static pressure presented in Figure 49.

Measured absolute air angles are shown in Figure 50. As discussed before, the flow in the hub region of stator 1 was highly separated with regions of reverse flow. The angle measurements in this region are suspect and therefore indicated by dashed lines in the figure. The comparison of the radial variation of incremental flow coefficient presented in Figure 51 for the treated and the untreated cases shows no significant differences. Part of the data for throttle setting 422 in Figure 51a was suspect and therefore was not included in the Figure.

Since the baffled wide blade angle slot treatment was not effective in modifying compressor performance, it was felt that the circumferential groove treatment would not be effective either. Therefore, the circumferential groove spools were not tested.

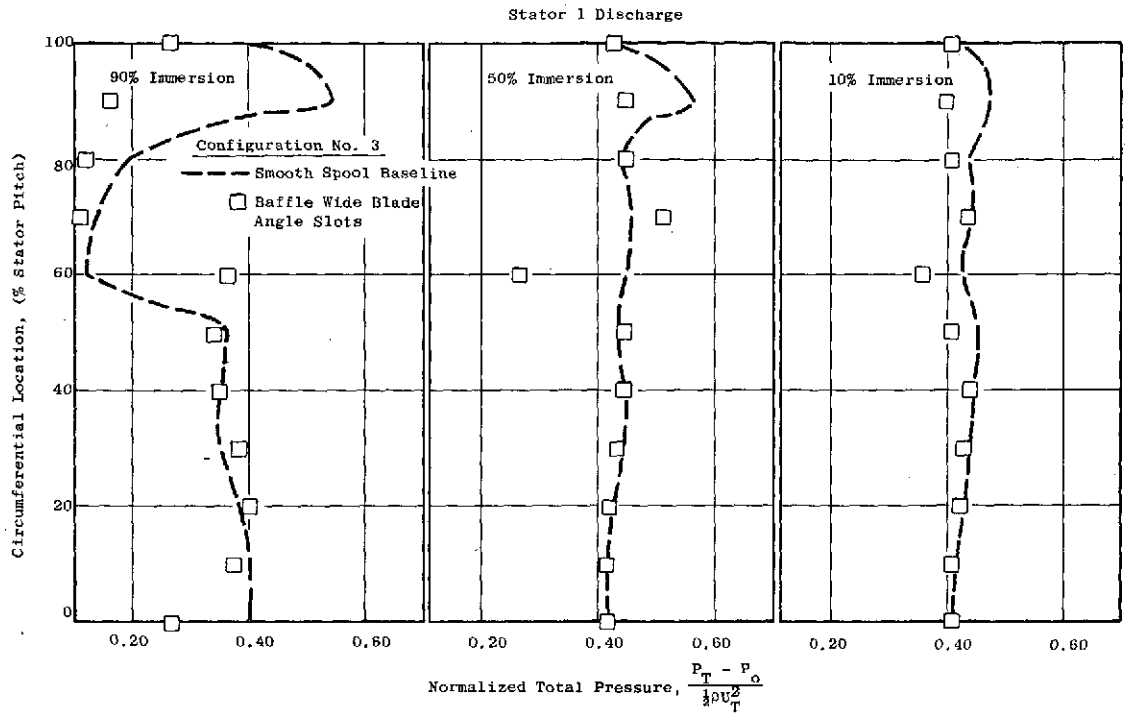

ϕ = 0.368, Throttle 180

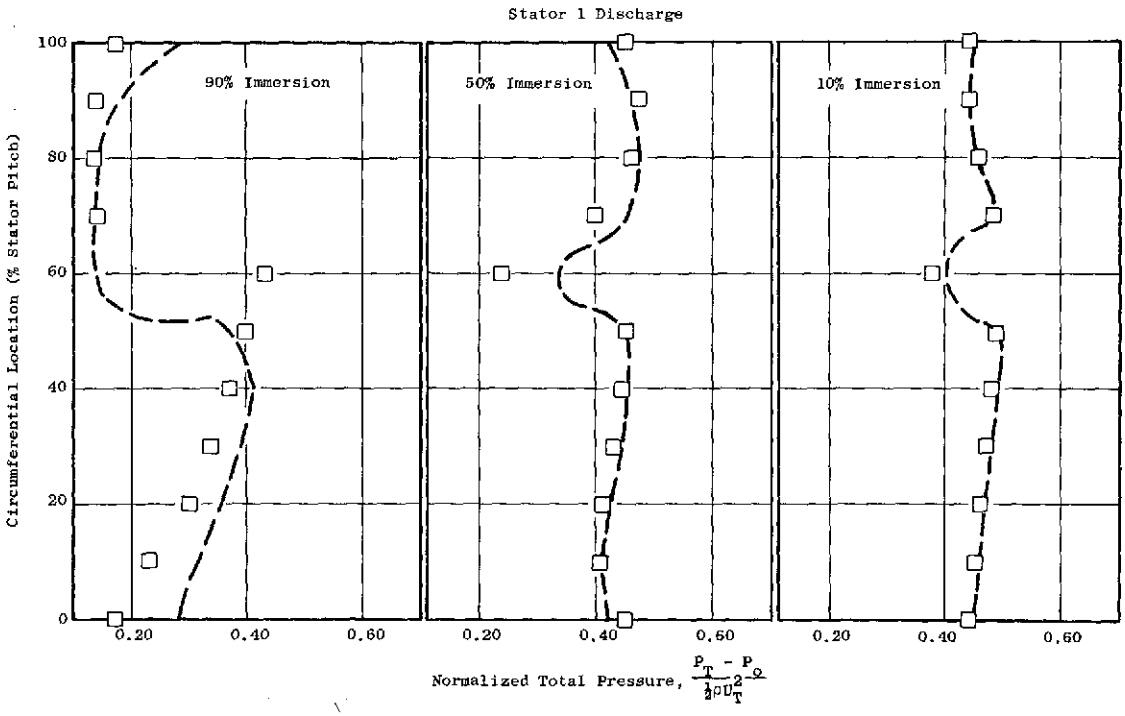

ϕ = 0.330, Throttle 155

Figure 46. Comparison of the Circumferential Variation of Normalized Total Pressure for the Smooth Spool Baseline and Baffled Wide Blade Angle Slot Treatment Configurations No. 3, U_t = 45.7 m/sec (150 ft/sec).

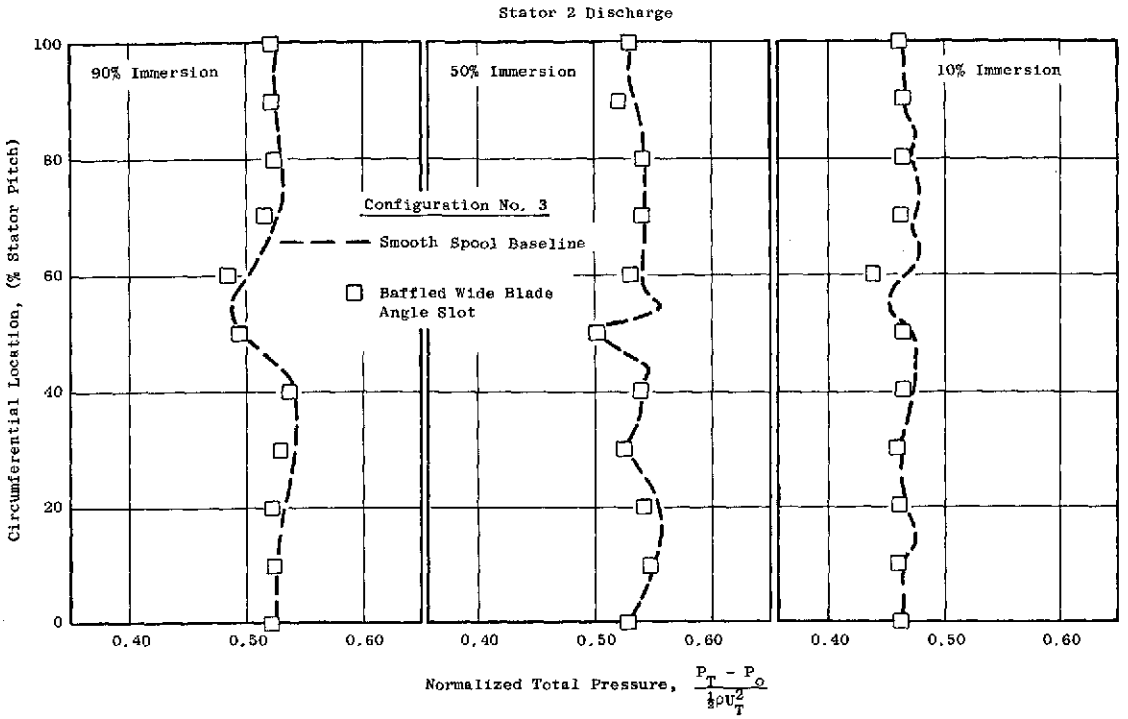

(a) ϕ = 0.368, Throttle 180

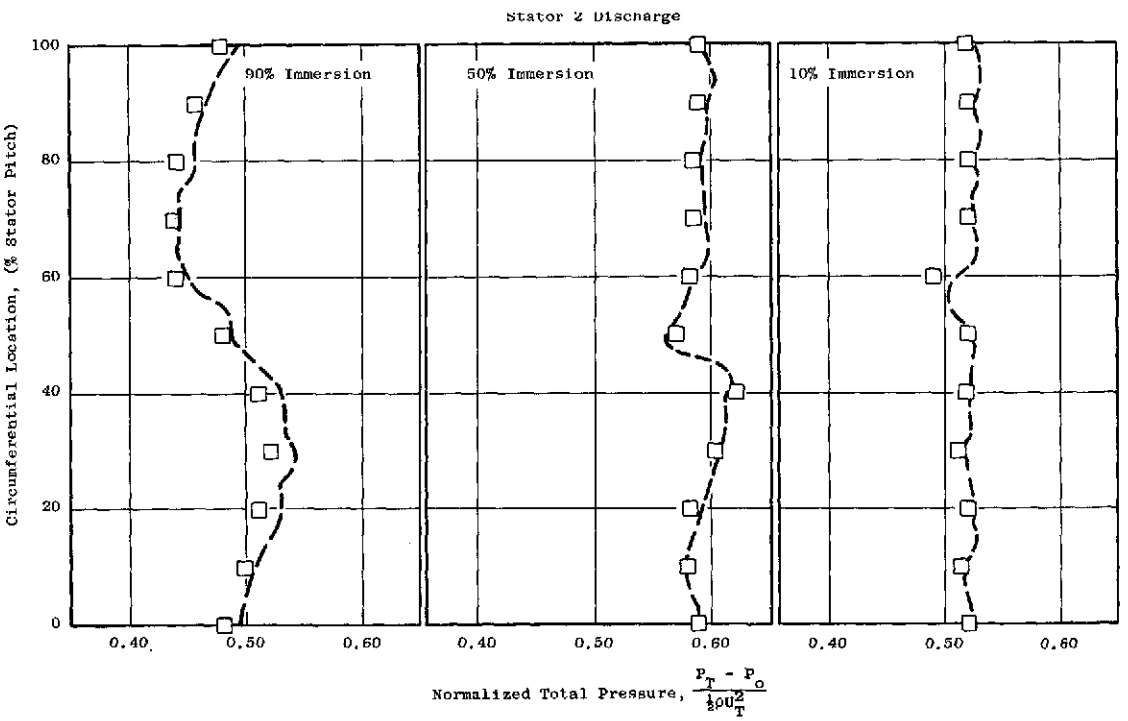

(b) ϕ = 0.330, Throttle 155

Figure 47. Comparison of the Circumferential Variation of Normalized Total Pressure for the Smooth Spool Baseline and Baffled Wide Blade Angle Slot Treatment Configurations No. 3, U_t = 45.7 m/sec (150 ft/sec).

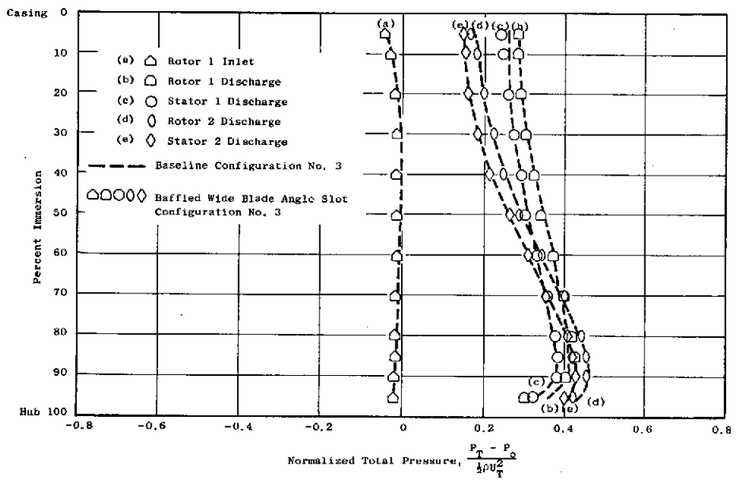

(a) ϕ = 0.456, Throttle 422

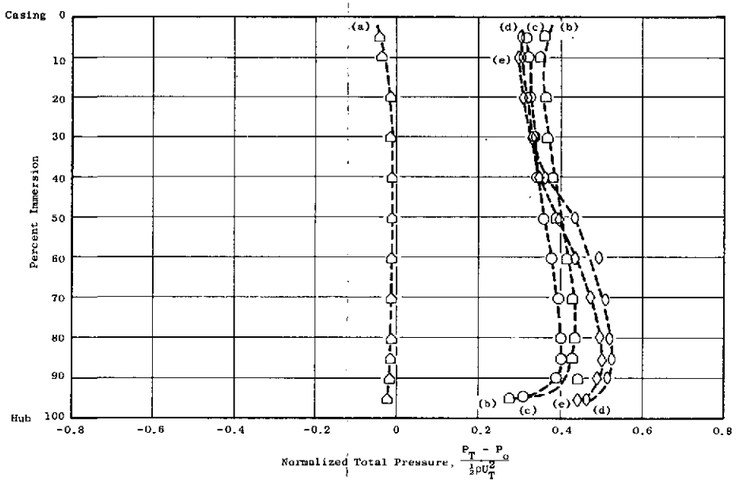

(b) ϕ = 0.422, Throttle 250

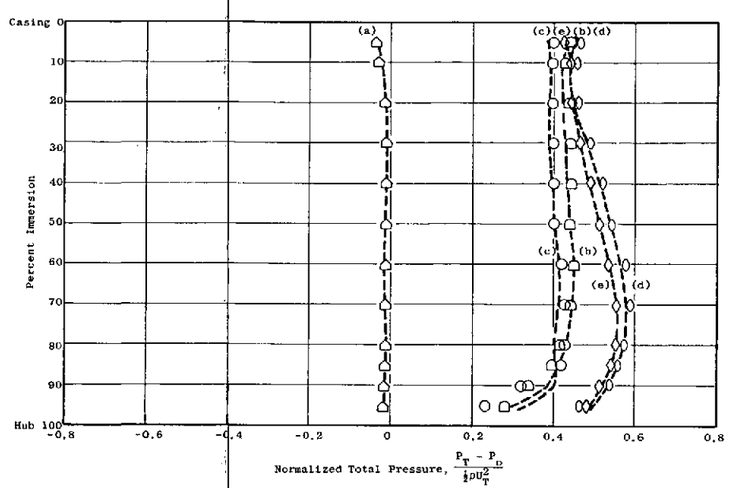

(c) ϕ = 0.379, Throttle 190

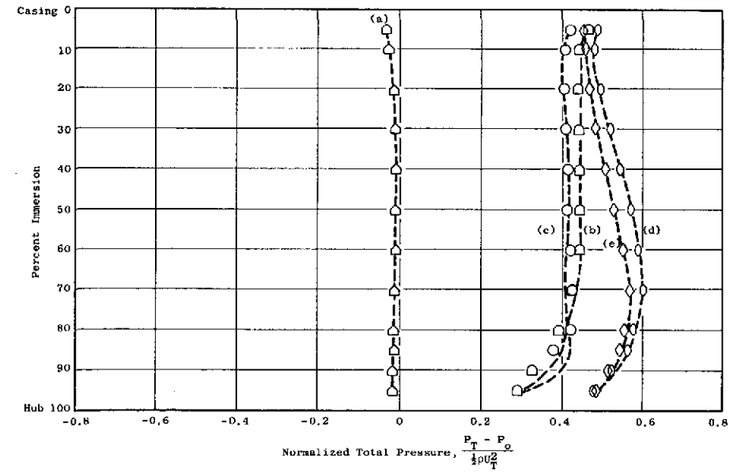

(d) ϕ = 0.368, Throttle 180

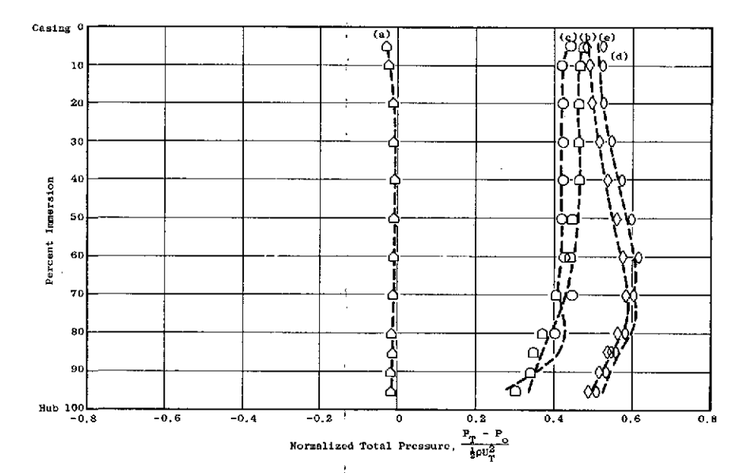

(e) ϕ = 0.340, Throttle 170

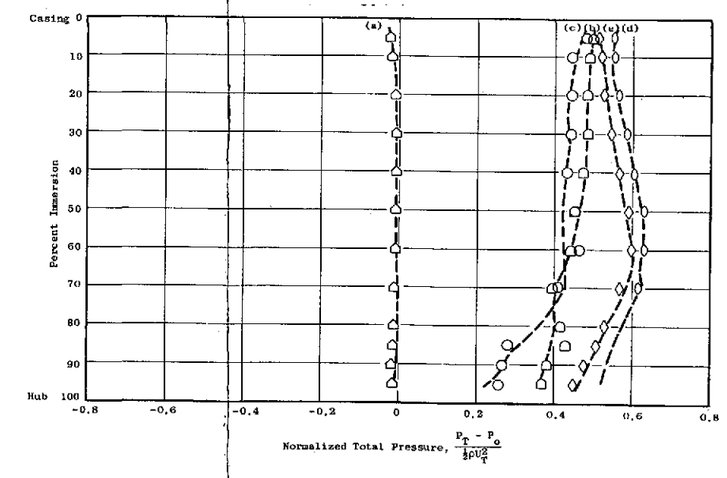

(f) ϕ = 0.330, Throttle 155

Figure 48. Comparison of the Radial Variation of Normalized Total Pressure for the Smooth Spool and the Baffled Wide Blade Angle Slot Treatment Configurations No. 3, U_t =45.7 m/sec (150 ft/sec).

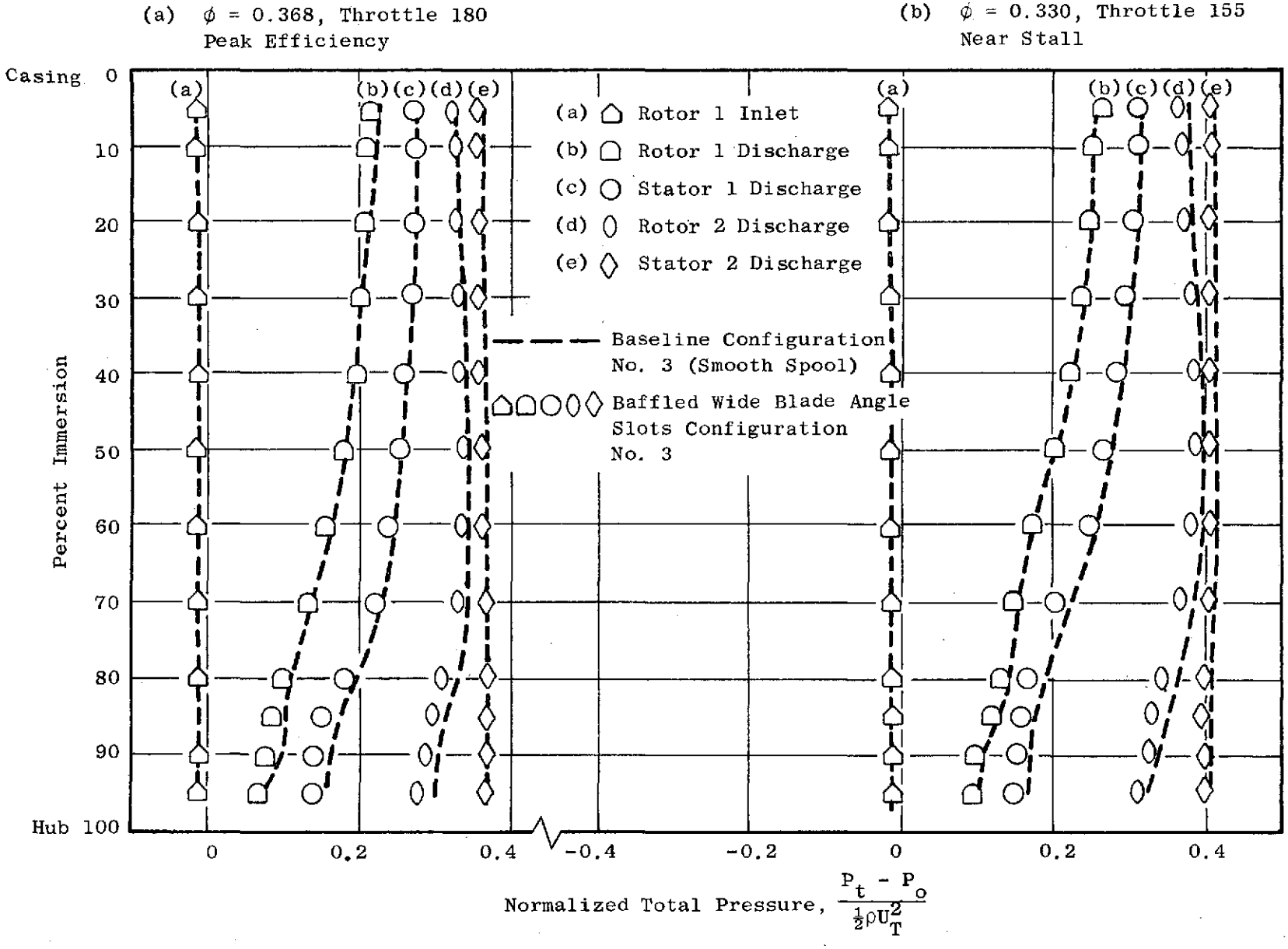

Figure 49. Comparison of the Radial Variation of Normalized Total Pressure for the Smooth Spool and Baffled Wide Blade Angle Slot Treatment Configurations No. 3, U_t = 45.7 m/sec (150 ft/sec).

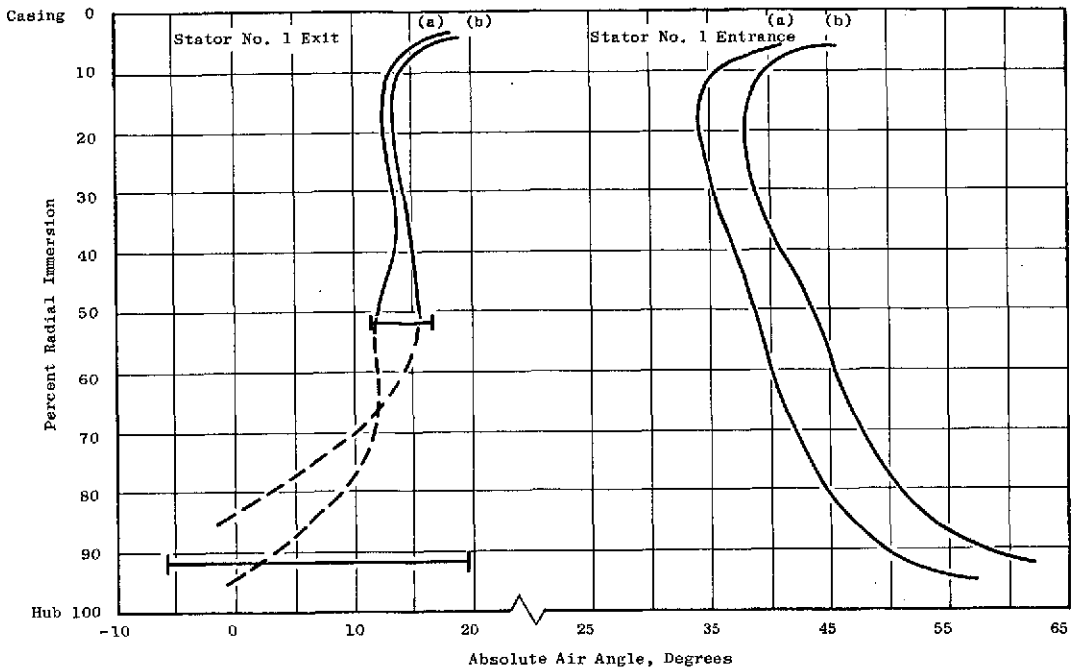

(a) First Stage Stator Entrance and Exit Absolute Air Angles

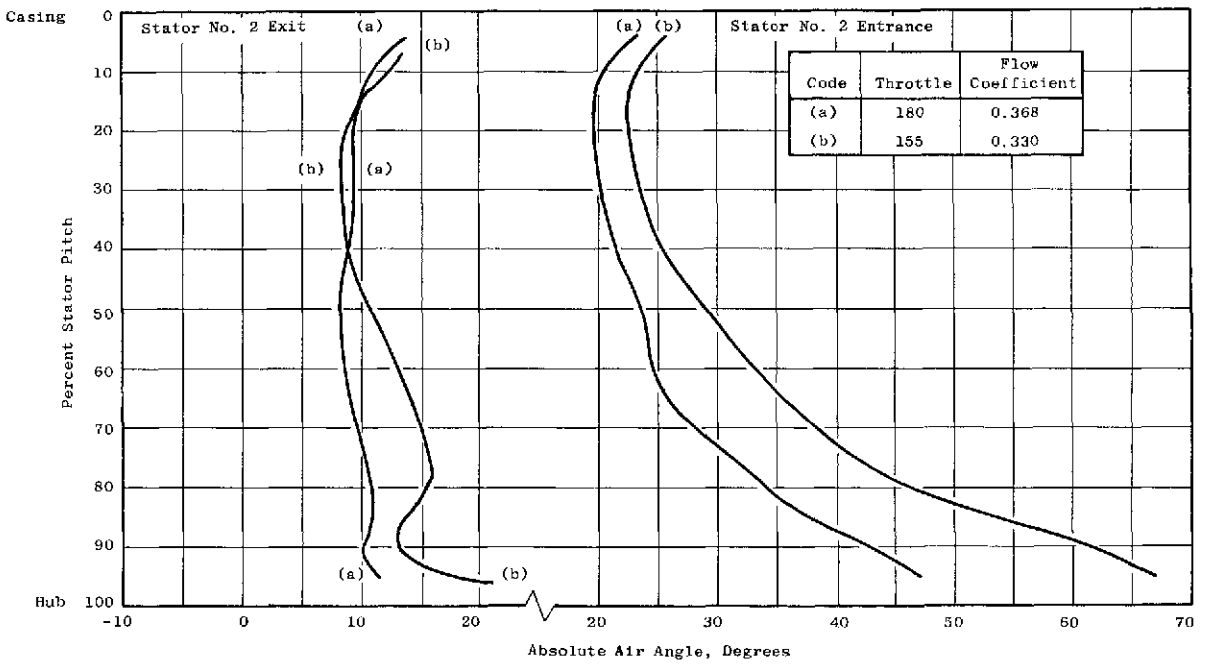

(b) Second Stage Stator Entrance and Exit Absolute Air Angles

Figure 50. Measured Absolute Air Angles Versus Percent Radial Immersion for Various Flow Coefficients, Configuration No. 3, U_t = 45.7 m/sec (150 ft/sec).

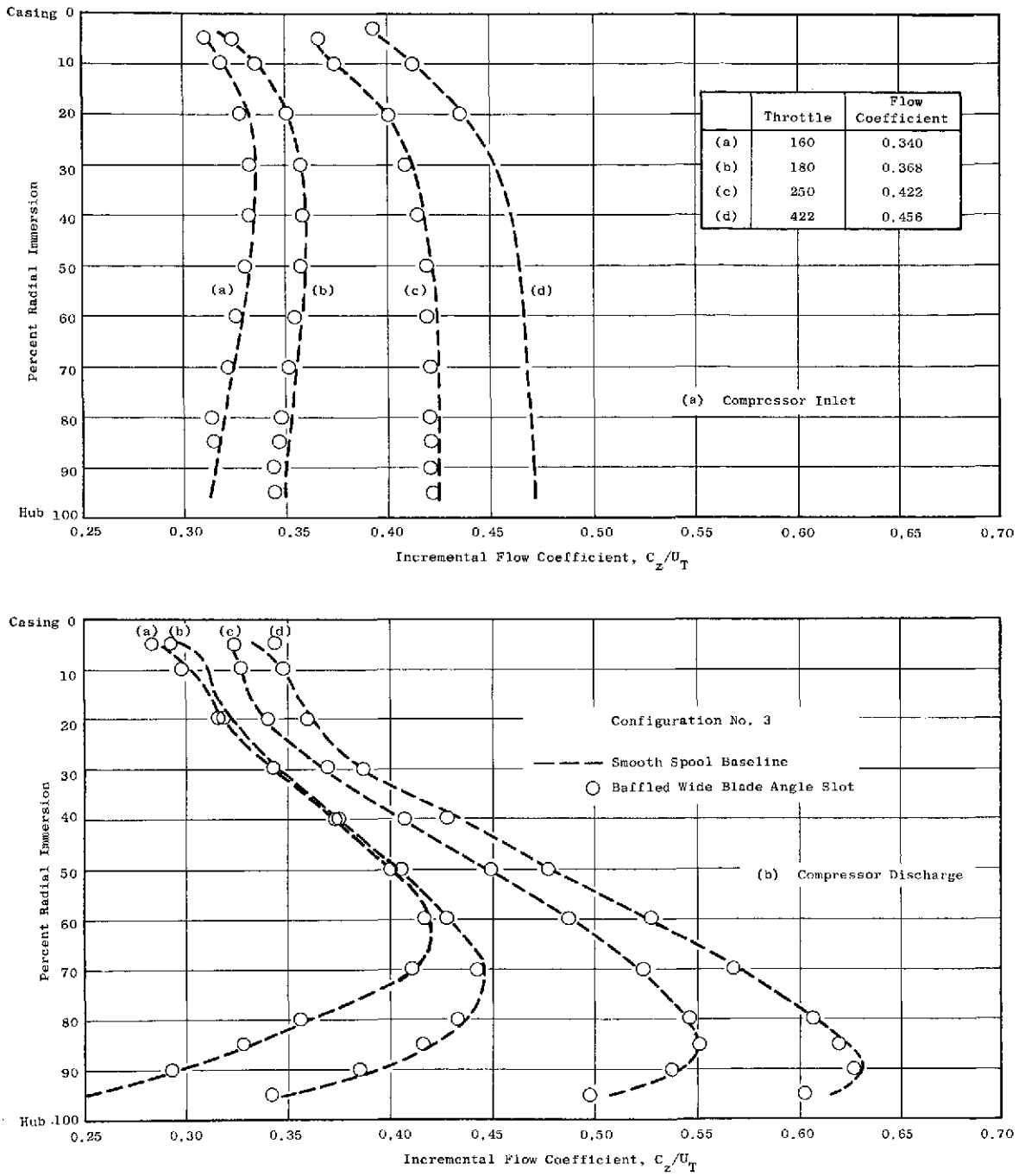

Figure 51. Comparison of the Radial Variation of Incremental Flow Coefficient for the Smooth Spool (Baseline) Configuration No. 3 and the Baffled Wide Blade Angle Slot Treatment Configuration No. 3, U_t = 45.7 m/sec (150 ft/sec).

DISCUSSION

Several observations can be made concerning the experimental results:

- The tuft probing measurements presented in Figures 13, 35, 39 and 40 show that the test compressor was hub critical.
- Stator hub treatment was ineffective in modifying the compressor performance in any discernible fashion. This conclusion is based on the results presented in Figures 15-23, 37 and 44-51.
- There is no change in work input or efficiency with the application of treatment as shown in Figures 15-17, 37, 44 and 45.

Casing treatment has been shown to be effective in increasing the stable operating range for rotors which are tip critical. The question then arises "Since this compressor was shown to be hub critical, why wasn't the treatment effective in reducing the flow at which the instability occurs (for this case the instability was the onset of rotating stall)?" An answer to this question would fall into one of two categories: first, the rotating stall is originating in a region other than the stator hub region, e.g., in the rotor hub region and, therefore, any treatment applied to the stator hub would probably be ineffective; or secondly, the rotating stall is originating in the stator hub region but the treatment cannot delay or prevent it.

Following the first line of reasoning, it is possible that the treatment is ineffective because stall originates in the rotors. Trying to determine whether rotating stall is triggered by the rotor or the stator is difficult at best. There is some inconclusive evidence, obtained from restaggering the compressor that stall could be originating in the rotor for Configuration No. 2. This restaggering was accomplished in steps and a comparison of stalling throttles and stalling flow coefficients for the various stagger changes is shown in Table VI. One must be cautious in making such comparisons; however, some trends are apparent. Comparing row VIc with VId shows that opening stator No. 2 (loading it) has a very small effect on stalling throttle. This would indicate that stator No. 2 is not limiting. Comparing row VId with VIe shows that opening stator No. 1 by 8 degrees gives a significant loss in stalling throttle. This result is indeterminate since this would happen if either stator No. 1 or rotor No. 2 were limiting. Closing rotor No. 2 by 2 degrees (unloading it) allows stalling throttle to be regained, as can be seen by comparing row VIe with VIf. Closing the second rotor by two more degrees gives a further increase in stalling flow. This trend seems to indicate that rotating stall could be originating in rotor No. 2 since, as this rotor is progressively unloaded, an improvement in stalling flow is obtained. Unfortunately, this result is still inconclusive because the effect on the first stage of a change in stagger angle of the second stage rotor has not been determined. Thus the evidence is not conclusive enough to determine whether stall is originating in rotor No. 1, stator No. 1 or rotor No. 2 for Configuration No. 2. For Configuration No. 3, in which the stator loading was significantly increased, there is no experimental evidence available to determine in which blade or vane row stall is originating.

Table VI. Stalling Throttle and Stalling Flow Configurations for Various Treatment Configurations.

	Configuration	Stalling Throttle[5]	Stalling Flow Coefficient	Stagger Angle Change - Degrees[4]			
				R1	S1	R2	S2
a.	Smooth[1]	147.4	0.347	0	0	0	0
b.	GG[2]	149.1	0.350	0	0	0	0
c.	BWBAS[3]	147.4	0.347	0	0	0	0
d.	BWBAS	149.6	N.A.	0	0	0	+8
e.	BWBAS	147.1	N.A.	0	+8	0	+8
f.	BWBAS	150.6	N.A.	0	+8	−2	+8
g.	BWBAS	146.3	0.331	0	+8	−4	+8
h.	Smooth	147.5	0.333	0	+8	−4	+8
i.	Smooth	152.8	0.327	0	0	0	0
				(1/2 stators removed)			
j.	BWBAS	153.8	0.329	0	0	0	0
				(1/2 stators removed)			

(1) Smooth spool baseline configuration
(2) Circumferential groove treatment configuration
(3) Baffled wide blade angle slot treatment configuration
(4) − indicates closing, + indicates opening
(5) Wide open throttle setting is 422. Decreasing throttle numbers imply a closing of the throttle toward stall. A one count change in throttle number is equivalent to approximately 0.00178 change in flow coefficient near the stall throttle.

Following the second line of reasoning, it is possible that stall is originating in the stator hub region but the treatment is not able to delay or prevent it. Some thoughts on why stator hub treatment might not be effective are listed below.

- The centrifugal effect of the rotating hub could inhibit flow into the cavities. The rotating hub would tend to sling the flow out of the cavity. Any low energy boundary layer flow would also tend to be slung away from the rotating hub wall. Thus, any fluid impinging on the cavity would have to overcome the centrifugal effect. This is in contrast to the flow over the rotor tip, particularly low energy boundary layer or separated flow, which tends to be slung off the rotor into the treatment cavities.

- There could be flow separation off the rotor No. 1 hub region making any treatment placed in the separated flow region ineffective. The fact that there is no measured efficiency loss with treatment could mean that the flow is not going into or out of the cavities but is simply bypassing the treatment.

- The stall initiation region could cover a large enough radial portion of the stator span that the effect of the treatment is too localized to help. It is noted that the separated flow region measured in this program extended from 70-100 percent radial immersion.

- There could be a difference in driving force for the flow into the cavity due to the compressor reaction. The static pressure at the exit of a blade or vane row is generally larger than the static pressure at the entrance. This tends to create axial re-circulation of flow in the treatment cavity. That is the flow would tend to enter the cavity at the aft (downstream) end and exit the cavity at the forward (upstream) end. A very high reaction compressor would have a much larger static pressure rise across the rotor than it would have across the stator. The recirculation driving force could be quite small for the stator of such a compressor. Thus the high reaction of the compressor used in the Stator Hub Treatment Program (approximately 75-80%) would provide a small recirculation driving force in the stators.

- The relative dynamic pressure of the fluid in the hub region is lower than that in the tip region, (note that $U^2_{HUB}/U^2_{TIP} = 1/4$ for this test compressor). If the effectiveness of the treatment were a function of the magnitude of the relative dynamic pressure, then the effectiveness of the treatment would be less at the hub. However, it is difficult to believe that the effectiveness of the treatment depends upon the magnitude of the wheel speed. If that were the case, then casing treatment which is effective at transonic speeds would probably not be effective at the wheel speeds of 45.7 m/sec (150 ft/sec) and 22.8 m/sec (75 ft/sec) described in Reference 8.

CONCLUDING REMARKS

It should not be concluded from this program that hub treatment is generally ineffective, even though the treatment had no discernible effect on the compressor performance. The test compressor was not designed specifically for the Stator Hub Treatment Program but was chosen instead from among existing hardware as one that was hub sensitive. Indeed, gross separation and backflow, indicating stall, existed over the hub region of the first stage stators. This stall was circumferentially uniform in all the vanes of the first stage; however, the operation of the compressor was stable. Two questions arise: (1) When does a compressor go from a condition of stable operation with "bad" flow (separation, reverse flow, uniform stall) to a condition of rotating stall?; and, (2) What is the instability limit? The concept of what triggers rotating stall and what delays the onset of instability needs to be better understood.

This improved understanding could be effectively applied to further investigations of stator hub treatment phenomenon and should be considered for future study.

APPENDIX

NOMENCLATURE

D-factor	Diffusion Factor
P_o	Barometric pressure
P_S	Static pressure
P_T	Total pressure
Plane 0.0	Flow measuring plane of calibrated bellmouth
Plane 1.0	First rotor inlet
Plane 1.5	First rotor discharge, first stator inlet
Plane 2.0	First stator discharge, second rotor inlet
Plane 2.5	Second rotor discharge, second stator inlet
Plane 3.0	Second stator discharge
Q	Free stream dynamic pressure
U_t	Rotor tip speed
$\Delta P/Q$	Loading parameter
δ	Boundary layer thickness
η	Torque efficiency based on total pressure
η_s	Torque efficiency based on static pressure
ρ	Density
$1/2\rho U_t^2$	Normalization parameter
ϕ	Flow coefficient, C_z/U_t
Ψ	Stream function
ψ	Work coefficient
ψ'	Pressure coefficient based on total pressure
ψ_s'	Pressure coefficient based on static pressure

REFERENCES

1. Bailey, E.E., and Voit, C.H.; "Some Observations of Effects of Porous Casing on Operating Range of a Single Axial Flow Compressor Rotor", NASA TM X-2120, October 1970.

2. Osborn, W.M., Lewis, G.E., Heidelberg, W., "Effect of Several Porous Casing Treatments on Stall Limit and on Overall Performance of an Axial Flow Compressor Rotor", NASA TN D-6537, November 1971.

3. Moore, R.D., Kovich, G., Blade, R.; "Effect of Casing Treatment on Overall and Blade Element Performance of a Compressor Rotor", NASA TN D-6538, November 1971.

4. Tesch, W.A.; "Evaluation of Range and Distortion Tolerance for High Mach Number Transonic Fan Stages: Task IV Stage Data and Performance Report for Casing Treatment Investigations", NASA CR-72862, May 1971.

5. Bailey, E.E.; "Effects of Grooved Casing Treatment on the Flow Range Capability of a Single-Stage Axial-Flow Compressor", NASA TM X-2459, January 1972.

6. NASA-Lewis Research Center Technical Staff, Aircraft Propulsion, Proceedings of Conference, NASA SP259, November 18, 1970.

7. Brent, J.A.; "Single Stage Experimental Evaluation of Compressor Blading with Slots and Vortex Generators", NASA CR-72793, March 1972.

8. Prince, D.C., Jr., Wisler, D.C., Hilvers, D.E.; "Study of Casing Treatment Stall Margin Improvement Phenomena", NASA CR-134552, March 1974.

DISTRIBUTION LIST

		Group 1 Data & Perf. Reports	Group 2 Anal. & Des. Reports, Final Perf. & Anal. Reports
1. NASA-Lewis Research Center			
21000 Brookpark Road			
Cleveland, Ohio 44135			
Attention:			
Report Control Office	MS 5-5	1	1
Technical Utilization Office	MS 3-19	1	1
Library	MS 60-3	2	2
Fluid System Components Division	MS 5-3	1	1
Compressor Branch	MS 5-9	5	5
W.L. Stewart	MS 3-5	1	1
R.S. Ruggeri	MS 5-9	1	1
M.J. Hartmann	MS 5-9	1	1
W.A. Benser	MS 5-9	1	1
D.M. Sandercock	MS 5-9	1	1
L.J. Herrig	MS 501-4	1	1
T.F. Gelder	MS 5-9	1	1
C.L. Ball	MS 5-9	1	1
L. Reid	MS 5-9	1	1
L.W. Schopen	MS 500-206	1	1
C.L. Meyer	MS 60-4	1	1
W.L. Beede	MS 5-3	1	1
D.W. Drier	MS 21-4		1
E.E. Bailey (AAMRDL)	MS 77-5	1	1
N.T. Musial	MS 500-311	1	1
C.H. Winzig	MS 5-3	1	1
2. NASA Scientific and Technical Information Facility			
P.O. Box 33			
College Park, Maryland 20740			
Attention: Acquisitions Branch		10	10
3. NASA Headquarters			
Washington, D.C. 20546			
Attention: N.F. Rekos (RLC)		1	1
4. U.S. Army Aviation Material Laboratory			
Fort Eustis, Virginia 23604			
Attention: John White		1	1

DISTRIBUTION LIST (Continued)

	Group 1	Group 2
5. Headquarters Wright-Patterson AFB, Ohio 45433		
Attention: A.J. Wennerstrom ARL/LF	1	1
S. Kobelak, AFAPL/TBP	1	1
R.P. Carmichael, ASD/XRHP	1	1
6. Department of the Navy Naval Air Systems Command Propulsion Division, AIR 536 Washington, D.C. 20360	1	1
7. Department of Navy Burear of Ships Washington, D.C. 20360		
Attention: G.L. Graves	1	1
8. NASA-Langley Research Center Technical Library Hampton, Virginia 23365		
Attention: Mark R. Nichols	1	1
John V. Becker	1	1
9. The Boeing Company Commerical Airplane Group P.O. Box 3707 Seattle, Washington 98124		
Attention: G.J. Schott, G-8410, MS 73-24	1	1
10. Douglas Aircraft Company 3855 Lakewood Boulevard Long Beach, California 90801		
Attention: J.E. Merriman Technical Information Center C1-250	1	1
11. Pratt & Whitney Aircraft Florida Research & Development Center P.O. Box 2691 West Palm Beach, Florida 33402		
Attention: J. Brent	1	1
H.D. Stetson	1	1
W.R. Alley	1	1
R.E. Davis		1
R.W. Rockenbach	1	1
B.A. Jones	1	1
J.A. Fligg	1	1

DISTRIBUTION LIST (Continued)

			Group 1	Group 2
12.	Pratt & Whitney Aircraft			
	400 Main Street			
	East Hartform, Connecticut 06108			
	Attention: R.E. Palatine		1	1
	T.G. Slaiby			1
	H.V. Marman			1
	M.J. Keenan		1	1
	B.B. Smyth			1
	A.A. Milolajczak		1	1
	Library (UARL)		1	1
	W.M. Foley (UARL)		1	1
13.	Allison Division, GMC			
	Department 8894, Plant 8			
	P.O. Box 894			
	Indianapolis, Indiana 46206			
	Attention: J.N. Barney	U-26	1	1
	G.E. Holbrook	T-22		1
	J.A. Korn	T-26	1	1
	R.F. Alverson	U-28	1	1
	Library	S-5	1	1
	A. Medlock	U-28	1	1
	P. Tramm	U-23	1	1
14.	Northern Research and Engineering			
	219 Vassar Street			
	Cambridge, Massachusetts 02139			
	Attention: K. Ginwala		1	1
15.	General Electric Company			
	Flight Propulsion Division			
	Cincinnati, Ohio 45215			
	Attention: D.C. Prince	H43	1	1
	J.F. Krapproth	K96		1
	J.W. McBride	E217		1
	L.H. Smith	H43	1	1
	J.B. Taylor	J40		1
	Tech. Infor. Center	N32	1	1
	Marlen Miller	H50	1	1
	C.C. Koch	H43	1	1
16.	General Electric Company			
	1000 Western Avenue			
	Lynn, Massachusetts 01910			
	Attention: D.P. Edkins - Bldg. 2-40			1
	F.F. Ehrich - Bldg. 2-40			1
	L.H. King - Bldg. 2-40		1	1
	R.E. Neitzel-Bldge. 2-40			1
	Dr. C.W. Smith - Library-Bldg. 2-40M		1	1

DISTRIBUTION LIST (Continued)

		Group 1	Group 2
17.	Curtiss-Wright Corporation Wright Aeronautical Wood-Ridge, New Jersey 07075		
	Attention: S. Lombardo	1	1
	G. Provenzale		1
18.	AiResearch Manufacturing Company 402 Sourth 36th Street Phoenix, Arizona 85034		
	Attention: Robert O. Bullock	1	1
	W.F. Waterman	1	1
	Jack Erwin	1	1
	Don Seyler	1	1
	Jack Switzer	1	1
	G.L. Perrone	1	1
19.	AiResearch Manufacturing Company 2525 West 190th Street Torrance, California 90509		
	Attention: R. Kobayashi	1	1
	R. Carmody	1	1
	Library	1	1
	R. Jackson	1	1
20.	Union Carbide Corporation Nuclear Division Oak Ridge Gaseious Diffusion Plant P. O. Box "P" Oak Ridge, Tennessee 37830		
	Attention: R.G. Jordan	1	1
	D.W. Burton, K-1001, K-25	1	1
21.	Avco Corporation Lycoming Division 550 South Main Street Stratford, Connecticut 06497		
	Attention: Clause W. Bolton	1	1
22.	Teledyne CAE 1330 Laskey Road Toledo, Ohio 43601		
	Attention: Eli H. Benstein	1	1
	Howard C. Walch		1
23.	Solar San Diego, California 92112		
	Attention: P.A. Pitt	1	1
	J. Watkins	1	1

DISTRIBUTION LIST (Continued)

	Group 1	Group 2
24. Goodyear Atomic Corporation Box 628 Piketon, Ohio 45661 Attention: C.O. Langebrake	1	2
25. Iowa State University of Science & Tech. Ames, Iowa 50010 Attention: Professor George K. Serovy Dept. of Mechanical Engrg.	1	1
26. Hamilton Standard Division of United Aircraft Corporation Windsor Locks, Connecticut 06096 Attention: Mr. Carl Rohrback Head of Aerodynamics and Hydrodynamics	1	1
27. Westinghouse Electric Corporation Small Steam and Gas Turbine Engineering B-4 Lester Branch P.O. Box 9175 Philadelphia, Pennsylvania 19113 Attention: Mr. S.M. DeCorso	1	1
28. Williams Research Corporation P.O. Box 95 Walled Lake, Michigan 48088 Attention: J. Richard Joy Supervisor, Analytical Section	1	1
29. Lockheed Missile and Space Company P.O. Box 879 Mountain View, California 94040 Attention: Technical Library	1	1
30. Eaton Research Center 26201 Northwestern Highway Southfield, Michigan 48076 Attention: Librarian	1	1
31. Chrysler Corporation Research Office Department 9000 P.O. Box 1118 Detroit, Michigan 48231 Attention: James Furlong (418-18-40) Ronald Pampreen (418-38-31)	1 1	1 1

DISTRIBUTION LIST (Concluded)

		Group 1	Group 2
32.	Elliott Company Jeannette, Pennsylvania 15644 Attention: J. Rodger Schields Director, Engineering	1	1
33.	California Institute of Technology Pasadena, California 91109 Attention: Professor Duncan Rannie	1	1
34.	Massachusetts Institute of Technology Cambridge, Massachusetts 02139 Attention: Dr. J.L. Kerrebrock	1	1
35.	Caterpillar Tractor Company Peoria, Illinois 61601 Attention: J. Wiggins	1	1
36.	Penn State University Department of Aerospace Engineering 233 Hammond Building University Park, Pennsylvania 16802 Attention: Professor B. Lakshminarayana	1	1
37.	Texas A&M University Department of Mechanical Engineering College Station, Texas 77843 Attention: Dr. Meherwan P. Boyce P.E.	1	1